Understanding the Molecular Mechanism of Mgm1 Function in Mitochondrial Dynamics

by

Jarungjit Rujiviphat

A thesis submitted in conformity with the requirements
for the degree of Doctor of Philosophy

Graduate Department of Biochemistry
University of Toronto

Understanding the Molecular Mechanism of Mgm1 Function in Mitochondrial Dynamics

Jarungjit Rujiviphat

Doctor of Philosophy

Graduate Department of Biochemistry
University of Toronto

2014

Abstract

Given the debilitating effect that mitochondrial dysfunction has on human health, it is important to understand mitochondrial dynamics that are vital for the maintenance of mitochondrial function, genome, morphology, and quality control. Mitochondrial dynamics result from a balance in mitochondrial fusion and fission. Although the mechanism and regulation of mitochondrial fission are largely elucidated, less is known about mitochondrial fusion. Mgm1 is a protein that mediates mitochondrial fusion in yeast. However, the molecular mechanism of Mgm1 function in mediating mitochondrial fusion is unclear. In this thesis, first, I show that Mgm1 contains a lipid-binding domain by demonstrating that purified Mgm1 has lipid-binding activity and by identifying mutations in conserved residues that abrogate these interactions. Second, I show that Mgm1 assembles into hexameric rings and undergoes nucleotide-dependent structural transitions that, I believe, initiate membrane fusion. Lastly, I demonstrate that Mgm1 exhibits membrane-remodeling activities that are crucial for the tethering and lipid-mixing steps in the membrane fusion event. Together, I propose a mechanistic model of Mgm1 function in mediating mitochondrial fusion that advances the fields of mitochondrial biology, cellular protein-membrane dynamics, and the etiology of neurodegenerative diseases.

Acknowledgements

"Angus, you are the best." Haha… yes, I do use this sentence to start my acknowledgement! I have to thank Angus a lot throughout my graduate studies from him asking me for an interview to hosting a very memorable defense exam and party. Five years in the McQuibban lab for graduate study is definitely the most memorable time of my life. I would like to thank Angus for his supervision, support, and his patience with my English. I have learned so much science and non-science knowledge from Angus.

I would like to acknowledge my committee members, Dr. Alan Davidson and Dr. John Rubinstein, for critical discussions at my committee meetings. Alan has also helped me a lot with my protein *in vitro* experiments and analyses. Without John, I would not have such a complete electron microscopy analysis. I would also like to thank all my exam committee members, Dr. R. Blake Hill, Dr. Rick Collins, Dr. David Williams, and Dr. Trevor Moraes, for offering insightful discussions and comments.

To all the McQuibban lab members, thank you for being awesome labmates and friends, and for trying to understand my work that is quite different from the rest of the lab. I would also like to extend special thanks to Riya Shanbhag, Rediet Taddese, and Dr. Mauro Serricchio for critical reading of my thesis, and Eliana Chan, Yuqing Wang, and Guang Shi for critical discussions during my practice defense talk. Lastly, I would like to acknowledge my mentors, Gaby Meglei who helped my started off the project and Dr. Saranya Kittanakom who first introduced me to research.

Lastly, I would like to thank my family, Sumalee, Viroj, and Chacree Rujiviphat for supporting me and trusting me that I would not turn into a *"crazy"* scientist after grad school. Jay Yang, thank you for helping me find ways to convince my parents, for convincing me that I can succeed in grad school, and for helping me throughout my graduate studies. To all my friends in Toronto, you are like my extended family who supports me during good and bad time. In addition to Angus and Jay who have read every word of this thesis, I would also like to acknowledge Jim Lyons for reading and helping me with the thesis editing.

This piece of work would not have happened without the help of everyone I have acknowledged here, especially Dr. G. Angus McQuibban. Thank you very much!

Table of Contents

ABSTRACT ..... **ii**

ACKNOWLEDGEMENTS ..... **iii**

LIST OF FIGURES ..... **IX**

LIST OF ABBREVIATIONS ..... **XI**

CHAPTER 1 ..... **1**

1 GENERAL INTRODUCTION **1**

1.1 THE MITOCHONDRION IS AN ESSENTIAL ORGANELLE WITH UNIQUE ORIGIN AND CHARACTERISTICS 1

1.1.1 Mitochondria possess their own genetic material *2*

1.1.2 Mitochondria have unique organization and compartmentalization *3*

1.1.3 Mitochondria are more than just cellular powerhouses *7*

1.2 MITOCHONDRIA ARE DYNAMIC IN NATURE TO MAINTAIN VARIOUS MORPHOLOGIES AND FUNCTIONS 10

1.2.1 Mitochondria are dynamic organelles that constantly undergo fusion and fission *12*

1.2.2 Genetic screens in S. cerevisiae have identified molecular machineries in mitochondrial dynamics *13*

1.2.3 Studies in multicellular organisms have revealed the cellular and physiological roles of mitochondrial dynamics *18*

1.2.4 Mitochondrial fission relies on a sole mechanoenzyme with multiple levels of regulation *22*

1.2.5 Mitochondrial fusion requires two separable membrane fusion events and machineries. *24*

1.3 DYNAMIN-RELATED PROTEINS ARE THE MAIN PLAYERS THAT MEDIATE MITOCHONDRIAL FUSION AND FISSION 29

1.3.1 Dynamin superfamily proteins are membrane-remodeling molecules *29*

1.3.2 Members of the dynamin superfamily share conserved domains *30*

1.3.3 Dynamin superfamily proteins polymerize and constrict membranes to mediate membrane fission *33*

1.3.4 DRPs mediate membrane fusion via unique mechanisms *37*

1.4 MITOCHONDRIAL GENOME MAINTENANCE 1 (MGM1) IS A DRP THAT MEDIATES MITOCHONDRIAL INNER MEMBRANE FUSION 41
1.4.1 Mgm1 was first discovered and characterized in 1990s 42
1.4.2 Mgm1 plays a role in mitochondrial morphology, fusion, and cristae maintenance 43
1.4.3 Mgm1 precursor is transported to the IM and processed into l-Mgm1 and s-Mgm1 isoforms 43
1.4.4 Mgm1 contains core domains and possesses characteristics of the dynamin superfamily proteins 45
1.4.5 Mgm1 mediates mitochondrial inner membrane fusion 49
1.5 THESIS RATIONALE 50

CHAPTER 2 52

2 MATERIAL AND METHODS 52
2.1 REAGENTS 52
2.1.1 Plasmids 52
2.1.2 Antibodies 52
2.1.3 Lipids 52
2.2 RECOMBINANT PROTEIN EXPRESSION, PURIFICATION, AND MODIFICATION 53
2.2.1 s-Mgm1 protein expression 53
2.2.2 s-Mgm1 protein purification 54
2.2.3 s-Mgm1 probe conjugation 54
2.2.4 l-Mgm1 protein expression 54
2.2.5 l-Mgm1 protein purification 55
2.2.6 l-Mgm1 liposome reconstitution 55
2.3 MODEL MEMBRANES PREPARATION 56
2.3.1 Large unilamellar vesicles preparation 56
2.3.2 Giant unilamellar vesicles preparation 56
2.3.3 Lipid monolayer preparation 57
2.3.4 Supported lipid bilayer preparation 57
2.4 ACTIVITY ASSAYS 58
2.4.1 GTPase activity assay 58
2.4.2 Enzyme-linked immunosorbent assay 58
2.4.3 Lipid turbidity assay 59

2.4.4 NBD/rhodamine lipid-mixing assay *59*
2.4.5 HPTS/DPX content-mixing assay *59*
2.5 CHROMATOGRAPHY 60
2.5.1 Size exclusion chromatography *60*
2.6 SPECTROSCOPY 60
2.6.1 Circular dichroism *60*
2.7 MICROSCOPY 61
2.7.1 Negative stain electron microscopy *61*
2.7.2 Cryo-electron microscopy *61*
2.7.3 Epifluorescence microscopy *62*
2.7.4 Confocal fluorescence microscopy *62*
2.7.5 Atomic force microscopy *63*
2.8 YEAST 63
2.8.1 In vivo complementation assay and imaging morphology *63*

CHAPTER 3 64

3 PHOSPHOLIPID ASSOCIATION IS ESSENTIAL FOR MGM1 FUNCTION IN MITOCHONDRIAL MEMBRANE FUSION 64
3.1 SUMMARY 65
3.2 INTRODUCTION 65
3.3 RESULTS 66
3.3.1 Conserved lysines constitute a lipid-binding domain within s-Mgm1 ..... *66*
3.3.2 s-Mgm1 GTPase activity is stimulated by phospholipids *69*
3.3.3 s-Mgm1 lipid binding is required for stimulated GTPase activity *69*
3.3.4 s-Mgm1 displays positive cooperativity in GTPase activity *71*
3.3.5 In vivo complementation of s-Mgm1 requires lipid association *72*
3.3.6 s-Mgm1 causes aggregation of IM liposomes *74*
3.3.7 s-Mgm1 assembles onto IM liposomes and forms a two-dimensional crystalline array *75*
3.4 DISCUSSION 76
3.4.1 Mgm1-phospholipid associations *77*
3.4.2 s-Mgm1 GTP hydrolysis is stimulated by lipid binding and s-Mgm1 oligomerization *78*
3.4.3 A possible lipid-binding domain of Mgm1 ..... *79*
3.4.4 A possible role of s-Mgm1 in the tethering step of IM fusion *80*

CHAPTER 4 82

4 MEMBRANE TETHERING AND GTP-DEPENDENT CONFORMATIONAL CHANGES DRIVE MGM1-MEDIATED MITOCHONDRIAL FUSION 82

4.1 SUMMARY 83

4.2 INTRODUCTION 83

4.3 RESULTS 84

4.3.1 s-Mgm1 assembles onto the surface of liposomes and forms protein bridges to promote membrane tethering 84

4.3.2 s-Mgm1 lipid-bound oligomers undergo a nucleotide-dependent conformational transition 88

4.3.3 s-Mgm1 secondary structures may undergo conformational changes 90

4.3.4 GTP enhances the lipid-mixing activity of s-Mgm1 91

4.4 DISCUSSION 93

4.4.1 Possible morphology and trans interactions of s-Mgm1 to tether membranes 93

4.4.2 Possible GTP-dependent structural transitions of s-Mgm1 to promote phospholipid mixing and fusion of bilayers 93

4.4.3 A proposed mechanism of Mgm1 function 94

CHAPTER 5 96

5 MGM1 ALTERS MEMBRANE TOPOLOGY AND PROMOTES LOCAL MEMBRANE BENDING .. 96

5.1 SUMMARY 97

5.2 INTRODUCTION 97

5.3 RESULTS 100

5.3.1 s-Mgm1 promotes lateral lipid movement and lipid clustering 100

5.3.2 s-Mgm1 alters membrane topology 103

5.3.3 s-Mgm1 deforms liposomes 104

5.3.4 s-Mgm1 promotes local membrane bending 106

5.3.5 GTP binding enhances Mgm1-mediated local membrane bending 109

5.3.6 GTP promotes liposome fusion in the presence of both s-Mgm1 and l-Mgm1 112

5.4 DISCUSSION 115

5.4.1 Lipid clustering activity of s-Mgm1 may be important for IM fusion 115

5.4.2 s-Mgm1 is a membrane-remodeling protein 116

5.4.3 A possible fusion initiation step of s-Mgm1-mediated IM fusion 116
5.4.4 A possible role of s-Mgm1 in the lipid-mixing step of IM fusion 117
5.4.5 A possible role of l-Mgm1 in IM fusion 119

CHAPTER 6 120

6 GENERAL DISCUSSION AND FUTURE DIRECTIONS 120
6.1 SUMMARY 120
6.2 MGM1 DOMAIN STRUCTURE AND FUNCTION 120
6.2.1 Requirement for lipid-binding activity 121
6.2.2 Possible effector roles of lipid-binding activity 122
6.2.3 Possible unique lipid-binding domain of Mgm1 124
6.3 MGM1 STRUCTURE 124
6.4 MODEL MECHANISM OF MGM1-MEDIATED IM FUSION 126
6.5 REGULATION OF MGM1-MEDIATED IM FUSION 129
6.6 CONCLUSION 129

REFERENCES 131

List of Figures

Figure 1.1. **Mitochondrial organization** **5**

Figure 1.2. **Schematic summary of mitochondrial functions** **8**

Figure 1.3. **Mitochondrial morphology** **11**

Figure 1.4. **Mitochondrial dynamics** **13**

Figure 1.5. **Mitochondrial morphology in *Saccharomyces cerevisiae*** **14**

Figure 1.6. **Mechanistic models of yeast mitochondrial fusion and fission** **26**

Figure 1.7. **Domain structure of the dynamin superfamily** **30**

Figure 1.8. **Dynamin structure and dynamin-mediated membrane fission mechanism** **36**

Figure 1.9. **Hemifusion model of membrane fusion** **38**

Figure 1.10. **Model mechanism of Fzo1-mediated membrane fusion** **40**

Figure 1.11. **Mgm1 processing into l-Mgm1 and s-Mgm1 isoforms** **45**

Figure 3.1. **s-Mgm1 contains a lipid-binding domain that directly binds to lipids of the mitochondrial IM** **68**

Figure 3.2. **s-Mgm1 binding to lipids results in stimulated GTPase activity** **71**

Figure 3.3 **Oligomerization induces stimulated GTPase activity** **72**

Figure 3.4. **s-Mgm1 mutants defective in IM binding and stimulated GTPase activity have impaired function *in vivo*** **73**

Figure 3.5. **s-Mgm1 promotes liposome aggregation** **74**

Figure 3.6. **s-Mgm1 assembles onto IM liposomes as oligomeric rings** **76**

Figure 3.7. **Model of s-Mgm1 mechanistic actions during the tethering step of mitochondrial IM fusion** **81**

Figure 4.1. **s-Mgm1 assembles onto and tethers liposomes** **86**

Figure 4.2. **s-Mgm1 can transform liposomes into protein-decorated tubes** **87**

Figure 4.3. **s-Mgm1 oligomeric arrays undergo a nucleotide-dependent structural transition that enhances s-Mgm1 membrane fusion activity** **89**

Figure 4.4. **GTP binding may alter s-Mgm1 secondary structure** **90**

Figure 4.5. **s-Mgm1 promotes lipid mixing of IM liposomes that is enhanced by nucleotide** **92**

Figure 4.6. **Model of Mgm1 structural transitions during mitochondrial IM fusion** **95**

Figure 5.1. **s-Mgm1 lipid-binding activity causes phospholipid clustering and fibre-like structure formation** **101**

Figure 5.2. **s-Mgm1 does not cause clustering of NBD-PC** **102**

Figure 5.3. **s-Mgm1 promotes immediate phospholipid lateral lipid movement and clustering and fibre-like structure formation** **103**

Figure 5.4. **s-Mgm1 alters the topology of the supported lipid bilayer** **104**

Figure 5.5. **s-Mgm1 deforms liposomes** **105**
Figure 5.7. **s-Mgm1 requires a functional lipid-binding domain to bind to liposomes** **107**
Figure 5.8. **s-Mgm1 binds to liposomes and causes local membrane bending** **108**
Figure 5.9. **Lipid-binding mutant K795A does not promote local membrane bending** **108**
Figure 5.10. **GTP binding enhances local membrane bending by s-Mgm1** **110**
Figure 5.11. **The enhancement in membrane bending is specific to GTP but not GDP** **111**
Figure 5.12. **s-Mgm1 segregates to promote local membrane bending upon GTP binding** **112**
Figure 5.13. **l-Mgm1 is reconstituted into IM liposomes and stimulates s-Mgm1 activity** **113**
Figure 5.14. **GTP promotes s-Mgm1-dependent liposome deformation and membrane fusion** **114**
Figure 5.15. **Model of s-Mgm1 mechanistic actions in the lipid-mixing step of mitochondrial IM fusion** **118**
Figure 6.1. **Schematic representation of Mgm1 and Mgm1 variants used to generate l*-Mgm1 and s*-Mgm1** **122**
Figure 6.2. **Model of Mgm1-mediated IM fusion** **127**

List of Abbreviations

ADL	*Arabidopsis thaliana* dynamin-like
AFM	Atomic force microscopy
AIF	Apoptosis-inducing factor
ANT	Adenine nucleotide translocator
ATP	Adenosine 5'-triphosphate
AUC	Analytical ultracentrifucation
BCL-2	B cell CLL/lymphoma-2
BDLP	Bacterial dynamin-like protein
BSE	Bundle signal elements
CCP	Cytochrome *c* peroxidase
CCV	Clathrin-coated vesicle
CD	Circular dichroism
CL	Cardiolipin
CM	Cristae membrane
DAPI	4',6-diamidino-2-phenylindole
DIC	Differential interference contrast
DNA	Deoxyribonucleic acid
DNM	Dynamin
DRP	Dynamin-related protein
EM	Electron microscopy
ER	Endoplasmic reticulum
ETC	Electron transport chain
FZO	Fuzzy onions
GBP	Guanylate-binding protein
GDP	Guanosine 5′-diphosphate
GED	GTP effector domain
GEF	GTP exchange factor
GFP	Green fluorescent protein
GTP	Guanosine 5′-triphosphate
HR	Heptad repeat
IBM	Inner boundary membrane
IM	Inner membrane
IMS	Intermembrane space
MAVS	Mitochondrial antiviral-signaling protein
MDM	Mitochondrial distribution and morphology
MFF	Mitochondrial fission factor
MFN	Mitofusin
MGM	Mitochondrial genome maintenance
MMM	Mitochondrial morphology maintenance
MPP	Mitochondrial processing peptidase

mtDNA	Mitochondrial DNA
MTS	Mitochondrial targeting sequence
NSF	*N*-ethylmaleimide sensitive fusion protein
OM	Outer membrane
OPA	Optic atrophy
OXPHOS	Oxidative phosphorylation
PA	Phosphatidic acid
PA-GFP	Photoactivatable green fluorescent protein
PARL	Presenilin-associated rhomboid-like protein
PC	Phosphatidylcholine
PCP	Processing of cytochrome *c* peroxidase
PD	Parkinson's disease
PDH	Pyruvate dehydrogenase
PE	Phosphatidylethanolamine
PH	Pleckstrin homology
PHB	Prohibitin
PI	Phosphatidylinositol
PLD	Phospholipase D
PRD	Proline-rich domain
PS	Phosphatidylserine
PSD	Phosphatidylserine decarboxylase
RBD	Rhomboid
RCR	Rhomboid cleavage region
RFP	Red fluorescent protein
RNA	Ribonucleic acid
ROS	Reactive oxygen species
rRNA	Ribosomal ribonucleic acid
SLB	Supported lipid bilayer
SNARE	Soluble NSF attachment protein receptor
TCA	Tricarboxylic acid
TIM	Translocase of the inner membrane
TIRF	Total internal reflection fluorescence
TM	Transmembrane segment
TOM	Translocase of the outer membrane
tRNA	Transfer ribonucleic acid
UBP	Ubiquitin protease
UPS	Unprocessed
VDAC	Voltage-dependent anion channel
VPS	Vacuolar protein sorting

Chapter 1

1 GENERAL INTRODUCTION

Eukaryotes rely on functional mitochondria as a major source of energy production and as a site for metabolic pathways and cellular signaling to control cell life and death. These functions require mitochondria to maintain their proper morphology and dynamics. The dynamics of mitochondria result from a balance in mitochondrial fusion and fission. Disruption in mitochondrial fusion or fission alters mitochondrial morphology, genome integrity, and overall cell health. Altered mitochondrial dynamics have been linked to neurodegenerative diseases such as Parkinson's disease. Genetic diseases such as autosomal optic atrophy are caused by mutations in mitochondrial fusion and fission genes. Therefore, it is important to understand the function and regulation of these disease-related genes or their homologues. This thesis work focuses on understanding the molecular mechanism of the dynamin-related protein Mgm1, which mediates mitochondrial inner membrane fusion in yeast. Although Mgm1 localization and function have been described, it is poorly understood how Mgm1 mechanistically mediates mitochondrial fusion. The goal of my thesis is to understand the molecular mechanism of Mgm1 function in mitochondrial dynamics.

1.1 THE MITOCHONDRION IS AN ESSENTIAL ORGANELLE WITH UNIQUE ORIGIN AND CHARACTERISTICS

The mitochondrion is a cellular organelle that uniquely evolved from an ancient endosymbiotic event (Andersson and Kurland 1999, Gray, Burger et al. 1999). Sequence analysis studies on mitochondrial DNA (mtDNA) have confirmed that mitochondria have eubacteria roots, supporting the endosymbiosis hypothesis of a bacterium being engulfed and then evolving into an organelle (Lang, Burger et al. 1997, Andersson, Zomorodipour et al. 1998). Phylogenetic analyses show that the obligate intracellular parasite *Rickettsia prowazekii* is more closely related to mitochondria than any other known microorganisms (Andersson, Zomorodipour et al. 1998). More than 150 nuclear-encoded mitochondrial targeted proteins in the yeast *Saccharomyces cerevisiae* have significant sequence similarity to *R. prowazekii* proteins. These proteins include

proteins that function in ATP production and transport, which are the hallmark functions of mitochondria. This unusual origin of the mitochondrion gives rise to its distinct characteristics such as having its own genetic material and a unique ultrastructural organization. Mitochondrial gene products make mitochondria a major site for energy production for their hosts. In addition, mitochondria also play a role in cell development, cell signaling, and cellular quality control mechanisms, which make the mitochondrion an essential cellular organelle. The unique characteristics of mitochondria are described below.

1.1.1 Mitochondria possess their own genetic material

Mitochondrial DNA (mtDNA) was first identified in 1963 when Sylan and Margit Nass noticed fibres inside mitochondria (Nass and Nass 1963). These fibres were found to be sensitive to ribonuclease and deoxyribonuclease, which indicated that they were composed of nucleic acid material. In addition, these fibres were previously shown to have fixation and staining properties similar to those of bacterial nucleoplasm (Schatz 1963). Like bacterial genomes, most mitochondrial genomes in multicellular organisms are circular, except for rare cases such as some species in the *Cnidaria* phylum. However, unicellular organisms including yeasts and algae have linear mtDNA. Mammals have a circular 16.5 kb mitochondrial genome (Anderson, Bankier et al. 1981), whereas the budding yeast *Saccharomyces cerevisiae* has a linear 75 kb mitochondrial genome (Williamson 2002). The mammalian mitochondrial genome is tightly packed without non-coding sequences and encodes 37 genes: 22 tRNA genes and 2 rRNA genes that are essential for the translation of mtDNA transcripts, and 13 genes whose translated proteins are subunits of respiratory complexes I, III, IV, and V (Chan 2006). Although the yeast mitochondrial genome encodes a similar number of genes as the mammalian mitochondrial genome, the yeast mitochondrial genome is five times larger because it contains long non-coding introns (Williamson 2002). The mitochondrial-encoded respiratory complexes function in the oxidative phosphorylation (OXPHOS) pathway, which generates most of the cellular supply of chemical energy in the form of adenosine triphosphate (ATP). This cellular respiration and ATP production is a hallmark function of mitochondria.

1.1.2 Mitochondria have unique organization and compartmentalization

In addition to their unique genome, mitochondria have a distinct ultrastructural organization. Unlike other cellular organelles, mitochondria have double membranes that create four discrete compartments: the outer membrane (OM), the inner membrane (IM), the intermembrane space (IMS), and the mitochondrial matrix (**Figure 1.1**). The four compartments contain different proteins and lipids to carry out distinct functions as described below.

1.1.2.1 Four mitochondrial compartments are unique in their compositions and functions

The four discrete compartments carry out unique functions. The OM allows proteins to pass in and out between the cytoplasm and the IMS via channels, whereas the IM only allows specific proteins to translocate across and to be imported to the mitochondrial matrix. The OM contains a large number of channels called porins or voltage-dependent anion channels (VDAC) that allow molecules smaller than 5 kDa to diffuse across, while larger molecules have to go through the translocase of outer membrane (TOM) complexes. The translocase of inner membrane (TIM) complexes reside in the IM and require membrane potential ($\Delta\Psi$) for their protein import function (Chacinska, Koehler et al. 2009). The OM contains metabolic enzymes that function in fatty acid oxidation, tryptophan metabolism, and monoamine neurotransmitter metabolism. The IM is filled with OXPHOS complexes that generate ATP. OXPHOS complexes pump protons to the IMS to generate a proton gradient, which is necessary for ATP synthesis. The IMS also contains other signaling molecules, including cytochrome *c,* that function in the apoptosis pathway. The mitochondrial matrix is where the mitochondrial genome is stored, transcribed, and translated. The matrix is also the home for enzymes in the tricarboxylic acid (TCA) cycle to convert nicotinamide adenine dinucleotide (NAD^+) to NADH, which is necessary for the OXPHOS pathway (**Figure 1.2**). Given these functions that each of the four compartments has, mitochondrial compartmentalization is crucial to support different functions of mitochondria.

1.1.2.2 The mitochondrial inner membrane has two unique membrane structures

The IM does not only add another layer of encapsulation; it also has unique features and functions. In comparison to the OM, the IM has a larger surface that partly folds into special structures called cristae. Therefore, the IM can be separated into two distinct subdomains: the inner boundary membrane (IBM) and the cristae membrane (CM). The IBM is the membrane area that is opposed to the OM, and the CM is the membrane area inside cristae folds. Cristae were originally thought to be simple random infoldings of the IM, but evidence has shown that they are rather internal compartments formed by invagination of the IM (Mannella 2006). Cristae junctions define the boundary between the IBM and the CM, which are morphologically distinct in their membrane structure and protein distribution (Mannella 2006, Vogel, Bornhovd et al. 2006) (**Figure 1.1B**). Cristae junctions in rat liver mitochondria have an inner diameter of 10-15 nm, which is wide enough to allow the flow of metabolites and soluble proteins, but is narrow enough to restrict diffusion rates (Mannella, Pfeiffer et al. 2001). By detecting and quantitatively measuring the amount of mitochondrial proteins in yeast mitochondria using immuno-electron microscopy (immuno-EM), Vogel et al. showed that the IBM and CM have different protein distributions (Vogel, Bornhovd et al. 2006). For instance, the majority of OXPHOS complexes localize to the CM, whereas the majority of TIM complexes localize to the IBM.

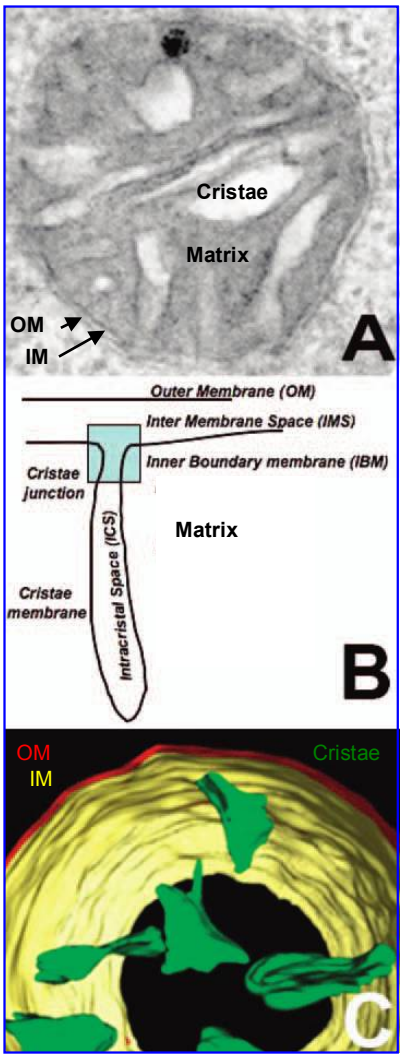

Figure 1.1. Mitochondrial organization

Mitochondria have four compartments: the outer membrane (OM), the intermembrane space (IMS), the inner membrane (IM), and the mitochondrial matrix. The IM folds into cristae, separating the IM into the inner boundary membrane (IBM) and the cristae membrane (CM). (**A**) Sectional view an electron micrograph of a mitochondrial tubule taken from HeLa cells grown in a glucose-deprived medium. (**B**) Different membrane compartments of the mitochondrial ultrastructure. (**C**) Tomographic view of the mitochondrial network. Source: Adapted from Benard and Rossignol (2008).

1.1.2.3 The mitochondrial inner membrane plays crucial roles in energy production and phospholipid synthesis

Cristae are the home to respiratory OXPHOS complexes and, therefore, the sites for ATP production. OXPHOS complexes are enriched in the CM (Vogel, Bornhovd et al. 2006). For example, by immuno-EM, 67.1% of Core1 (complex III) are found in the CM, and subunits of complex IV and complex V are also found in the CM at a similar extent. The unique membrane structure of cristae junctions results in limited gradient diffusion, kinetically controlled proton flow, and the enrichment of OXPHOS protein complexes, thereby supporting efficient ATP production (Mannella 2006). Besides ATP production, the IM is also the site for the synthesis of cardiolipin (CL, a mitochondria-specific phospholipid) and for the synthesis of phosphatidylethanolamine (PE) (Osman, Voelker et al. 2011). CL is synthesized from phosphatidic acid (PA) by a cascade of enzymes that are localized within the IM. The IM also contains a phosphatidylserine decarboxylase (PSD) enzyme that converts phosphatidylserine (PS) to PE. After their syntheses, some CL is transported to the OM, and PE is transported to the OM as well as to other cellular membranes such as the plasma membrane. In addition to their roles in serving as building blocks for membrane biogenesis, these mitochondrial-synthesized phospholipids are involved in several mitochondrial protein functions and cellular pathways. For instance, CL levels affect the assembly of β-barrel proteins in the OM (Gebert, Joshi et al. 2009), and mitochondrial-synthesized PE provides a PE pool for autophagosome biogenesis, which is necessary for the autophagic pathway (Luo, Chen et al. 2009).

1.1.2.4 Mitochondrial membrane lipids are made up of mostly phospholipids

In addition to CL and PE, which are synthesized in the IM, mitochondrial membranes contain other phospholipids: PS, PA, phosphatidylcholine (PC), and phosphatidylinositol (PI) (Osman, Voelker et al. 2011). These phospholipids make up 90% of all the lipids in the mitochondrial membrane. Although the exact composition of each of the phospholipids varies from one organism to another, PE and PC are the most abundant phospholipids in mitochondrial membranes, making up approximately 30% and 40% of all phospholipids, respectively (Zinser and Daum 1995, Osman, Voelker et al. 2011). Mitochondrial membranes usually contain 10-

15% of PI and CL, and 1-5% of PS and PA. CL distinguishes mitochondrial membranes from other intracellular membranes. The majority of CL is accumulated within the IM, where it plays a role in different mitochondrial processes, including maintaining the structural stability of OXPHOS complexes. By native gel electrophoresis, OXPHOS supercomplexes were dissociated in CL-deficient yeast cells (Pfeiffer, Gohil et al. 2003). With the unique cristae structure, the important function in ATP production, and the distinct phospholipid composition, the IM makes mitochondria different from other cellular organelles.

1.1.3 Mitochondria are more than just cellular powerhouses

Mitochondria have a multitude of important cellular functions. In addition to ATP production and lipid synthesis as described above, other important mitochondrial functions include (1) serving as a site for metabolic pathways, (2) Ca^{2+} buffering, (3) controlling apoptosis, a programmed cell death pathway, as well as Fe-S clustering and thermogenesis (Martinou and Youle 2011, Pizzo, Drago et al. 2012, Rizzuto, De Stefani et al. 2012, Tait and Green 2012, Pandey, Gordon et al. 2013) (**Figure 1.2**). Mitochondria contain enzymes in metabolic pathways for amino acids, nitrogen, lipids, nucleic acids, and metabolic intermediates. Mitochondria control Ca^{2+} buffering via voltage-dependent anion channels (VDAC) (Pizzo, Drago et al. 2012). Moreover, mitochondria regulate apoptosis by releasing signaling molecules and serving as the site for interactions and the activation of proteins in the apoptosis pathway (Martinou and Youle 2011). Mitochondria also maintain overall cell health by influencing three interconnected pathways: (1) by sensing cellular stresses, (2) by regulating quality control mechanisms, and (3) by regulating programmed cell death (Tait and Green 2012).

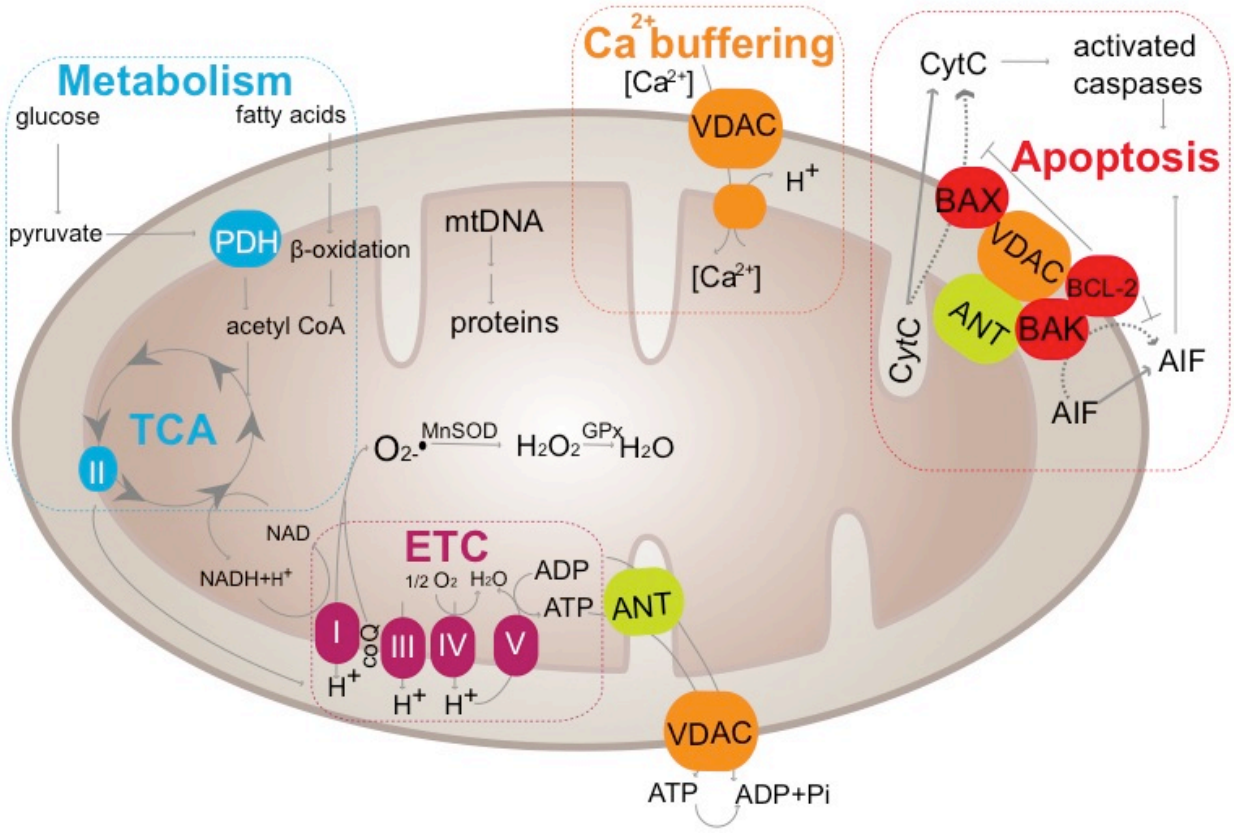

Figure 1.2. Schematic summary of mitochondrial functions

Mitochondria function in several cellular processes, from left to right: metabolism, cellular respiration via electron transport chain (ETC), calcium buffering, and the apoptosis pathway. Metabolic pathways in mitochondria include the oxidation of fatty acids and the conversion of pyruvate to acetyl CoA by pyruvate dehydrogenase (PDH) to enter the tricarboxylic acid (TCA) cycle. Transferring electrons and respiring oxygen in ETC results in ATP production. O_2^- is one of the reactive oxygen species (ROS) that are byproducts of cellular respiration. ROS are inactivated by a mitochondrial superoxide dismutase (MnSOD). The mitochondrial genome encodes subunits of the respiratory chain complexes. Adenine nucleotide translocator (ANT) and voltage-dependent anion channels (VDAC) mediate the shuttling of ATP and ADP. Calcium ion homeostasis is maintained by the function of VDAC in the outer membrane and Ca^{2+}/H^+ antiporter in the inner membrane. ANT and VDAC also function with proteins in BCL-2 family shown in red in apoptotic pathway. Pro-apoptotic members, BAK and BAX, facilitate the release of apoptosis-inducing factor (AIF) and cytochrome *c* (CytC), respectively, activating caspases to trigger apoptosis. On the other hand, anti-apoptotic members, BCL-2 and BCL-X, inhibit the release of CytC and AIF, negatively regulating apoptosis. Source: Taken from Chan, Rujiviphat et al. (2011).

1.1.3.1 Mitochondria sense cellular stresses and regulate cellular quality control mechanisms

Mitochondria sense and react to perturbations of intracellular homeostasis such as oxidative stress and nutrient deprivation, and to the invasion by extracellular materials such as viral infections. In an innate immunity response to viruses, mitochondrial antiviral-signaling protein (MAVS) localizes to the OM to function in antiviral immunity by detecting viral cytoplasmic double-stranded RNA (Seth, Sun et al. 2005). If the foreign matter is not removed, this can damage the cell. The damage can be eliminated by a cellular detoxification mechanism called autophagy. Mitochondria can influence the autophagic process by providing autophagic membranes and regulating autophagic flux (Rambold and Lippincott-Schwartz 2011). Mitochondria provide phospholipids for autophagosomal membrane formation during nutrient deprivation (Hailey, Rambold et al. 2010). An increase in reactive oxygen species (ROS) produced in mitochondria can induce autophagic flux (Scherz-Shouval, Shvets et al. 2007). Damaged mitochondria themselves are degraded by an autophagic process called mitophagy that protects the cell from cell death (Rambold and Lippincott-Schwartz 2011).

1.1.3.2 Mitochondria play a role in apoptosis

Ultimately, if the cellular defense mechanisms and autophagy induction can no longer reverse cellular damage, eukaryotic cells undergo apoptosis to prevent the spread of foreign materials to other cells. Mitochondria directly play a role in apoptosis by serving as the sites for protein-protein interactions of the B cell CLL/lymphoma-2 (BCL-2) family proteins and regulating the release of the pro-apoptotic molecule cytochrome *c,* which activates downstream cascades. Pro-apoptotic stimuli such as DNA damage can activate two key BCL-2 family proteins, BAK and BAX, that interact on the OM and cause the permeabilization of the OM (Tait and Green 2012). Upon membrane permeabilization, cytochrome *c* is released from the IMS through the OM to the cytosol to activate different caspases. Caspases are the proteases that cleave proteins and activate enzymes that cleave nucleic acids, leading to rapid apoptotic cell death (Taylor, Cullen et al. 2008). Cells deficient in both BAX and BAK are resistant to an induced cytochrome *c* release and apoptosis (Wei, Zong et al. 2001). Given the crucial roles that mitochondria play in the maintenance of cell health, it is important to understand the cell biology of mitochondria.

1.2 MITOCHONDRIA ARE DYNAMIC IN NATURE TO MAINTAIN VARIOUS MORPHOLOGIES AND FUNCTIONS

In different cell types, mitochondria adopt different localizations and morphologies that may associate their functions with specific cellular demands (Kuznetsov, Hermann et al. 2009) (**Figure 1.3**). For instance, in cardiomyocytes, mitochondria cluster around nuclei. This perinuclear localization may be crucial for supplying more ATP to the nucleus to support nuclear import. In elongated cells like neurons, mitochondria have elongated morphologies, and it is very important that they are localized to cell extremities to ensure ATP production and distribution to all parts of the cell (Lovas and Wang 2013). To ensure proper localization and maintain proper morphology, mitochondria move along the cytoskeleton and constantly fuse and divide.

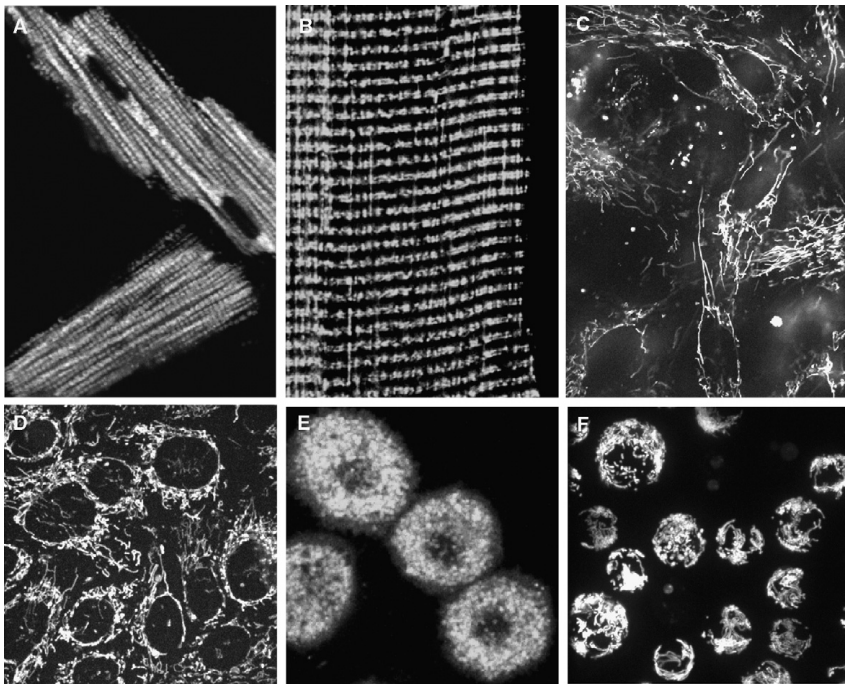

Figure 1.3. Mitochondrial morphology

Mitochondrial morphology differs in various cell types. Confocal fluorescence live microscopy images show various mitochondrial morphologies: regular arrangement of mitochondria in (**A**) adult rat cardiomyocytes and (**B**) skeletal muscles from rat *M. soleus*, long mitochondrial threads in (**C**) human pancreatic cells, and mitochondrial network in (**D**) in HL-1 cells with cardiac phenotype. (**E**) Mitochondrial arrangement in isolated rat liver cells (hepatocytes) and (**F**) in small promyeloid cells. Mitochondria were visualized in living primary or cultured cells by means of fluorescence confocal imaging using mitochondria-specific fluorescent probes TMRM or MitoTracker (A, B, C, D, and F) or autofluorescence of mitochondrial flavoproteins (E). Source: Taken from Kuznetsov, Hermann et al. (2009).

In addition to organellar morphology, dynamic changes in morphology are also observed in the ultrastructural organization of mitochondria. Mitochondria are described to be in either the condensed or orthodox morphologic state (Mannella, Pfeiffer et al. 2001). In the condensed state, mitochondria are very dense and have a contracted matrix compartment with wide cristae. On the other hand, in the orthodox state, mitochondria are less dense. Cristae are more widened, tubular, or flattened. The changes from the condensed to orthodox state are observed during respiration and can be induced by changing the osmotic pressure. These morphological changes were detected by dynamic light scattering and observed in three dimensions by electron tomography (Mannella 2008). To mediate morphological changes in response to osmotic and

metabolic changes, the IM has to undergo membrane remodeling as well as fusion and fission events. Therefore, these findings suggest that the cellular energetic state and the organellar environment regulate the ultrastructural membrane morphology and the dynamics of mitochondria.

1.2.1 Mitochondria are dynamic organelles that constantly undergo fusion and fission

The first direct evidence of mitochondrial fusion and fission was observed in the budding yeast *Saccharomyces cerevisiae* using three-dimensional wide-field fluorescence microscopy (Nunnari, Marshall et al. 1997). Mitochondria were observed as continuous dynamic reticular organelles giving rise to the term mitochondrial network. From the time-lapse fluorescence images, the reticular structure was speculated to be dependent on mitochondrial fusion and fission events (Nunnari, Marshall et al. 1997) (**Figure 1.4**). The authors also showed that these mitochondrial fusion and fission events are crucial for mitochondrial inheritance, since mitochondrial fusion was directly observed during yeast mating. Subsequent advancements in imaging techniques have provided more detailed understanding of mitochondrial dynamics. Mitochondrial plasticity was observed from three-dimensional mitochondrial structures that were reconstructed from a series of electron tomographs (Perkins, Sun et al. 2009). A single set of mitochondria can be tracked using photo-activatable green fluorescent protein (PA-GFP) (Patterson and Lippincott-Schwartz 2002). Super-resolution fluorescence microscopy allows for the monitoring of the mitochondrial structures and the detecting of protein machineries in live cells at 40 nm resolution, at which point it is possible to resolve most protein complexes (Shim, Xia et al. 2012). While imaging approaches have elucidated the structure and morphology of the mitochondrial network, genetic approaches have revealed the protein machineries that mediate mitochondrial dynamics.

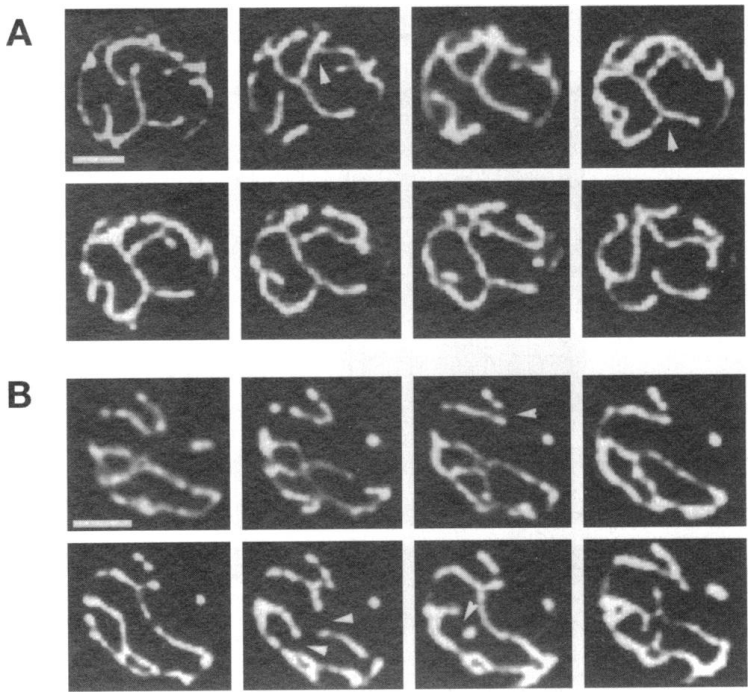

Figure 1.4. Mitochondrial dynamics

Mitochondria constantly fuse and divide. Time-resolved images from a single optical section of 0.2 μm. Time increases from left to right in 3-minute increments. Representative fusion events are indicated by *arrowheads* in (**A**), and representative fission events are indicated by *arrowheads* in (**B**). *Scale bars* represent 1 μm. Source: Taken from Nunnari, Marshall et al. (1997).

1.2.2 Genetic screens in *S. cerevisiae* have identified molecular machineries in mitochondrial dynamics

Mitochondrial dynamics are not only crucial for the maintenance of mitochondrial morphology and inheritance; they are also important for the maintenance of the mitochondrial genome and regulating quality control mechanisms (Chan 2012). Genetic tools and model organisms have been used to elucidate essential genes that regulate mitochondrial dynamics and to understand the roles of mitochondrial dynamics in mitochondrial morphology, mitochondrial functions, and cell development. Since the first direct observation of mitochondrial dynamics, the budding yeast *S. cerevisiae* has been an important model organism due to the availability of genomic information and genetic techniques (McConnell, Stewart et al. 1990, Jones and Fangman 1992, Burgess, Delannoy et al. 1994, Hermann, King et al. 1997, Dimmer, Fritz et al. 2002). *S.*

cerevisiae is one of the most commonly used yeast species in biological studies, and it is one of the first eukaryotes to have had its genome sequenced. Moreover, *S. cerevisiae* is particularly suitable to study mitochondrial morphology because aberrant mitochondrial morphologies can be clearly distinguished from the normal reticular morphology. Yeast that are defective in mitochondrial fusion have fragmented mitochondria, while yeast that are defective in mitochondrial fission have an elongated and interconnected net-like mitochondrial network. Therefore, mitochondrial morphologies are usually categorized as being reticular, fragmented, aggregated, or elongated (**Figure 1.5**). Several mitochondrial dynamics-related genes were first identified in the budding yeast *S. cerevisiae.*

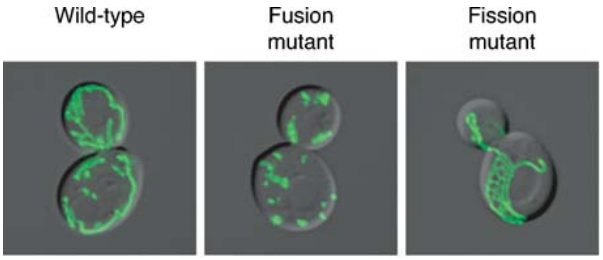

Figure 1.5. Mitochondrial morphology in *Saccharomyces cerevisiae*

Wild-type yeast have reticular mitochondria (*left panel*). Mutant yeast defective in mitochondrial fusion (*fzo1Δ*) have fragmented and aggregated mitochondria (*middle panel*). Mutant cells defective in mitochondrial fission (*dnm1Δ*) have elongated net-like mitochondria (*right panel*). Mitochondria were visualized by a matrix-targeted GFP. Differential interference contrast (DIC) and GFP fluorescence images were superimposed for each cell. Source: Adapted from Okamoto and Shaw (2005).

1.2.2.1 Temperature sensitive screens identified *DNM1* and *MGM1*

One of the genetic approaches that is commonly used to reveal important genes and pathways is the screen for temperature sensitive mutants. To do this, yeast are randomly mutated by a DNA damaging agent, and thousands of mutated strains are grown at a permissive temperature and shifted to a non-permissive temperature. Temperature sensitive strains have mutations that cause a protein to become non-functional at the non-permissive temperature but functional at the permissive temperature because the rise in temperature quickly ablates protein function (Tan,

Chen et al. 2009). To identify genes that are essential for the maintenance of mitochondrial morphology, mutated yeast were stained with mitochondria-specific probes to observe their mitochondrial morphology (McConnell, Stewart et al. 1990, Burgess, Delannoy et al. 1994, Hermann, King et al. 1997). A temperature sensitive mutant would have normal morphology at the permissive temperature but disrupted morphology at the non-permissive temperature. A temperature sensitive screen was performed to identify genes that are involved in mitochondrial inheritance into daughter cells (McConnell, Stewart et al. 1990). These genes were identified as being important for mitochondrial distribution and morphology (MDM). For example, Mdm29 was one of the identified gene products that was later called Dnm1 and characterized as a mitochondrial fission protein (Bleazard, McCaffery et al. 1999). Dnm1 was first identified from molecular and genetic mapping to have sequence homology to human dynamin-1 (Gammie, Kurihara et al. 1995). Dnm1 was shown to play a role in endosomal trafficking in yeast and later shown to regulate mitochondrial morphology (Gammie, Kurihara et al. 1995, Sesaki and Jensen 1999). *DNM1* knockout yeast has an interconnected net-like mitochondrial network, suggesting that Dnm1 plays a role in mitochondrial fission (Otsuga, Keegan et al. 1998, Sesaki and Jensen 1999).

Other screens that did not specifically look for genes involving in mitochondrial morphology also contributed to the discovery of important players in mitochondrial dynamics. Jones and Fangman screened for nuclear genes that are involved in mitochondrial genome maintenance (MGM) (1992). In this screen, mutants that have cellular respiratory defects and loss of mtDNA were selected. An adenine-requiring strain (*ade1 ade2* strain, BS127) was used to select for respiratory defective mutants. BS127 strain forms red colonies if it respires but white colonies if it cannot respire. BS127 was mutagenized by ethylmethanesulfonate, and mutated strains that formed white colonies were selected and were subsequently confirmed that they were respiratory deficient. 4',6-diamidino-2-phenylindole (DAPI) was used to stain for mtDNA to select for mutants that had lost mtDNA. Mitochondrial genome maintenance 1 (*MGM1*) was identified from this screen and subsequently shown to function to maintain mitochondrial morphology and to directly mediate fusion of the IM (Guan, Farh et al. 1993, Wong, Wagner et al. 2000, Wong, Wagner et al. 2003) (see section **1.4**).

1.2.2.2 Genome-wide gene deletion screens identify several *MDM* genes

Since *S. cerevisiae* is a facultative anaerobic yeast that does not require mitochondrial ATP, very few mitochondrial proteins are essential for cell viability under normal growth conditions. Therefore, systematic genome-wide screening of a yeast deletion mutant library is useful for identifying non-essential genes that are involved in the maintenance of mitochondrial morphology. Dimmer et al. screened a collection of 4,794 yeast gene deletion strains to identify mutant yeasts that had aberrant mitochondrial morphology (Dimmer, Fritz et al. 2002). The mitochondria of knockout strains were labeled with a mitochondria-specific probe and the authors determined whether the knockout strains had abnormal mitochondrial morphology by fluorescence microscopy. *mdm* mutants were categorized into three classes based on their phenotypes. Class I mutants have mutations that disrupt mitochondrial morphology; Class II mutants have abnormal mitochondrial morphology only under certain conditions; Class III mutants have abnormal mitochondrial morphology and are defective in cellular respiration. This screen identified eight genes from the Class I mutants that are known to maintain mitochondrial morphology and 10 unknown genes that were thought to play a role in mitochondrial morphology. The list of uncharacterized genes includes *MDM30*, *MDM33*, *MDM36*, and *NUM1* that were later confirmed to have direct functions in the maintenance of mitochondrial morphology (see section **1.2.4.2** and **1.2.5.2**).

1.2.2.3 Genome-wide gene deletion screens identified mitochondrial fusion genes *UGO1* and *RBD1*

Since the first proposal in 1997 that mitochondrial dynamics require a balance in mitochondrial fusion and fission events, the concept of mitochondrial fission as an antagonistic process to mitochondrial fusion has been employed to develop a screen to identify genes involved in mitochondrial fusion (Sesaki and Jensen 2001). Yeast Fzo1, which was first identified in flies (see section **1.2.3.1**), was shown to work antagonistically with the mitochondrial pro-fission protein Dnm1 to maintain mitochondrial morphology and dynamics by acting as a mitochondrial pro-fusion molecule (Hales and Fuller 1997, Hermann, Thatcher et al. 1998, Bleazard, McCaffery et al. 1999, Sesaki and Jensen 1999). Double mutations of *DNM1* and *FZO1* restore normal tubular mitochondrial morphology, confirming the hypothesis that mitochondrial

dynamics require a balance in mitochondrial fusion and fission (Sesaki and Jensen 1999). Furthermore, the loss of mtDNA phenotype observed in an *fzo1* mutant can be suppressed by inactivating Dnm1 function to maintain the dynamic balance. This idea of rescuing phenotypes by restoring the balance of mitochondrial fusion and fission was used to screen for genes involved in mitochondrial fusion (Sesaki and Jensen 2001). Using this approach, Ugo1 (Ugo means fusion in Japanese) was revealed as the third key component in mitochondrial fusion machinery. Ugo1 was later shown to potentially play a role in the lipid-mixing step of the mitochondrial fusion process (see section **1.2.5**).

Another mutant *ugo2* was shown to be defective in *PCP1* (processing of cytochrome *c* peroxidase 1) gene (Sesaki, Southard et al. 2003). Pcp1 was first identified as a transmembrane protein that contains a mitochondrial targeting sequence (MTS) and a rhomboid motif (Esser, Tursun et al. 2002). Pcp1 is also called Rbd1 (Rhomboid 1). McQuibban et al. identified cytochrome *c* peroxidase 1 (Ccp1) and Mgm1 as two substrates of Rbd1 (McQuibban, Saurya et al. 2003). *rbd1Δ* has fragmented mitochondria and lacks mtDNA similar to the phenotypes of *mgm1Δ*, suggesting that Rbd1 may have a role in the maintenance of mitochondrial morphology. Rbd1/Pcp1 belongs to the highly conserved rhomboid serine protease family and directly functions in the processing of Mgm1, which in turn regulates mitochondrial morphology (Herlan, Vogel et al. 2003, McQuibban, Saurya et al. 2003) (see section **1.2.5.3**). *rbd1Δ* phenotypes and s-Mgm1 processing were rescued by expressing wild-type Rbd1 but not a catalytically dead Rbd1 mutant, confirming that the proteolytic activity of Rbd1/Pcp1 is essential for its function.

1.2.2.4 Prohibitins were identified in yeast screens as a regulator of mitochondrial phospholipid homeostasis and Mgm1 processing

In addition to temperature sensitive screens and gene deletion screens, yeast multi-copy suppressor screens have been conducted to identify genes involving in mitochondrial dynamics. A multi-copy suppressor screen of *MDM12* identified *PHB2,* which belongs to a highly conserved family of prohibitins (Berger and Yaffe 1998). Mdm12 was thought to localize to OM and play a role in mitochondrial distribution by interacting with cytoskeletal elements. Mitochondria in *mdm12Δ* cells collapse into large giant mitochondria that cannot be inherited

into daughter cells. This abnormal morphology is suppressed by the overexpression of *PHB2*. Mitochondria in *mdm12Δ* cells that overexpress *PHB2* are smaller and can be distributed to the daughter cells, suggesting that the function of *PHB2* can bypass the requirement of *MDM12* in the maintenance of mitochondrial morphology and inheritance in *S. cerevisiae.* Phb1 is another yeast prohibitin that also localizes to mitochondria and is likely to function together with Phb2. The double deletion of *PHB1* and *PHB2* yeast is respiratory deficient. Moreover, double mutations in *PHB1* or *PHB2* with other *MDM* genes, *MDM12* and *MDM10,* are synthetically lethal, suggesting that *PHB1* and *PHB2* genetically interact with *MDM* genes (Berger and Yaffe 1998). Synthetic lethality arises when a combination of mutations in two or more genes leads to cell death; while cells are viable if there are mutations in only one of the genes (Tucker and Fields 2003). Assuming that at least two genes are required in a cellular process, either working in two parallel pathways or in the same pathway, the deletion of two genes that work in the same pathway will not worsen the phenotypes. On the other hand, if two genes work in two parallel pathways, the reducing the expression of both genes will worsen the phenotype. The synthetic genetic array is widely used to identify genome-wide genetic interactions (Baryshnikova, Costanzo et al. 2010). The interactome of prohibitins provides insights into the function of prohibitins in yeast by identifying genes that regulate the level of lipids and affect the processing of Mgm1. These findings suggest a crucial role for prohibitins in phospholipid homeostasis that may be linked to the regulation of Mgm1 processing and the maintenance of mitochondrial morphology (Osman, Haag et al. 2009). Prohibitin may play a role in maintenance of PE and CL levels that affect s-Mgm1 processing and, thereby, mitochondrial fusion (Chan and McQuibban 2012).

1.2.3 Studies in multicellular organisms have revealed the cellular and physiological roles of mitochondrial dynamics

In addition to genetic studies in yeast, studies in fruit flies, worms, cultured cells, and mouse models have led to important discoveries in mitochondrial dynamics. The first mitochondrial fusion protein and the importance of mitochondrial fusion in cell development were shown in the fruit fly *Drosophila melanogaster* (Hales and Fuller 1997). A study in the roundworm *Caenorhabditis elegans* demonstrated the relationship between the maintenance of mitochondrial function and morphology (Ichishita, Tanaka et al. 2008). Human genes involved in

mitochondrial dynamics have been largely characterized using tissue culture systems (Chan 2012). Mouse models have been used to study disease-related genes and to understand the pathophysiological role of mitochondrial dynamics in neurodegenerative diseases (Davies, Hollins et al. 2007).

1.2.3.1 Fzo is the first mitochondrial fusion protein identified in *Drosophila*

Drosophila is a widely used model organism for genetic studies. A study in *Drosophila* identified the main protein that mediates mitochondrial fusion: *fuzzy onions* (*fzo)* (Hales and Fuller 1997). During *Drosophila* spermatogenesis, mitochondria aggregate, fuse, and elongate to form an onion-like structure called the Nebenkern that results from two giant mitochondria wrapping around each other. In male *fzo* mutated *Drosophila*, in the early post-meiotic spermatids, mitochondria fail to fuse, resulting in misshaped Nebenkern structures that contain multiple smaller mitochondria instead of two giant onion-like mitochondria (Hales and Fuller 1997). This finding indicates the important role that mitochondrial fusion plays during cell development and identifies *fzo* as a gene responsible for mitochondrial fusion process.

1.2.3.2 Proper mitochondrial morphology is required for the maintenance of mitochondrial function in *Caenorhabditis elegans*

RNA interference (RNAi) is a genetic manipulation approach commonly used in *C. elegans* to silence specific genes. An RNAi screen in *C.elegans* was conducted to identify mitochondrial proteins that are required for the maintenance of mitochondrial morphology (Ichishita, Tanaka et al. 2008). To silence genes, worms were fed with *E.coli* cells expressing dsRNAs targeting different genes. These worms also expressed a fluorescently tagged OM protein, allowing for the examination of mitochondria in the worms' body-wall muscles. Out of 719 genes encoding for mitochondrial proteins, 80% were identified to be required genes for the maintenance of proper mitochondrial morphology. Mutations in most of these identified genes cause mitochondrial fragmentation, and the other mutant strains have elongated mitochondria. Most of

these genes function in metabolism and cellular respiration, suggesting a relationship between the maintenance of mitochondrial function and morphology.

1.2.3.3 Tissue culture experiments demonstrated the function of human DRP1

Cultured mammalian cells have been used to investigate the function of human genes. Similarly to the RNAi approach in worms, various gene interference approaches are used in cultured mammalian cells to investigate gene functions. For example, HeLa cells treated with DRP1 targeted RNAi have reduced DRP1 protein level and elongated mitochondria (Lee, Jeong et al. 2004). Elongated mitochondrial morphology resulted from ongoing mitochondrial fusion in the absence of mitochondrial fission, suggesting a role for DRP1 in mitochondrial fission. Inhibiting DRP1 by expressing the dominant negative mutant of DRP1 K38A also resulted in elongated morphology of mitochondria (Smirnova, Griparic et al. 2001). Similar approaches have been used to investigate the function of human genes that are involved in mitochondrial fusion and fission (Chan 2012).

1.2.3.4 Mouse models revealed physiological roles of mitochondrial dynamics

Mouse models have been used to study the role of mitochondrial dynamics in cell development and in the pathophysiology of related diseases. Mitofusin 1 and 2 (MFN1 and MFN2) were first discovered in 2001 and identified as homologues of Fzo1 from a mouse cDNA library (Santel and Fuller 2001, Chen, Detmer et al. 2003). MFN1 and MFN2 have 81% similarity to each other, and both MFN1 and MFN2 have 52% similarity to *Drosophila* Fzo. Consistently, both mitofusins were shown to play a role in mitochondrial fusion (Chen and Chan 2005). MFN-deficient mouse embryonic fibroblast cells have altered mitochondrial morphology and disrupted mitochondrial dynamics. Both *MFN1* and *MFN2* knockout mice show embryonic lethality in homozygous mutants, suggesting that MFN1 and MFN2 are crucial for mitochondrial fusion during embryogenesis (Chen, Detmer et al. 2003). Mutations in MFN2 cause a neurodegenerative disease called Charcot-Marie-Tooth neuropathy type 2A, suggesting a

pathophysiological link between mitochondrial dynamics and neurodegenerative diseases (Zuchner, Mersiyanova et al. 2004).

Optic atrophy 1 (OPA1) is the human homologue of Mgm1 (Delettre, Lenaers et al. 2000). OPA1 was given its name because several mutations found in dominant optic atrophy type Kjer, which is an autosomal dominant eye disease, are mapped to the *OPA1* gene region (Eiberg, Kjer et al. 1994). Homozygous *Opa1* null mice show early embryonic lethality, and heterozygous *Opa1* mice are viable but their inter-crosses give no live progeny of $Opa1^{-/-}$ (Davies, Hollins et al. 2007). Similar to studies on mitofusin, these findings indicate the requirement of mitochondrial dynamics during cell development. Moreover, OPA1 is crucial for neuronal cell health and plays a direct role in mitochondrial fusion (Chan 2012). Heterozygous *Opa1* mice displayed fragmented mitochondria, abnormal optic nerve anomalies in myelination and structure, and impaired visual functions.

Another neurodegenerative disease that could have a direct link to the maintenance of mitochondrial dynamics is Parkinson's disease (PD). Presenilin-associated rhomboid-like protein (PARL) is the human homologue of Rbd1, and its mutations have been linked to PD, further emphasizing the pathophysiological role of mitochondrial dynamics (Shi, Lee et al. 2011). A mutation from serine to alanine at amino acid position 77 was found in the PD population at a 1 in 1291 frequency, and this mutation impairs the ability of PARL to cause mitochondrial fragmentation. *PARL* knockout mice have been used as a model for investigating the disease mechanisms of PD and have revealed the role of OPA1 in apoptotic pathways and in cytochrome *c* release (Sanjuan Szklarz and Scorrano 2012). Heat shock induces PARL-dependent accumulation of soluble OPA1 that upregulates apoptosis via cytochrome *c* release and, upon thermal stress, mitochondria become fragmented due to OPA1 cleavage. This disrupted mitochondrial dynamics could lead to mitochondria dysfunction and unregulated apoptosis, which could be an underlying cause of neurodegenerative diseases such as Parkinson's disease.

Together, the genetic studies in higher eukaryotic model organisms have elucidated the role of mitochondrial dynamics in cellular functions, implicating the role of mitochondrial dynamics in neurodegenerative diseases.

1.2.4 Mitochondrial fission relies on a sole mechanoenzyme with multiple levels of regulation

As described above, Dnm1/DRP1 (yeast/human homologue) is a crucial protein for mitochondrial fission. Dnm1/DRP1 is a key mechanoenzyme that mediates mitochondrial fission. Structural characterizations have revealed the mechanistic action of Dnm1/DRP1: it polymerizes around mitochondria and undergoes a GTP cycle to cause mitochondrial membrane scission (see section **1.3.3**). Subsequent findings have identified other components in the mitochondrial fission machinery that have regulatory roles rather than mechanistic roles (Otera, Ishihara et al. 2013). Mitochondrial fission is regulated by multiple pathways as described below.

1.2.4.1 Dnm1/DRP1 membrane recruitment regulates mitochondrial fission

Mitochondrial fission is regulated by controlling the Dnm1/DRP1 recruitment to mitochondria. Three different pathways have been shown to recruit Dnm1 to the OM in yeast (Otera, Ishihara et al. 2013) (**Figure 1.6**). Dnm1 exists as puncta in the cytosol and at the mitochondria. Fis1 is an integral membrane protein that recruits Dnm1. The localization of Dnm1 to mitochondria is reduced in the absence of Fis1. The crystal structures of Fis1 cytosolic domain show a concave surface and an extended domain called the Fis1 arm that allows for the binding to Dnm1 and consequently promotes mitochondrial fission (Wells, Picton et al. 2007, Tooley, Khangulov et al. 2011). Fis1 is conserved from yeast to human (Dohm, Lee et al. 2004). However, the role of human Fis1 (hFis1) in DRP1 recruitment is still unclear. Overexpression of hFis1 results in mitochondrial fragmentation and perinuclear clustering, which are phenotypes similar to that of DRP1 overexpression (Otera, Wang et al. 2010). However, DRP1 recruitment to the OM is not affected by the reduction in the expression level of hFis1 (Otera, Wang et al. 2010). DRP1 recruitment is dependent on the mitochondrial fission factor (Mff), and the mitochondrial dynamics proteins of 49 and 51 kDa (MiD49 and MiD51) were found to directly recruit DRP1 (Otera, Wang et al. 2010, Palmer, Osellame et al. 2011). The reduced expression of Mff causes DRP1 to be released from the OM, while the overexpression of Mff stimulates DRP1 recruitment and mitochondrial fission (Otera, Wang et al. 2010). MiD49/51 is a newly identified protein

complex that forms rings around mitochondria, which is similar to DRP1 rings (Palmer, Osellame et al. 2011). Interfered MiD49/51 expression reduces DRP1 recruitment to the OM and consequently reduces the rate of mitochondrial fission, suggesting the direct of role of MiD49/51 in recruiting DRP1, which in turn regulates mitochondrial fission (Palmer, Osellame et al. 2011). To clarify the role of these possible Drp1 adaptors, a recent study examined mouse embryonic fibroblast cell lines with null alleles of Fis1, Mff, MiD49 or MiD51 (Loson, Song et al. 2013). The authors showed that both Fis1 and Mff are important for mitochondrial fission, while Mff plays a larger role. MiD49 and MiD51 can also recruit Drp1 but in Fis1 and Mff independent manner. This finding is consistent with another recent study (Palmer, Elgass et al. 2013), supporting the notion that there are multiple pathways to recruit Drp1 to the OM. There is no known yeast homologue of Mff, MiD49, and MiD51. This further supports the notion that even though the mitochondrial fission mechanoenzyme Dnm1/DRP1 is conserved from yeast to human, its membrane recruitment pathways evolved diversely.

1.2.4.2 Mitochondrial fission is regulated by protein localization and post-translational modifications

In addition to the regulation at the membrane recruitment step, other molecules affecting protein localization and post-translational modification pathways are involved in mitochondrial fission. Num1 and Mdm36 are multi-copy suppressors of the dominant-negative mutant of Dnm1 (Dimmer, Fritz et al. 2002). Num1 was shown to play a role in mitochondrial division and inheritance, and Num1 co-localizes with Dnm1 at the cell cortex (Cerveny, Studer et al. 2007). This cortical localization of the Num1/Dnm1 complex is maintained by Mdm36 (Hammermeister, Schodel et al. 2010). Altering DRP1 levels by overexpressing wild-type DRP1 does not alter mitochondrial morphology, suggesting that the rate of mitochondrial fission is not dependent on the protein level of DRP1, but rather could be due to the level of DRP1 activity (Smirnova, Shurland et al. 1998). DRP1 activity and consequently the rate of mitochondrial fission are regulated by post-translational modifications. To date, mitochondrial fission is known to be regulated by phosphorylation, s-nitrosylation, SUMOylation, ubiquitylation, and O-GlucNAcylation (Otera, Ishihara et al. 2013). Moreover, differential expression of dynamin-like protein variants suggests that Drp1 splicing is another possible mode of Drp1 regulation (Kamimoto, Nagai et al. 1998, Chen, Howng et al. 2000). These multiple regulatory pathways of

mitochondrial fission further emphasize the importance of maintaining a delicate balance in mitochondrial dynamics.

1.2.5 Mitochondrial fusion requires two separable membrane fusion events and machineries

The mitochondrial fusion event is distinct from other intracellular membrane fusion events because it requires the fusion of two separate membranes. The fusion of the OM and IM are two separable events that are mechanistically distinct, but both events require guanosine 5′-triphosphate (GTP) and are tightly coordinated (Meeusen, McCaffery et al. 2004).

1.2.5.1 Fzo1/MFN mediates OM fusion while Mgm1/OPA1 mediates IM fusion

In yeast, Fzo1 and Mgm1 mediate OM and IM fusion, respectively, while Ugo1 may be a protein that coordinates the two membrane fusion events (Meeusen, McCaffery et al. 2004, Sesaki and Jensen 2004, Meeusen, DeVay et al. 2006) (**Figure 1.6**). Meeusen et al. developed an *in vitro* cytological mitochondrial fusion assay that revealed different mitochondrial fusion intermediates and stages of mitochondrial fusion, suggesting that OM and IM fusion are separable events (Meeusen, McCaffery et al. 2004). In this assay, mitochondria containing matrix-targeted green fluorescent protein (m-GFP) are mixed with mitochondria containing matrix-targeted Discosoma red fluorescent protein (m-dsRed) in the presence of cytosolic extract, ATP, GTP, and an energy regeneration system. Mitochondrial fusion is assessed by the co-localization of m-GFP and m-dsRed, which indicates content mixing upon fusion. Tethered mitochondrial intermediates suggest a deficiency in OM fusion. OM fusion requires GTP and Fzo1 *trans* interactions on opposing mitochondria. Electron microscopy images show mitochondrial fusion intermediates that have OM encapsulating two separate opposing IMs, suggesting impaired IM fusion. IM fusion requires higher GTP concentration and functional Mgm1 (Meeusen, DeVay et al. 2006). Ugo1 is a multispan transmembrane OM protein that is crucial for both OM and IM fusion events (Sesaki and Jensen 2004, Coonrod, Karren et al. 2007, Hoppins, Horner et al. 2009). Ugo1 forms a complex with Fzo1 and Mgm1, and their tight interactions were shown by co-

immunoprecipitation experiments (Sesaki and Jensen 2004). Using the *in vitro* fusion assay described above, it was found that Ugo1 is essential for both OM and IM fusion, suggesting that Ugo1 functions at the lipid-mixing step (Hoppins, Horner et al. 2009). Lipid mixing is crucial at the final step of a membrane fusion event to mix the lipids of the two bilayers into a single bilayer. In humans, MFNs and OPA1, which are the human homologues of Fzo1 and Mgm1, also mediate fusion of the OM and IM, respectively. However, there is no known human homologue of Ugo1. Although the key proteins that function in mitochondrial fusion have been identified, the molecular mechanism of mitochondrial fusion is still unclear due to the lack of detailed structural information. Therefore, obtaining structural information to understand the molecular mechanism of mitochondrial fusion is a focus of this thesis work.

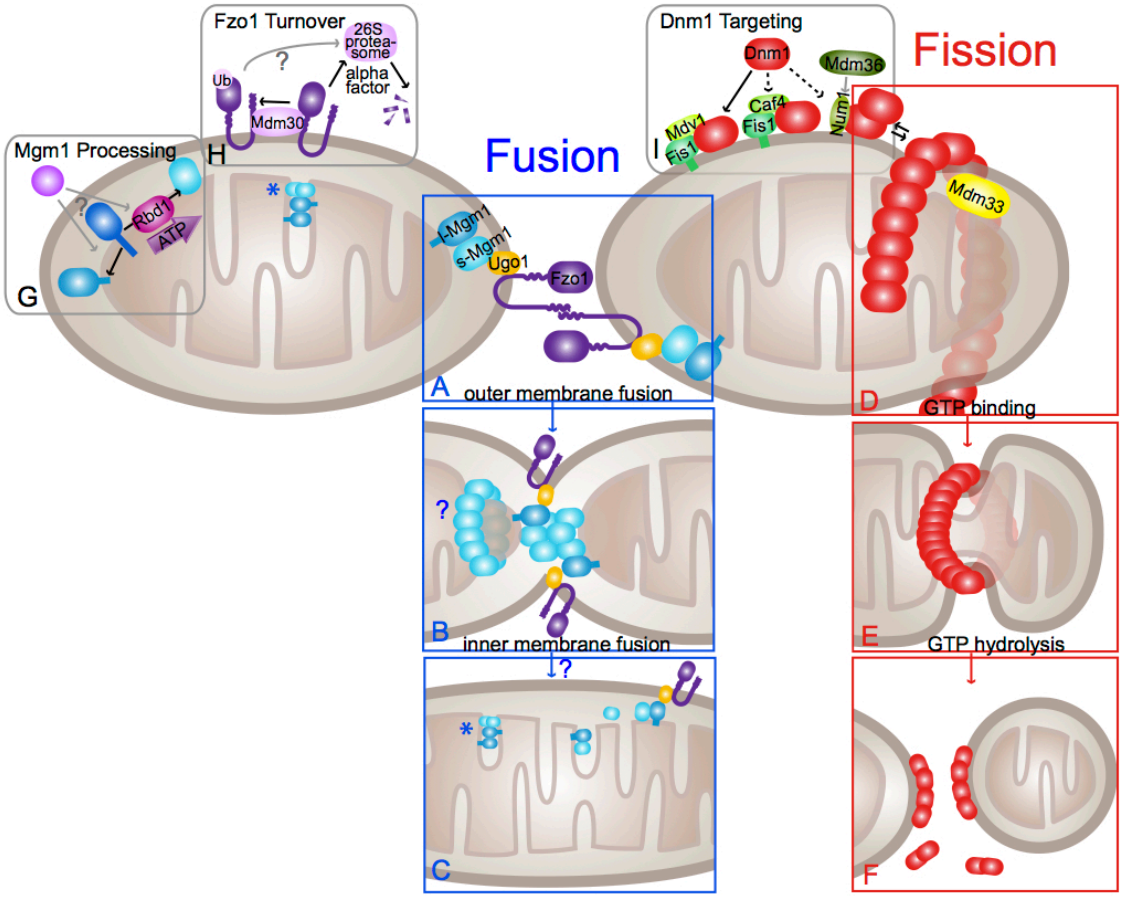

Figure 1.6. Mechanistic models of yeast mitochondrial fusion and fission

The diagram illustrates proposed models of mitochondrial dynamics and mechanisms of actions by the key players. Blue boxes, **A** to **C**, show sequential steps of mitochondrial fusion whereas Red boxes, **D** to **F**, present the proposed mitochondrial fission event. Grey boxes, **G** to **I**, show the currently known regulatory pathways in mitochondrial fusion and fission. See text for details. Source: Taken from Chan, Rujiviphat et al. (2011).

1.2.5.2 Ubiquitylation regulates Fzo1/MFN function in OM fusion

In addition to the three core protein machineries, accessory proteins also regulate mitochondrial fusion events via (1) ubiquitylation, (2) proteolytic processing, and (3) lipid metabolism. Proper mitochondrial morphology requires the maintenance of adequate Fzo1 protein levels that are regulated via ubiquitin-proteasome-dependent degradation (Cohen, Leboucher et al. 2008). In a cyclohexamide chase experiment where protein synthesis is inhibited and steady states of

proteins can be monitored over time, Fzo1 is quickly turned over within three hours (Cohen, Leboucher et al. 2008). This Fzo1 degradation is also dependent on functional proteasomes (Cohen, Leboucher et al. 2008). Fzo1 degradation is slower in a proteasome mutant strain and is completely inhibited in another proteasome mutant strain. This degradation is also dependent on an F-box family protein Mdm30, which is a substrate recognition component of a Skp1-Cullin-F-box family ubiquitin ligase. Mdm30 ubiquitylates Fzo1 and targets Fzo1 for proteasome-dependent degradation. Fzo1 proteasome-dependent degradation can also be triggered by alpha-factor pheromone, suggesting that there are multiple pathways that Fzo1 protein levels are regulated (Escobar-Henriques, Westermann et al. 2006). Similarly, human MFN1 and MFN2 are ubiquitylated by the ubiquitin ligase Parkin and degraded by proteasomes (Ziviani, Tao et al. 2010, Glauser, Sonnay et al. 2011, Chen and Dorn 2013). Overexpressing Parkin promotes the ubiquitylation of MFN1, and proteasome inhibition by MG132 causes an accumulation of ubiquitylated MFN1 (Glauser, Sonnay et al. 2011). Phosphorylated MFN2 serves as a site for Parkin recruitment to mitochondria and is ubiquitylated by Parkin (Ziviani, Tao et al. 2010, Chen and Dorn 2013).

1.2.5.3 Proteolytic processing regulates Mgm1/OPA1 function in IM fusion

Proteolytic processing of Mgm1/OPA1 regulates the level of different isoforms of Mgm1/OPA1, which in turn regulates mitochondrial fusion. Precursor Mgm1 is processed into the long isoform l-Mgm1 by the mitochondrial processing peptidase (MPP) and the short isoform s-Mgm1 by the rhomboid family serine protease Rbd1/Pcp1, as mentioned above (see section **1.4.3**) (Herlan, Bornhovd et al. 2004). Unprocessed 1 (Ups1) is an IMS protein that is shown to regulate the proteolytic processing of s-Mgm1 (Sesaki, Dunn et al. 2006). The deletion in *UPS1* gene abolishes s-Mgm1 formation. PARL, which is the human homologue of Rbd1, proteolytically processes OPA1 into a short isoform of OPA1 (Sanjuan Szklarz and Scorrano 2012). The deletion in *PARL* gene abolishes the accumulation of this short isoform of OPA1. Since these proteolytic events produce Mgm1/OPA1 isoforms that are essential for the fusion function, these proteolytic events in turn activate mitochondrial fusion. Conversely, proteolysis could also inactivate mitochondrial fusion. The ATP-independent metalloprotease OMA1 plays a role in the proteolytic inactivation of OPA1 (Quiros, Ramsay et al. 2012) and OMA1-

dependent processing of OPA1 has also been reported by other groups (Ehses, Raschke et al. 2009, Head, Griparic et al. 2009). Therefore, proteolytic events regulate mitochondrial fusion by regulating the processing of Mgm1/OPA1 isoforms.

1.2.5.4 Phospholipid homeostasis plays a role in regulating both OM and IM fusion events

In addition to regulating mitochondrial fusion by altering protein levels, altering mitochondrial membrane lipid composition and metabolism may affect mitochondrial fusion. Lipid metabolism has been shown to regulate mitochondrial fusion (Furt and Moreau 2009). mitoPLD, which is the enzyme that converts CL into PA, is a pro-fusion molecule (Choi, Huang et al. 2006). The reduced expression of mitoPLD causes reduced levels of mitochondrial fusion, but the overexpression of mitoPLD leads to the aggregation of mitochondria. These aggregated mitochondria resemble tethered mitochondria because the separation distance is equivalent to half the size of an MFN molecule. Therefore, these findings indicate the role of mitoPLD in the lipid-mixing step of the OM fusion process. As mentioned above, prohibitins, *PHB1* and *PHB2*, have genetic interactions with several genes involved in mitochondrial morphology maintenance, *MMM1* and *MDM10*, as well as lipid metabolism genes, *UPS1*, *GEP1*, *CRD1*, and *PSD1* that work together to regulate the level of CL and PE. CL and PE have overlapping functions in mitochondrial fusion in yeast (Joshi, Thompson et al. 2012). Ups1, which regulates the proteolytic processing of Mgm1, functions antagonistically with Ups2/Gep1 in regulating the level of CL (Tamura, Endo et al. 2009). Ups1 and Ups2 regulate the level of CL that is synthesized by cardiolipin synthase 1 (Crd1). Psd1 is a decarboxylase that converts PS into PE. The lack of *CRD1* does not lead to abnormal mitochondrial morphology. However, the mutant lacking both Crd1 and Psd1 has fragmented mitochondria, reduced levels of mtDNA, and altered membrane potential, which are all phenotypes of *mgm1Δ*. The level of s-Mgm1 processing was lower in *psd1Δ*, and the level of both s-Mgm1 and l-Mgm1 are reduced in *crd1Δpsd1Δ,* which overall affects the level of mitochondrial fusion. Given these findings, phospholipid homeostasis may influence mitochondrial dynamics at multiple levels, including the membrane architecture, protein activities, and mitochondrial genome. Hence, further studies are required to understand the role of lipids in mitochondrial dynamics at a mechanistic level.

1.3 DYNAMIN-RELATED PROTEINS ARE THE MAIN PLAYERS THAT MEDIATE MITOCHONDRIAL FUSION AND FISSION

All the key mechanoenzymes that mediate mitochondrial fusion and fission events (Dnm1/DRP1, Fzo1/MFN, and Mgm1/OPA1) are dynamin-related proteins (DRPs) that belong to the dynamin superfamily. The dynamin superfamily proteins have crucial roles in the cell as membrane-remodeling molecules and possess unique domains and characteristics as described below.

1.3.1 Dynamin superfamily proteins are membrane-remodeling molecules

The dynamin superfamily is a diverse superfamily of large GTPases in eukaryotes with unique domain architecture (Praefcke and McMahon 2004). They are distinguished from other GTPases due to their ability to self-assemble, self-stimulate, and bind to lipids (Praefcke and McMahon 2004). Proteins in the dynamin superfamily are either classical dynamins or dynamin-related proteins (DRPs). Classical dynamins include dynamin 1, 2, and 3, which function in the scission of clathrin-coated vesicles (CCVs) during endocytosis as well as synaptic vesicle recycling, Golgi trafficking, phagocytosis, and cytokinesis (Ferguson and De Camilli 2012). DRPs function in various cellular membrane-remodeling processes. Four well-characterized DRPs in yeast are Vps1, Dnm1, Mgm1, and Fzo1. Vps1 mediates Golgi vesicle formation, while the other three DRPs function in mitochondrial dynamics. Dnm1 directly mediates the fission of mitochondria, while Mgm1 and Fzo1 are the key players for mitochondrial fusion. These DRPs are highly conserved proteins since the higher eukaryote counterparts of Dnm1, Mgm1, and Fzo1 are also membrane-remodeling molecules (Praefcke and McMahon 2004). In other organisms, Myxovirus resistance protein (Mx)-like proteins, which are found in higher eukaryotes and in *A. thaliana*, function in a viral resistance pathway. Guanylate-binding proteins (GBPs) and atlastins are two groups of similar proteins found in *H. sapiens*, *D. melanogaster*, and *C. elegans*. GBPs play a role in interferon II-induced pathogenic resistance, while atlastins mediate vesicle trafficking at the cis-Golgi and mediate homotypic fusion of the endoplasmic reticulum (ER)

tubes (Orso, Pendin et al. 2009). Plants also have a dynamin-like protein ARC-5 to mediate chloroplast division and *Arabidopsis thaliana* dynamin-like (ADL) proteins to function in cytokinesis, chloroplast division, and trans-Golgi vesicle scission (Praefcke and McMahon 2004). Even though different DRPs function in diverse pathways, they all utilize their core domains to self-assemble and hydrolyze GTP to remodel membranes. Although it is largely known how dynamin 1 mediates the scission of CCVs, the molecular mechanisms by which DRPs function in membrane fusion are mostly unknown.

1.3.2 Members of the dynamin superfamily share conserved domains

The dynamin superfamily is subdivided into two subclasses: classical dynamins and DRPs. All members in the dynamin superfamily contain at least three conserved domains: the GTPase domain, the middle domain, and the GTP Effector Domain (GED) (**Figure 1.7**). Crystal structures characterize the structure of dynamin and several DRPs into four distinct regions: head, bundle signal elements (BSE) or neck, stalk, and foot regions (Ferguson and De Camilli 2012) (**Figure 1.8**).

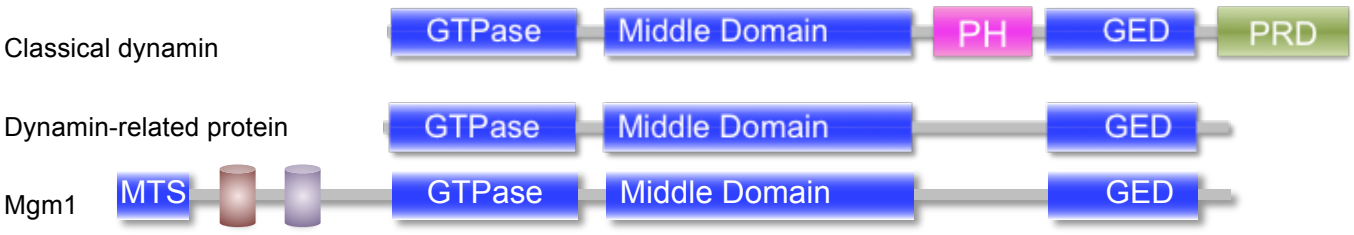

Figure 1.7. Domain structure of the dynamin superfamily

All classical dynamins and dynamin-related proteins contain the GTPase domain, the middle domain, and the GTP effector domain (GED), which are shown in *blue*. Classical dynamins also contain C-terminal proline-rich domain (PRD) shown in *green*. In addition, classical dynamins interact with lipids via a pleckstrin homology (PH) domain, which is shown in *pink*. Mgm1 is a dynamin-related protein that contains all core domains of dynamin. In addition, Mgm1 contains an N-terminal mitochondrial targeting sequence (MTS) and two hydrophobic segments between its MTS and GTPase domain.

1.3.2.1 The head region consists of a GTPase domain and BSE

The catalytic GTPase domain serves as the site for GTP binding and hydrolysis. The GTPase domain is the most conserved domain that contains four conserved motifs G1-G4 that have specific roles. G1 and G4 are the sites for GTP binding; G1 and G3 are the sites for phosphate coordination; G2 contains catalytic threonine residues; and G3 coordinates a portion of the GTP molecule (Praefcke and McMahon 2004). Since dynamin superfamily proteins have low affinities for GTP and GDP, they do not require exchange factors to release nucleotides during the GTP cycle. The GTPase domain is near the N-terminus and makes up a region called G domain or head region. BSE serves as the lever arm between the GTPase domain and the stalk region.

1.3.2.2 The stalk region contains the middle domain and the GED

The stalk region is referred to as the bundle of the middle domain and the GED that are essential for protein oligomerization and self-assembly. The stalks of dynamin and Myxovirus resistance protein 1 (MxA) contain antiparallel four-helix bundles (Gao, von der Malsburg et al. 2010, Ford, Jenni et al. 2011, Gao, von der Malsburg et al. 2011). Dynamin and MxA dimerize via the interaction of the stalks into a cross shape, where the head region points to one side and the foot region points to the other side (Gao, von der Malsburg et al. 2010, Ford, Jenni et al. 2011). The crosses interact with one another, allowing dynamin to polymerize (Ferguson and De Camilli 2012). The self-assembly of dynamin stimulates its GTPase activity, and the oligomerization of MxA at the stalk region influences the nucleotide release (Gao, von der Malsburg et al. 2010). A point mutation in the middle domain of Dnm1 causes deficient Dnm1 oligomerization and reduced GTPase activity (Ingerman and Nunnari 2005). The GED is important for self-assembly of dynamin superfamily proteins. The interaction between the GED and the GTPase domain is required for the oligomerization and the stimulation of GTPase activity (Muhlberg, Warnock et al. 1997).

1.3.2.3 The foot region of dynamin binds to membrane

In addition to the three core domains, the region between the middle domain and the GED is called the foot region and serves as the site for lipid interactions. This region is the site for the pleckstrin homology (PH) domain (Praefcke and McMahon 2004). PH domains have affinities for negatively charged phospholipids. The PH domain of classical dynamin binds to phosphatidylinositols (PIs) such as phosphotidylinositol-(4,5)-bisphosphate (PI(4,5)P2) (Klein, Lee et al. 1998). Instead of a PH domain, the foot region between the middle domain and the GED in several DRPs is also the site for lipid interactions, as shown by molecular structures and protein-lipid binding assays (Kim, Park et al. 2001, Low and Lowe 2006, von der Malsburg, Abutbul-Ionita et al. 2011). Crystal structures and three-dimensional reconstruction of electron microscopy images of protein-lipid tubes of the bacterial dynamin-like protein (BDLP) identified the two helices in the region between the middle domain and the GED, which is in the same region as the foot region and is theorized to be the site for membrane interaction (Low and Lowe 2006). MxA contains an L4 loop in the similar region that allows it to bind to negatively charged phospholipids (von der Malsburg, Abutbul-Ionita et al. 2011). MxA is co-sedimented with liposomes containing negatively charged PS and found assembled on the liposomes by electron microscopy. ADL2 also specifically binds to phosphatidylinositol-4-phosphate (PI4P) in a Fat western blot analysis (Kim, Park et al. 2001). In this analysis, a nitrocellulose membrane is spotted by lipids and incubated with purified protein, and the nitrocellulose-bound ADL2 is detected by an antibody against ADL2. Moreover, by a liposome flotation assay, *Arabidopsis* dynamin-related protein 1A (*At*DRP1A) was also shown to bind to liposomes containing phospholipid compositions similar to that found in the plasma membrane (Backues and Bednarek 2010). Recently, Meglei and McQuibban demonstrated that purified s-Mgm1 interacts with certain negatively charged phospholipids (2009) (see section **1.4.4.3**). Altogether, these findings suggest that lipid binding is a characteristic of the dynamin superfamily proteins and is crucial for their functions. However, in addition to the PH domain, other lipid-binding regions of DRPs are yet to be elucidated.

Specific interactions with certain phospholipids suggest that the PH domain of classical dynamin and other lipid-binding regions of DRPs may have unique effector roles. Bethoney et al. showed that the PH domain does not play a role in targeting dynamin 1 to the membrane but rather has the converse role of recruiting PI(4,5)P2 to the dynamin bound areas on the membrane

(Bethoney, King et al. 2009). Immunofluorescence experiments showed that mutations in the PH domain of dynamin do not affect the subcellular localization of dynamin. Moreover, geometry analysis and fluorescence quenching experiments showed that dynamin may cluster PI(4,5)P2. This phospholipid clustering may be important for dynamin-mediated membrane scission. To date, little is known about the effector role of the lipid-binding activities of DRPs.

In addition to the dynamin core domains that are essential for their hallmark characteristics of GTP hydrolysis, oligomerization, and lipid interactions, dynamins have sequence motifs that serve for protein-protein interactions. Dynamin contains a proline-rich domain (PRD) that promotes protein-protein interactions, and Fzo1/MFN has coiled-coil heptad repeat regions that promote protein self-interaction. The findings on the domain functions and characteristics provide insights into the molecular mechanism of the dynamin superfamily proteins.

1.3.3 Dynamin superfamily proteins polymerize and constrict membranes to mediate membrane fission

Members of the dynamin superfamily are known as universal membrane tubulation and fission molecules because of their roles in membrane scission of a wide range of vesicles and organelles (Praefcke and McMahon 2004). The scission of clathrin-coated vesicles relies on classical dynamins, while DRPs mediate the fission of other membranes and organelles, such as mitochondria and peroxisomes. The membrane scission event involves binding to the membrane, severing the membrane, and releasing from the membrane (**Figure 1.8**). Classical dynamins, such as dynamin 1, directly bind to the sites of membrane fission via the PH domain, while other dynamin superfamily proteins like Dnm1/DRP1 are recruited to the membrane via adapter proteins. Following the membrane scission process, dynamin 1 is recycled back to the cytosol. It is still under debate how dynamin 1 is released from the membrane. Two studies showed that dynamin is released upon GTP hydrolysis, while other studies have shown that dynamin is still bound to the membrane under GTP hydrolysis conditions (Warnock, Hinshaw et al. 1996, Stowell, Marks et al. 1999, Marks, Stowell et al. 2001).

Since the 1990s, there have been studies to support the model that dynamin superfamily proteins sever membranes by membrane constrictions based on the findings that (1) dynamin polymerizes and tubulates liposomes; (2) dynamin polymer constricts upon GTP hydrolysis; and (3) dynamin constriction leads to fission (Praefcke and McMahon 2004). Dynamin superfamily proteins readily self-assemble, polymerize onto membranes, and deform the membrane. There have been extensive structural studies on the classical dynamin to demonstrate its membrane fission mechanism. Electron micrographs have shown that purified dynamin self-assembles and forms helical structures in solution under low salt conditions (Hinshaw and Schmid 1995, Carr and Hinshaw 1997). This helical structure is formed from a string of the cross-shaped dimers that interact with one another through the upper part and lower part of the stalk. The crosses align with a slight shift to allow the formation of helical structures, and weak interactions allow the helix to be flexible (Faelber, Posor et al. 2011, Ford, Jenni et al. 2011).

In addition to the evidence that dynamin can self-assemble in solution, dynamin self-assembles and polymerizes on negatively charged liposomes. Dynamin polymerization deforms spherical liposomes into tubulated and elongated structures. Dynamin-decorated lipid tubes have diameters of approximately 50 nm with a membrane diameter of 20 nm, which is comparable to the size of the neck of a clathrin-coated pit (Sweitzer and Hinshaw 1998, Takei, Slepnev et al. 1999). Dnm1-lipid tubes have larger diameters of around 120 nm (Mears, Lackner et al. 2011). However, under GTP hydrolysis conditions, Dnm1 constricts the lipid tubes to a diameter of approximately 60 nm (Mears, Lackner et al. 2011). Upon GTP addition, dynamin-lipid tubes also constricted from 50 nm to 40 nm in diameter. This constriction coexists with torsion, a reduction in the number of dimers per turn, and the radius of the helical structure (Chappie, Mears et al. 2011). It is thought that the GTP-dependent conformational changes cause membrane constriction (**Figure 1.8**).

The G interface in the GTPase domain is proposed to be the site that mediates contacts between neighboring dynamin filaments on the membrane (Morlot and Roux 2013). This contact region undergoes conformational changes upon GTP hydrolysis, and this structural change is proposed to cause membrane constriction. Sharp membrane bending at the edge of the dynamin coat is generated upon membrane constriction. Since this bending is highly energetically unstable and membrane scission would be favored to relieve this tension, it is proposed that membrane constriction is what drives membrane scission (Hurley and Hinshaw

2012, Morlot, Galli et al. 2012). Dynamin-lipid constricted tubules break into small vesicles, suggesting that membrane constriction could lead to membrane scission (Sweitzer and Hinshaw 1998). Nevertheless, recent studies showed that membrane constriction is essential but not sufficient to cause membrane fission (Morlot and Roux 2013). Other players and membrane mechanical parameters of tension, bending, and rigidity may play a role in promoting membrane fission. Although much is known at a mechanistic level about dynamin-mediated membrane fission, the mechanism of dynamin-mediated membrane fusion is yet to be elucidated.

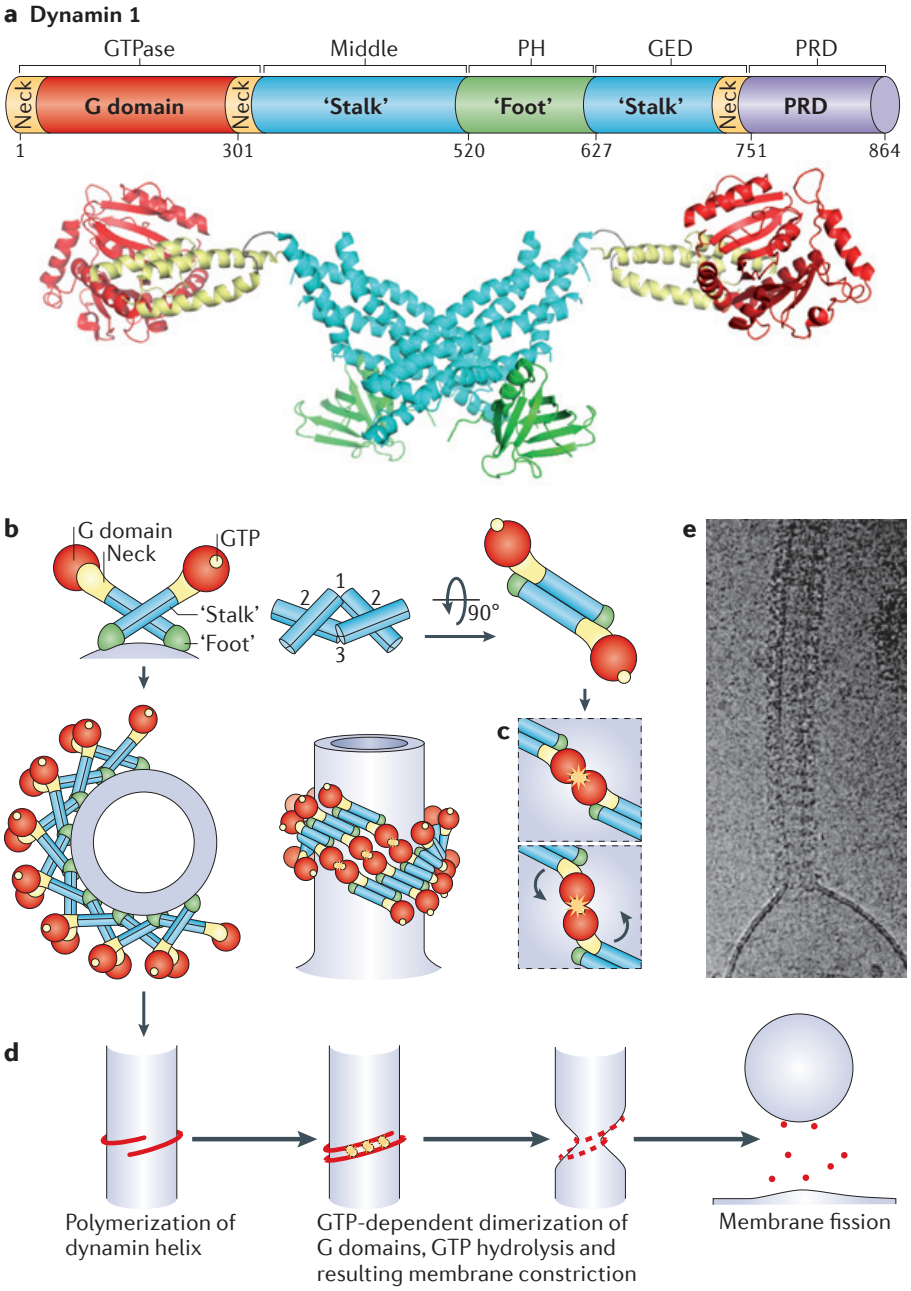

Figure 1.8. Dynamin structure and dynamin-mediated membrane fission mechanism

(**A**) Domain architecture and structure of a classical dynamin, dynamin 1. Numbers indicate amino acid positions within the primary sequence of the human dynamin 1 xa splice variant. Regions that belong to the same folded module are shown in the same color. (**B**) Schematic representation of dynamin dimers and of helical dynamin polymers around a tubular template in two different orientations (with 90° rotation between them). (**C**) Proposed GTP hydrolysis-dependent conformational changes at BSE relative to the G domain. (**D**) Key steps in dynamin-mediated membrane fission. (**E**) Cryo-electron microscopy image shows helical polymer of purified dynamin that has driven the formation of a tubule from a liposome. See text for details. Source: Taken from Ferguson and De Camilli (2012).

1.3.4 DRPs mediate membrane fusion via unique mechanisms

While most members of the dynamin superfamily are fission molecules, certain members are membrane fusion molecules. In addition to Fzo1/MFN and Mgm1/OPA1 that mediate mitochondrial fusion, atlastins mediate the fusion of ER membranes, and dynamin-like DynA and BDLP are proposed to mediate bacterial membrane fusion (Low, Sachse et al. 2009, Orso, Pendin et al. 2009, Burmann, Ebert et al. 2011). Even though polymerization and membrane constriction are largely known as mechanisms of dynamin-mediated membrane scission, it is largely unknown how proteins of the dynamin superfamily promote the opposing event of membrane fusion.

1.3.4.1 Intracellular membrane fusion proceeds through a hemifusion intermediate

Membrane fusion is a process that allows for the content mixing of two separate compartments. This process is crucial for inter- and intra-cellular communications. Membrane fusion involves merging of the two bilayers via two possible intermediates: hemifusion structures and fusion pores (Chernomordik and Kozlov 2008). In a hemifusion structure, the outer leaflets of the two bilayers are connected while the inner leaflets are separate. Therefore, there is no content mixing in hemifusion structures. In contrast, in a fusion pore intermediate, both outer and inner leaflets of both bilayers are connected, and the pore allows content mixing. Viral fusion, intracellular membrane fusion, and developmental cell fusion go through hemifusion intermediates (Chernomordik and Kozlov 2008). Most membrane fusion events rely on the function of fusion molecules (1) to bring membranes in close proximity, (2) to remodel the membranes to initiate the fusion event, and (3) to cause lipid mixing in the two fusing membranes and complete the fusion event (**Figure 1.9**). All these three steps contain high-energy barriers. One of the main functions of fusion proteins is to lower these energy barriers at the right time and place to mediate a membrane fusion event (Chernomordik and Kozlov 2008).

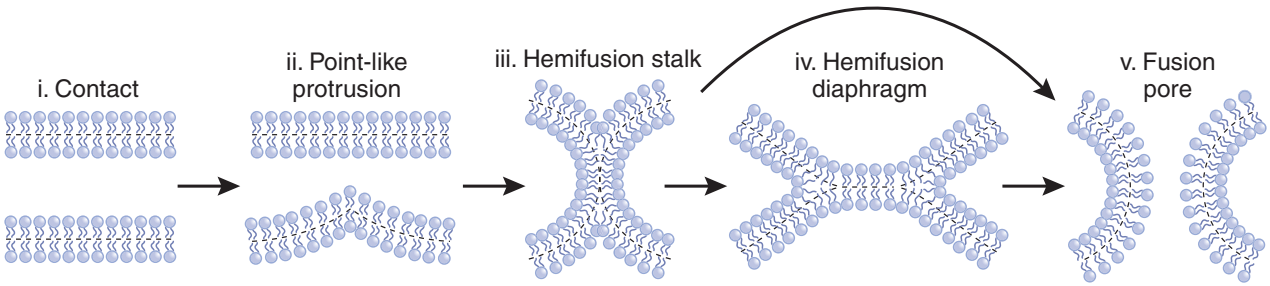

Figure 1.9. Hemifusion model of membrane fusion

The model shows how two bilayers fuse via a hemifusion intermediate through membrane tethering (**i**), fusion initiation (**ii**), and lipid-mixing steps (**iii-v**). (**i**) Pre-fusion contact. (**ii**) A point-like membrane protrusion minimizes the energy of the hydration repulsion between the proximal leaflets of the membranes coming into immediate contact. (**iii**) A hemifusion stalk with proximal leaflets fused and distal leaflets unfused. (**iv**) Stalk expansion yields the hemifusion diaphragm. (**v**) A fusion pore forms either in the hemifusion diaphragm bilayer or directly from the stalk. Dashed lines show the boundaries of the hydrophobic surfaces of monolayers. Source: Taken from Chernomordik and Kozlov (2008).

1.3.4.2 DRPs bind to and tether membranes to fuse opposing membranes

In a membrane fusion event, DRPs first localize to the fusion sites, bringing membranes together and tethering them to allow fusion. Fzo1/MFN and atlastins are already anchored to the membranes via their transmembrane domains. On the other hand, DynA, BDLP, and soluble isoforms of Mgm1/OPA1 have to be recruited to the membranes. The PH domain of the classical dynamin interacts directly with PI in the bilayer (Praefcke and McMahon 2004). BDLP binds to membrane in a nucleotide-dependent manner via a domain called paddle domain, which is in a similar region as the PH domain of dynamin. DynA binds to membranes independently of nucleotides (Burmann, Ebert et al. 2011). Recently, Meglei and McQuibban showed that Mgm1 binds to certain negatively charged phospholipids: PS, PA, and CL (2009). Similarly, OPA1 interacts and co-sediments with liposomes that contain CL (Ban, Heymann et al. 2010).

Upon recruitment to the fusion site, DRPs self-interact in *cis* to assemble onto membranes and in *trans* to tether the opposing membranes. Fzo1/MFN anchors to the OM by two transmembrane segments having both the N- and C-terminal tails exposed to the cytoplasm (Escobar-Henriques and Anton 2013). The N-terminal tail of Fzo1 contains two coiled-coil

heptad repeats, HR1 and HRN, which are downstream and upstream of the GTPase domain, respectively. MFN has the HR1 upstream of the GTPase domain as well as another coiled-coil heptad repeat, the HR2, near the C-terminal tail. Fzo1/MFN utilizes these coiled-coil domains to self-interact both in *cis* and in *trans*. Fzo1 interacts in *cis* on the same membrane to form dimers upon GTP binding (Anton, Fres et al. 2011). *Trans* interactions result in a larger complex of Fzo1, which can be detected by size exclusion chromatography. Atlastins, DynA, and BDLP also self-interact in *trans* to tether bilayers (Low, Sachse et al. 2009, Orso, Pendin et al. 2009, Burmann, Ebert et al. 2011).

Even though it is known that membrane tethering is an initial step of dynamin-mediated membrane fusion, it is unclear what subsequent steps are required to complete membrane fusion. To date, Fzo1 and atlastin studies have provided clues on how DRPs may promote membrane fusion. Mutagenesis studies have shown that self-interaction, structural transition, and post-translational modification are crucial for Fzo1-mediated OM fusion (Cohen, Amiott et al. 2011, Anton, Dittmar et al. 2013). Crystal structures of atlastin in different nucleotide-bound forms demonstrate conformational switching, suggesting a model of atlastin-mediated ER fusion (Bian, Klemm et al. 2011, Byrnes and Sondermann 2011, Byrnes, Singh et al. 2013).

1.3.4.3 Fzo1 undergoes protein modification and conformational changes to promote membrane fusion

Recent studies showed that the ubiquitylation of Fzo1 does not only regulate the Fzo1 protein level; it also acts directly in the fusion mechanism (Anton, Fres et al. 2011, Cohen, Amiott et al. 2011, Anton, Dittmar et al. 2013). In a proposed model of Fzo1 function, GTP binding promotes Fzo1 homo-dimerization and oligomerization in *trans* to tether mitochondria. Based on the structures of BDLP in different nucleotide stages, GTP hydrolysis is believed to promote conformational changes that may allow protein ubiquitylation (Anton, Dittmar et al. 2013). The ubiquitylation of Fzo1 at K464 triggers the formation of ubiquitin chains at K398 of the neighboring Fzo1 molecules and subsequently promotes OM fusion (Anton, Dittmar et al. 2013). Moreover, this activation by Mdm30-dependent ubiquitylation can be reversed by a ubiquitin protease, Ubp12 (Anton, Dittmar et al. 2013). This mode of action reveals the role of

ubiquitylation and nucleotide-dependent structural transitions in promoting membrane fusion (**Figure 1.10**).

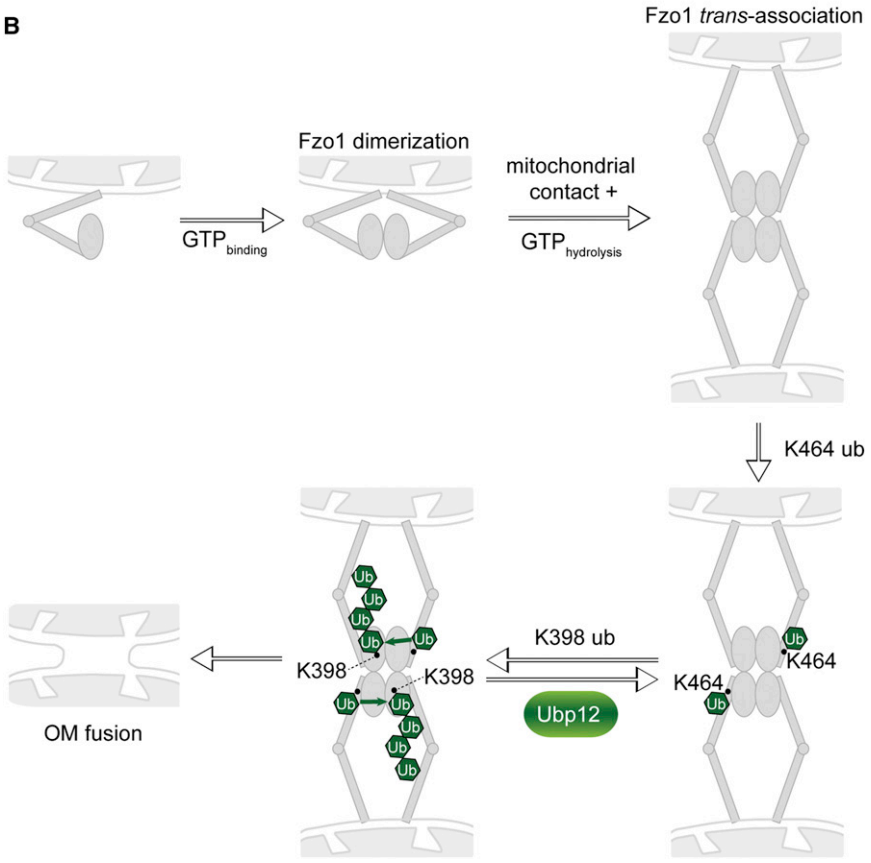

Figure 1.10. Model mechanism of Fzo1-mediated membrane fusion

GTP binding promotes Fzo1 homo-dimerization and further oligomerization. GTP hydrolysis induces a conformational change in Fzo1 that promotes K464 ubiquitylation. K464 mono-ubiquitylation promotes K398 polyubiquitylation. K398 polyubiquitylation and Fzo1 degradation drive the OM fusion. Source: Adapted from Anton, Dittmar et al. (2013).

1.3.4.4 Atlastin-mediated membrane fusion mechanism depends on GTP binding and hydrolysis

Atlastin in humans or Sey1 in yeast localizes to highly curved ER membranes and promotes the homotypic fusion of ER membranes. Biochemical studies and crystal structures have demonstrated the activities and the characteristics of atlastins to propose a model of atlastin-

mediated ER fusion (Orso, Pendin et al. 2009, Bian, Klemm et al. 2011, Byrnes and Sondermann 2011, Moss, Andreazza et al. 2011, Pendin, Tosetto et al. 2011, Liu, Bian et al. 2012, Byrnes, Singh et al. 2013). Similar to Fzo1, atlastin self-assembles in *cis* to oligomerize (Orso, Pendin et al. 2009). Upon GTP binding, atlastin interacts in *trans* to form a tethering complex. GTP hydrolysis-dependent conformational changes allow the tethered membranes to be in closer proximity. Atlastin also generates membrane curvature via its transmembrane domain, which destabilizes the membrane and promotes fusion (Liu, Bian et al. 2012). Similar to other dynamin superfamily proteins, GDP and inorganic phosphate (Pi), which are products of a GTP hydrolysis reaction, are likely disassociated and released after GTP hydrolysis, allowing the recycling of atlastin (Bian, Klemm et al. 2011). Cytosolic truncated atlastin 1 is found as dimers in the presence of a non-hydrolyzable analog, GTPγS or GDP by analytical ultracentrifucation (AUC) and gel filtration. AUC shows a broader dimer peak in the presence of GDP, suggesting that the GDP-bound atlastin dimer could be less stable, which would allow the release back into monomer form. Moreover, from the crystal structure, it was demonstrated that Pi release could trigger conformational changes (Byrnes, Singh et al. 2013). These findings suggest that nucleotide-dependent conformational changes play a crucial role in dynamin-mediated membrane fusion process.

To date, membrane tethering, nucleotide-dependent conformational changes, and membrane destabilization are thought be the main mechanisms of how DRPs mediate membrane fusion. Although the model mechanisms of how Fzo1/MFN and atlastins mediate membrane fusion have been proposed, it is still unclear how Mgm1/OPA1 mediates fusion of the IM of mitochondria.

1.4 MITOCHONDRIAL GENOME MAINTENANCE 1 (MGM1) IS A DRP THAT MEDIATES MITOCHONDRIAL INNER MEMBRANE FUSION

Another DRP known to function in membrane fusion is Mgm1/OPA1, which mediates mitochondrial IM fusion. Since its first discovery 20 years ago, much has been learned about the localization, domain architecture, and functions of Mgm1 (Jones and Fangman 1992, Shepard and Yaffe 1999, Wong, Wagner et al. 2000, Sesaki, Southard et al. 2003, Wong, Wagner et al.

2003). Recent and on-going studies have further characterized the molecular mechanism of Mgm1 activity. Using an *in vitro* mitochondrial fusion assay, Mgm1 was shown to directly mediate IM fusion (Wong, Wagner et al. 2003, Meeusen, DeVay et al. 2006). Key domains and residues of the GTPase domain and the GED have been identified (Wong, Wagner et al. 2003, Meeusen, DeVay et al. 2006), and biochemical approaches have been used to demonstrate the GTPase activity and oligomerization of Mgm1 (Meglei and McQuibban 2009).

1.4.1 Mgm1 was first discovered and characterized in 1990s

Mgm1 was first identified in a screen for genes required for mitochondrial genome maintenance in the yeast *S. cerevisiae*. Wild-type yeast strains were randomly mutagenized by ethylmethanesulfonate and selected for mutated strains that have petite colonies at the non-permissive temperature (Jones and Fangman 1992). The petite colony phenotype is due to the loss of or mutations in mtDNA causing respiratory deficiency, slow growth, and small size colony (Ferguson and von Borstel 1992). Upon shifting to the non-permissive temperature of 34°C, *mgm1-1* cells formed white colonies, a phenotype characteristic of respiration-deficient mutants, and grew at a slower rate (Jones and Fangman 1992). mtDNA synthesis rate and the total amount of mtDNA also decreased upon the temperature shift. The *mgm1-1* mutant was mapped to the deletion of *MGM1* gene. A subsequent study has confirmed the loss of mtDNA in *mgm1Δ* mutant. Together, these findings demonstrated that mitochondrial genome maintenance is dependent on the function of Mgm1 (Guan, Farh et al. 1993). In addition, the deletion of *MGM1* caused disruption in mitochondrial morphology and localization, suggesting another crucial role of Mgm1 in the maintenance of mitochondrial morphology. Therefore, these initial characterizations of temperature sensitive mutants and *mgm1Δ* mutant showed that although *MGM1* is a non-essential gene, it is required for the maintenance of mitochondrial genome, mitochondrial morphology, mitochondrial distribution, proper cellular respiration, and normal cell growth (Jones and Fangman 1992, Guan, Farh et al. 1993).

1.4.2 Mgm1 plays a role in mitochondrial morphology, fusion, and cristae maintenance

Sheppard and Yaffe showed that functional Mgm1 is required for mitochondrial inheritance (1999). Mitochondria are aggregated in the yeast lacking Mgm1, and after budding the majority of daughter cells are devoid of mitochondria. To examine the primary function of Mgm1, Wong et al. characterized temperature sensitive *MGM1* alleles (Wong, Wagner et al. 2000). By using an indirect immunofluorescence approach monitoring mitochondrial morphology, Wong et al. showed that the *mgm1Δ* mutant has a primary phenotype of fragmented mitochondria and a secondary phenotype of aggregated mitochondria. In addition, *mgm1Δ* was shown to have the same phenotype as *fzo1Δ*, which suggested a role for Mgm1 in mitochondrial fusion (Wong, Wagner et al. 2000).

The role of Mgm1 in mitochondrial fusion was confirmed by two separate experiments (Wong, Wagner et al. 2000). Mitochondrial fusion occurs during yeast mating, and inhibiting mitochondrial fission can restore mitochondrial fusion defects. Mitochondrial fusion is blocked in *mgm1Δ* during yeast mating. Mitochondrial fragmentation in *mgm1Δ* is reversed by the deletion of *DNM1*, which is required for mitochondrial fission. In an *in vitro* mitochondrial fusion assay, Mgm1 was shown to specifically mediate mitochondrial IM fusion, and the defective IM fusion negatively regulates OM fusion and overall mitochondrial fusion (Meeusen, DeVay et al. 2006). Electron microscopy images of temperature sensitive mutants of Mgm1 showed aberrant cristae morphology, suggesting a role for Mgm1 in cristae maintenance (Meeusen, DeVay et al. 2006). However, it is still unclear how Mgm1 mechanistically mediates mitochondrial IM fusion and maintains cristae morphology.

1.4.3 Mgm1 precursor is transported to the IM and processed into l-Mgm1 and s-Mgm1 isoforms

MGM1 encodes for a protein of 902 amino acids (Guan, Farh et al. 1993). From the N- to C-terminus, Mgm1 contains an MTS, two hydrophobic segments, and three conserved domains of the dynamin superfamily (**Figure 1.7**). Full-length Mgm1 is targeted to the mitochondria via its MTS and transported through the transporters in the OM and IM, TOM and TIM complexes, respectively. Mgm1 was first shown to localize to the OM by biochemical fractionation and

indirect immunofluorescence experiments (Shepard and Yaffe 1999, Wong, Wagner et al. 2000). However, treating intact mitochondria with proteinase K and trypsin does not degrade Mgm1, suggesting that Mgm1 is not an OM protein (Wong, Wagner et al. 2000). Upon rupturing the OM with osmotic shock, Mgm1 becomes sensitive to proteinase K digestion, suggesting that Mgm1 is exposed to the IMS. Indeed, Mgm1 is found to be associated to the IM by an immuno-gold labeling experiment (Wong, Wagner et al. 2000).

Once Mgm1 is translocated through the TIM complex, Mgm1 is anchored to the IM by its first hydrophobic segment. The MTS is cleaved by the mitochondrial processing peptidase (MPP), and Mgm1 stays tethered to the IM as l-Mgm1 (Herlan, Bornhovd et al. 2004) (**Figure 1.11**). Alternatively, ATP drives the import of precursor Mgm1, bypassing the first hydrophobic segment and causing Mgm1 to anchor to the IM by its second hydrophobic segment. This hydrophobic segment contains a rhomboid-processing site with a sequence specific to the rhomboid serine protease Rbd1, which is also known as Pcp1 (Herlan, Vogel et al. 2003, McQuibban, Saurya et al. 2003) (see section **1.2.2.3**). Rbd1 cleaves full-length Mgm1 into s-Mgm1 and releases it into to the IMS (**Figure 1.11**). By subcellular fractionation and immuno-EM, s-Mgm1 is found to be loosely associated to the IM (Wong, Wagner et al. 2000, Herlan, Vogel et al. 2003). s-Mgm1 co-immunoprecipitates with l-Mgm1, suggesting that s-Mgm1 is recruited to the IM by interacting with l-Mgm1 (Meeusen, DeVay et al. 2006). However, it is still unclear how s-Mgm1 is associated to the IM to mediate IM fusion.

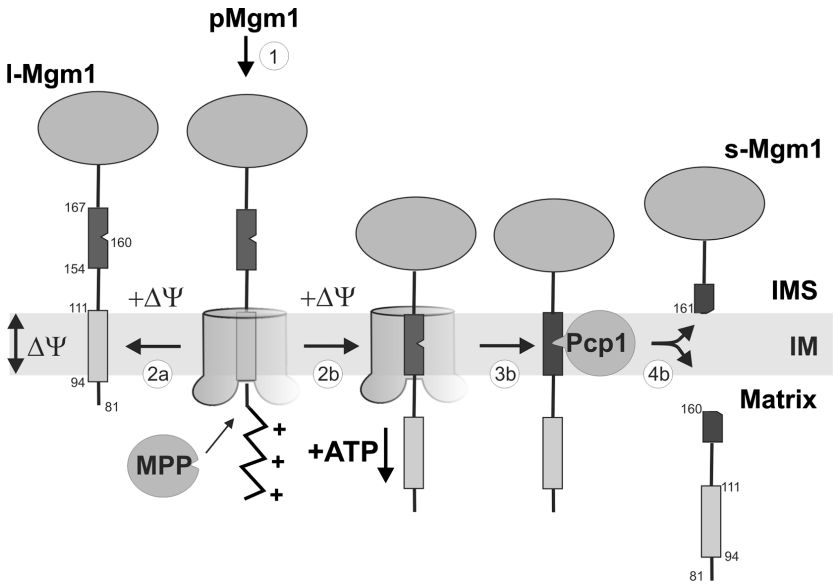

Figure 1.11. Mgm1 processing into l-Mgm1 and s-Mgm1 isoforms

Two pathways process precursor Mgm1 (pMgm1) into l-Mgm1 or s-Mgm1. pMgm1 is targeted to the IM by its MTS (**1**). MTS is cleaved off by MPP, resulting in l-Mgm1 anchored to the IM via the first hydrophobic segment (*light gray box*) (**2a**). Membrane potential (+ΔΨ) and ATP allow the first hydrophobic segment to bypass the transporter (**2b**). The second hydrophobic segment (*dark gray box*) contains a rhomboid-specific sequence that is recognized by a rhomboid serine protease Pcp1/Rbd1 (**3b**). The proteolytic cleavage releases s-Mgm1 into the IMS (**4b**). Source: Taken from Herlan, Bornhovd et al. (2004).

1.4.4 Mgm1 contains core domains and possesses characteristics of the dynamin superfamily proteins

Sequence analysis showed that *MGM1* is located on chromosome XV and contains N-terminal MTS and conserved GTP-binding motifs (Jones and Fangman 1992). *MGM1* has a 200-amino acid region that was characterized to be highly related to three different dynamin superfamily proteins from different organisms: dynamin D100 in vertebrates and *Drosophila*, MxA in vertebrates, and Vps1 in yeast (Jones and Fangman 1992). Mgm1 is most closely related to dynamin D100, a prototype protein of the dynamin superfamily that is frequently called dynamin 1 (Jones and Fangman 1992, Guan, Farh et al. 1993).

Mgm1 contains three conserved domains of the dynamin superfamily: the GTPase domain, the middle domain, and the GED (**Figure 1.7**). Sequence homology to these three

dynamin domains suggests that Mgm1 is a member of the DRP subfamily. The GTPase domain and the GED are highly conserved while the middle domain is more divergent (Meglei and McQuibban 2009). *In vivo* mutagenesis studies, *in vitro* mitochondrial fusion assays, and *in vitro* biochemical characterizations have shown that Mgm1 behaves like a DRP (Wong, Wagner et al. 2003, Meeusen, DeVay et al. 2006, Meglei and McQuibban 2009). Wong et al. was the first group to characterize the domains of Mgm1 based on mutational analyses and *in vivo* phenotypic analyses (Jones and Fangman 1992, Wong, Wagner et al. 2003). Mutations in the GTPase domain and the GED domain were shown to affect Mgm1 function *in vivo*. Subsequently, these mutations were found to directly affect the IM fusion function of Mgm1 by *in vitro* mitochondrial fusion assays (Meeusen, DeVay et al. 2006). More importantly, Meglei and McQuibban showed that purified s-Mgm1 has basal GTPase activity and the ability to oligomerize, which are the characteristics of DRPs (2009).

1.4.4.1 Mgm1 has a functional GTPase domain

The GTPase domain of Mgm1 contains four highly conserved canonical GTP-binding motifs and catalytic residues (Meglei and McQuibban 2009). Based on sequence homology, S224, which is located in the G1 motif of the GTPase domain of Mgm1, is predicted to be important for nucleotide binding. On the other hand, T244 in the G2 motif is thought to stabilize Mgm1 in the GTP-bound form permitting GTP hydrolysis to occur (Bourne, Sanders et al. 1991, Meglei and McQuibban 2009). The fragmented mitochondrial morphology of *mgm1Δ* is rescued by expressing wild-type Mgm1 but not S224A or T244A mutants (Wong, Wagner et al. 2003). Consistently, S224A and T244A cannot rescue mitochondrial fusion defect during yeast mating. Moreover, the overexpression of S224A and T244A Mgm1 interferes with wild-type Mgm1 function, which causes mitochondrial fragmentation. Together, these findings demonstrate that the GTPase domain and S224 and T244 residues are crucial for Mgm1 function.

The requirement of a functional GTPase domain of Mgm1 was also demonstrated by *in vitro* approaches (Meeusen, DeVay et al. 2006, Meglei and McQuibban 2009). In an *in vitro* mitochondrial fusion assay, mitochondria isolated from a temperature sensitive mutant, *mgm1-6,* that has mutations in the GTPase domain were shown to be defective in IM fusion (Meeusen, DeVay et al. 2006). A colorimetric malachite green GTPase assay showed that purified wild-

type s-Mgm1 has basal level of GTPase activity (Meglei and McQuibban 2009). However, GTP hydrolysis activity was abolished in S224A and T244A s-Mgm1 mutants. Together, these findings reveal that Mgm1 is an active GTPase and that its GTPase activity is essential for its function in mitochondrial fusion. The GTPase activity of proteins in the dynamin superfamily is stimulated by self-assembly and lipid interactions (Praefcke and McMahon 2004). However, it has not yet been shown whether the GTPase activity of Mgm1 can be stimulated in a similar manner.

1.4.4.2 Mgm1 oligomerizes via the GED

The GTPase effector domain or the GED is important for the GTPase activity stimulation, which is dependent on dynamin oligomerization and self-assembly (Praefcke and McMahon 2004). This oligomerization-dependent stimulation of GTPase activity involves lysine and arginine residues in the GED (Sever, Muhlberg et al. 1999, Sever, Damke et al. 2000). By making point mutations in all lysine and arginine residues in the predicted GED of Mgm1, Wong et al. showed that the R824 and K854 residues are crucial for Mgm1 function (Wong, Wagner et al. 2003). R824A and K854A Mgm1 mutants cannot rescue the fragmented mitochondrial morphology and the defective mitochondrial fusion during mating in *mgm1Δ*, indicating that functional GED and Mgm1 oligomerization could be important for Mgm1 function. Consistently, by using an *in vitro* mitochondrial fusion assay, Meeusen et al. showed that a temperature sensitive allele *mgm1-7*, which contains a mutation in the GED, has deformed mitochondria and is defective in mitochondrial fusion (Meeusen, DeVay et al. 2006).

Meglei and McQuibban (2009) investigated the oligomerization properties of purified s-Mgm1 by size exclusion chromatography and chemical crosslinking experiments. Purified s-Mgm1 elutes from a size exclusion column as two populations with apparent molecular sizes equivalent to s-Mgm1 monomer and a low-order oligomer, suggesting that s-Mgm1 oligomerizes in solution. By size exclusion chromatography, K854A s-Mgm1 was shown to have reduced ability to oligomerize. However, oligomers of K854A s-Mgm1 were still observed by chemical crosslinking. Basal GTPase activity requires the internal interaction between the GTPase domain and the GED, while stimulated GTPase activity is dependent on protein self-assembly. K854A has basal GTPase activity at similar level to that of the wild-type s-Mgm1, suggesting

that K854A does not disrupt the internal interaction between the GTPase domain and the GED. Instead, K854A mutation could affect Mgm1 self-assembly. Therefore, these findings suggest that Mgm1 oligomerizes and that K854 could be essential for Mgm1 self-assembly. However, the self-assembled structure of Mgm1 has not yet been observed, and the self-assembly dependent stimulation of the GTPase activity remains to be investigated.

1.4.4.3 Mgm1 interacts with certain negatively charged phospholipids

Classical dynamin contains a PH domain for its interaction with the negatively charged PI (Praefcke and McMahon 2004). However, by sequence analyses, a PH domain is not observed in Mgm1 and other DRPs (Praefcke and McMahon 2004, Meglei and McQuibban 2009). Despite the lack of PH domain, several DRPs have been shown to interact with negatively charged phospholipids (see section **1.3.2.3**). Meglei and McQuibban recently showed that Mgm1 also interacts with negatively charged phospholipids (2009). Mgm1-lipid interactions were tested by a lipid overlay assay similar to the Fat western blot assay that was used to detect the interaction of ADL2 with PI(4)P (Kim, Park et al. 2001). Serial dilutions of all IM phospholipids and all phospholipids that bind to PH domains were spotted on nitrocellulose membranes. The membranes were then incubated with purified 6xHis tagged s-Mgm1 and subject to western blotting using an anti-6xHis antibody. s-Mgm1 interacts with negatively charged CL, PA, PS, and PI(3,5)P2 but not with other negatively charged phospholipids. Moreover, Meglei and McQuibban identified a positively charged residue K795 to be crucial for binding to CL, PA, and PS (2009). K795 was identified as a conserved lysine residue along with seven other lysine and arginine residues by sequence alignment analyses with 22 fungal sequences that are homologous to Mgm1. The interactions of conserved residues with specific phospholipids suggest that the lipid binding activity of Mgm1 is selective and likely physiologically relevant. However, the functional significance of Mgm1-lipid interactions has yet to be elucidated.

1.4.5 Mgm1 mediates mitochondrial inner membrane fusion

Mgm1-mediated mitochondrial IM fusion likely involves at least two sequential steps: membrane tethering and lipid mixing. Mgm1 from opposing IMs are proposed to interact in *trans* and function together to mediate IM fusion (Wong, Wagner et al. 2003). The combination of two different temperature sensitive Mgm1 mutants, *mgm1-6* with a mutation in the GTPase domain and *mgm1-7* with a mutation in the GED, is able to partially compensate for the loss of function of one another to restore mitochondrial fusion. Moreover, mitochondria that are halted at the tethering step co-immunoprecipitate with both l-Mgm1 and s-Mgm1, indicating that both isoforms are required for IM fusion and that the two isoforms interact in *trans*. Together, these findings suggest that both isoforms of Mgm1 on both opposing IMs work together to mediate IM fusion. However, the *trans* interaction of Mgm1 from opposing membranes has not been directly observed.

Lipid mixing is an important step for any membrane fusion process. Mgm1-mediated IM fusion is likely dependent on the functional GTPase domain of Mgm1 (Meeusen, DeVay et al. 2006). Tethered IMs were observed during the fusion of mitochondria from *mgm1-6*, suggesting that the tethering step is not affected. Instead, the tethered IMs are unable to fuse due to the inhibition of the lipid-mixing step. In addition, Mgm1's lipid-binding activity could be a factor important for the lipid-mixing step. The PH domain of dynamin clusters PI(4,5)P2 and this phospholipid clustering was proposed to cause phase separation that could facilitate the lipid-mixing step (Bethoney, King et al. 2009). Therefore, Mgm1-lipid interactions could play a role in the membrane fusion process and possibly at the lipid-mixing step. However, a direct role for Mgm1's GTPase and lipid-binding domains functioning in the lipid-mixing step remains to be demonstrated.

Despite the fact that several studies have contributed to the understanding of the cellular localization, domain architecture, and functions of Mgm1, it is still unclear how Mgm1 mechanistically mediates mitochondrial IM fusion. The molecular details of Mgm1 function remain to be elucidated and are the focus of this thesis work.

1.5 THESIS RATIONALE

Although mitochondrial dynamics were first noticed in 1914, it was only 20 years ago that mitochondrial fusion and fission were directly observed and have become widely accepted. Mitochondria play a role in various cellular functions, and these functions rely on a proper balance in mitochondrial dynamics. Disrupted mitochondrial dynamics have been implicated in diseases including several neurodegenerative diseases. Greater understanding of the molecular mechanism of mitochondrial dynamics is crucial to advance our knowledge of the cellular and physiological implications of mitochondrial dynamics and their pathophysiological relevance to neurodegenerative diseases.

Mitochondrial dynamics result from a balance in mitochondrial fusion and fission. Genetic studies have revealed several players in mitochondrial dynamics and identified the dynamin-related protein Dnm1/DRP1 as the mediator of mitochondrial fission and Fzo1/MFN and Mgm1/OPA1 as mediators of mitochondrial fusion. Although it is largely known how Dnm1 mediates mitochondrial fission and how Fzo1 mediates OM fusion, it is unclear how Mgm1 mediates IM fusion in yeast.

Mgm1 is a nuclear-encoded protein that is targeted to the IM and processed into s-Mgm1 and l-Mgm1 in the IM. Mgm1 contains conserved domains of the dynamin superfamily, and Mgm1 can hydrolyze GTP and oligomerize like other dynamin superfamily proteins. Even though sequence analyses and genetic studies have proposed possible modes of action of Mgm1, the detailed mechanism of Mgm1 function and the IM fusion remains to be elucidated. *The goal of my thesis research is to understand the molecular mechanism of Mgm1 function in mediating inner membrane fusion of mitochondria.*

On the basis of the similarities of Mgm1's domain characteristics to those of dynamin superfamily proteins, I hypothesized that Mgm1 directly mediates fusion of the inner mitochondrial membrane via lipid interactions, oligomerization, and structural transitions. To test this hypothesis, I used biochemical assays and imaging techniques to study the activities of Mgm1. Since the lipid-binding region of Mgm1 has not yet been extensively characterized and it is unknown how Mgm1 utilizes its functional domains to mediate IM fusion, my objectives were the following: (1) to investigate the lipid-binding properties of Mgm1; (2) to determine how

Mgm1 oligomerizes and utilizes its GTPase activity in the tethering and lipid-mixing steps of IM fusion; and (3) to investigate how Mgm1 directly affects the IM to drive membrane fusion.

In this thesis, first, I identify a lipid-binding region and demonstrate that phospholipid interactions are essential for Mgm1 *in vivo* functions and *in vitro* activities (Chapter 3). Second, I demonstrate that s-Mgm1 self-assembles onto membranes with unique patterns that undergo nucleotide-dependent structural transitions, which could drive the membrane fusion (Chapter 4). Lastly, I provide evidence that lipid binding, GTP hydrolysis, and conformational changes of s-Mgm1 promote local membrane bending that could, together with l-Mgm1, cause IM fusion (Chapter 5). Taken together, I propose a model of how Mgm1 mediates mitochondrial IM fusion, which provide a better understanding of the mechanism and regulation of mitochondrial dynamics. Moreover, these findings also advance our knowledge of the mechanism of pro-fusion dynamin superfamily protein and cellular protein-membrane dynamics.

Chapter 2

2 MATERIAL AND METHODS

2.1 REAGENTS

2.1.1 Plasmids

s-Mgm1 plasmid was previously constructed in the lab (Meglei and McQuibban 2009). *MGM1* sequence containing 902 amino acids (aa) (Accession: CAA99426.1, GI:1420493) was used as the template. s-Mgm1 was cloned in the pET-21(+)b expression vector (Novagen) to contain amino acides 161-902 and a C-terminal 6xHis tag. Point mutations were generated by QuickChange® site-directed mutagenesis (Stratagene). l-Mgm1 plasmid was a gift from Dr. Andreas Reichert. The construct contains amino acids 61-805 and a C-terminal 6xHis tag in a pEH-1 plasmid.

2.1.2 Antibodies

Recombinant 6xHis tagged s-Mgm1 and l-Mgm1 were detected by a mouse monoclonal anti-His antibody (BioShop). Endogenous Mgm1 was detected by a rabbit polyclonal anti-Mgm1 antibody, which was a gift from Dr. Andreas Reichert. Antisera against Tom40 was a gift from Dr. Thomas Langer. Horseradish peroxidase-conjugated anti-mouse and anti-rabbit secondary antibodies were purchased from Sigma-Aldrich.

2.1.3 Lipids

All non-labeled phospholipids were purchased from Avanti Polar Lipids (Alabaster, AL): 1,2-dimyristoyl-*sn*-glycero-3-phosphocholine (DMPC, 14:0), 1,2-dimyristoyl-*sn*-glycero-3-

phosphoethanolamine (DMPE, 14:0), L-α-phosphatidylinositol (Liver, Bovine), 1',3'-bis[1,2-dimyristoyl-*sn*-glycero-3-phospho]-*sn*-glycerol (TMCL, 14:0), 1,2-dimyristoyl-*sn*-glycero-3-phospho-L-serine (DMPS, 14:0), and 1,2-dimyristoyl-*sn*-glycero-3-phosphate (DMPA, 14:0).

For NBD/Rhodamine lipid-mixing assay, head group-labeled phospholipids were purchased from Avanti Polar Lipids (Alabaster, AL): 1,2-dimyristoyl-*sn*-glycero-3-phosphoethanolamine-N-(7-nitro-2-1,3-benzoxadiazol-4-yl) (NBD-PE, 14:0), and 1,2-dimyristoyl-*sn*-glycero-3-phosphoethanolamine-N-(lissamine rhodamine B sulfonyl) (Rhodamine-PE, 14:0).

To fluorescently label supported lipid bilayers (SLB), the lipid mixture for the bilayer formation, including 1,2-dioleoyl-*sn*-glycero-3-phospho-L-serine-N-(7-nitro-2-1,3-benzoxadiazol-4-yl) (NBD-PS, 18:1) or 1-myristoyl-2-[12-[(7-nitro-2-1,3-benzoxadiazol-4-yl)amino]dodecanoyl]-*sn*-glycero-3-phosphocholine (NBD-PC, 14:0-12:0), was purchased from Avanti Polar Lipids (Alabaster, AL). Giant unilamellar vesicles were labeled with Texas Red® 1,2-dihexadecanoyl-*sn*-glycero-3-phosphoethanolamine (Texas Red® DHPE) (Life Technologies).

2.2 RECOMBINANT PROTEIN EXPRESSION, PURIFICATION, AND MODIFICATION

2.2.1 s-Mgm1 protein expression

C-terminal 6xHis tagged s-Mgm1 was transformed into *Escherichia coli* Rosetta-gami B cells (Novagen) for expression. Typically, 6-12 L of cultures were grown at 37 °C. Once they were grown to an optical density of 0.3 absorbance units, the cultures were cooled to 15 °C and induced by 50 μM isopropyl-1-thio-β-d-galactopyranoside (IPTG). Upon induction, the cultures were grown at 15 °C for 16 hours.

2.2.2 s-Mgm1 protein purification

Cultures were harvested and lysed with a French pressure cell press. Protein was purified using Ni^{2+}-NTA Superflow resin (Qiagen) according to the manufacturer's specifications. Fractions were tested by SDS-polyacrylamide gel electrophoresis (SDS−PAGE) and Coomassie Brilliant Blue staining. The collected fractions were exchanged into 25 mM HEPES, 25 mM PIPES, 500 mM NaCl, 1 mM dithiothreitol (DTT), pH 7.5 buffer (HP500), and concentrated using Amicon® Ultra centrifugal filter units (Millipore) prior to size exclusion chromatography. The concentrated samples were then subject to the size exclusion column Superdex 200 (GE Healthcare), and fractions were eluted with HP500 buffer. Collected fractions were concentrated and stored in HP500 buffer that contains 10% glycerol at -80 °C. Protein concentrations were determined using NanoDrop 2000 (Thermo Scientific). The molar extinction coefficient of s-Mgm1 was calculated by ExPASy ProtParam tool (http://web.expasy.org/protparam/) to be 43320 M^{-1} cm^{-1}, at 280 nm measured in water, assuming all cys pairs are reduced.

2.2.3 s-Mgm1 probe conjugation

Purified s-Mgm1 stock was diluted to 2-10 mg/mL in HP500 buffer. DTT was added to the final concentration of 10 mM. The sample was dialyzed overnight at 4°C into HP500 buffer without DTT in an oxygen free environment. After dialysis, 1 mM Alexa Fluor® 488 C5 Maleimide (Life Technologies) was slowly added to the sample with constant agitation for 2-5 minutes. The excess probe was removed by size exclusion chromatography using the Superdex 200 column. Eluted fractions were collected and concentrated using Amicon® Ultra-0.5 (Millipore). The dye and protein concentrations were determined using NanoDrop 2000.

2.2.4 l-Mgm1 protein expression

C-terminal 6xHis tagged l-Mgm1 was transformed into *Escherichia coli* SF100 cells for expression. SF100 cell was a gift from Dr. Andreas Reichert. Typically, 6-12 L of cultures were grown at 37 °C. Once they were grown to an optical density of 0.3, the cultures were cooled to

18 °C and induced by 50 μM IPTG. Upon induction, the culture were grown at 18 °C for 16 hours.

2.2.5 l-Mgm1 protein purification

Cultures were harvested and lysed with a French pressure cell press. Cell lysates were centrifuged at 10,000x g for 45 minutes at 4°C. Next, the supernatant was ultracentrifuged at 100,000x g for 90 minutes at 4°C. Pellet was resuspended by a homogenizer in 50 mM NaH_2PO_4, 300 mM NaCl, 10 mM imidazole, 10% Glycerol, 1 mM DTT, pH 8.0. 2% Triton X-100 was gradually added and incubated for 3 hours at 4°C. Ni-NTA resins were added and incubated overnight at 4°C. The flow-through was discarded, and the resins were washed with 50 mM NaH_2PO_4, 300 mM NaCl, 20 mM imidazole, 2%Triton-X 100, 10% Glycerol, 1 mM DTT, pH 8.0. 2% Triton-X 100 was exchanged to 1.5% MEGA-8 in the last wash. Ni-NTA resins were loaded onto the column for further washing and eluting. The purified fractions were concentrated and exchanged to 25 mM HEPES, 25 mM PIPES, 300 mM NaCl, 1.5% MEGA-8, 10% Glycerol, 1 mM DTT, pH 7.5 buffer and subject to size exclusion chromatography. The purified proteins were aliquoted, flashed frozen by liquid nitrogen, and stored at -80°C.

2.2.6 l-Mgm1 liposome reconstitution

l-Mgm1 was reconstituted into IM liposomes using a quick dilution method. Briefly, 4 μL of 1 mM IM liposomes were gently lysed with 1% MEGA-8 and incubated with purified 6 μL 1 mg/mL l-Mgm1 at room temperature for 1-2 hours. The mixture was diluted 10 times by adding 90 μL buffer that contains 25 mM HEPES, 25 mM PIPES, 300 mM NaCl, 10% Glycerol, 1 mM DTT, pH 7.5. The unbound l-Mgm1 aggregates were removed by centrifugation at 10,000x g for 10 minutes at 4°C. The pellet was saved and resuspended with 100 μL buffer for SDS-PAGE. Supernatant was used as liposome-reconstituted l-Mgm1. The efficiency of l-Mgm1 reconstitution was analyzed by centrifugation at 100,000x g for 90 minutes at 4°C of 10 μL. The pellet and supernatant fractions represent liposome-bound and unbound l-Mgm1, respectively. The amount of aggregated l-Mgm1, liposome-reconstituted l-Mgm1, and non-reconstituted l-Mgm1 was determined by performing SDS-PAGE and Coomassie staining of 5 μL of

resuspended pellet from the 10,000x g centrifugation, resuspended pellet from 100,000x g centrifugation, and supernatant from 100x g centrifugation, respectively.

2.3 MODEL MEMBRANES PREPARATION

2.3.1 Large unilamellar vesicles preparation

Liposomes were prepared from either 100% DMPS or mitochondrial IM phospholipid composition (Simbeni, Pon et al. 1991) as follows: 38% DMPC, 24% DMPE, 16% Liver PI, 16% TMCL, 4% DMPS, and 2% DMPA. A 10 mg/ml chloroform solution of lipid or lipid mixture was dried by rotary evaporation and vacuum pump, yielding a thin lipid film. The lipid film was rehydrated in physiological salt buffer, which contains 150 mM NaCl, and was extruded 15 times through a 0.1 μm polycarbonate Nucleopore™ track-etched membrane (Whatman) to generate large unilamellar vesicles. 1 μm polycarbonate Nucleopore™ track-etched membrane was used for electron microscopy experiments.

2.3.2 Giant unilamellar vesicles preparation

Liposomes were prepared from a lipid mixture, which contains 54% DMPC, 24% L-α-phosphatidylethanolamine (*E. coli* PE), 16% cardiolipin (*E. coli* CL), 4% DMPS, 2% DMPA, and 0.4% 1,2-dihexadecanoyl-sn-glycero-3-phosphoethanolamine (Texas Red®-DHPE, Life Technologies) (%mol). The total of 0.5 mg lipid mixture was diluted in 1 mL chloroform and transferred to a round bottom flask. The lipid mixture was dried by rotary evaporation for 2 hours at 37°C. 2 mL of Buffer A (20 mM Tris-Cl pH 7.5, 200 mM sucrose) was gently added, and the rehydration was allowed at room temperature for at least 3 hours. Alternatively, giant unilamellar vesicles (GUVs) were prepared through electroformation on platinum (Pt) wires. The chamber was constructed by sealing a circular glass slide in an aluminum fluid cell with an O-Ring and covered by a Teflon block that Pt wires are fixed to. 2 μL of 1 mg/mL lipid mixture in chloroform was deposited on each wire followed by placing the Teflon block in the vacuum for 30 minutes to ensure complete solvent evaporation. The lipid film was hydrated in 1.5 mL

Buffer A in the presence of alternated electric field at room temperature. The amplitude was progressively increased from 0.2 V to 1 V within an hour and was kept constant at 1 V for an hour with the frequency remained at 10 Hz. Vesicle detachment was done by decreasing the frequency from 10 Hz to 0.1 Hz within 30 minutes at 1 V. The electric field was applied using a function generator (Stanford Research Systems, DS345, Sunnyvale, California).

2.3.3 Lipid monolayer preparation

Lipid mixture was prepared to contain IM phospholipid composition as follows: 38% DMPC, 24% DMPE, 16% Liver PI, 16% TMCL, 4% DMPS, and 2% DMPA. Two-dimensional crystals were prepared from lipid monolayer covering the air-water interface in a Teflon well. A 0.5 μL drop of 0.1 mg/mL IM mixture, which was prepared in 9:1 chloroform/methanol, was dropped on a Teflon block filled with 20 mM Tris, 150 mM NaCl, pH 8.0 buffer. A 24-hour incubation was allowed for the lipid monolayer to form. Then, 1 mg/mL was added to on the side of the well and incubated for 24 hours. Lipid monolayer was picked up by gently placing a non-glow discharged carbon-coated grid to the surface of the well. The grids were negatively stained with 2% uranyl acetate.

2.3.4 Supported lipid bilayer preparation

Lipid mixture was prepared to contain IM phospholipid composition as follows: 38% DMPC, 24% DMPE, 16% Liver PI, 16% TMCL, 4% DMPS, and 2% DMPA (mol%). For confocal experiments, 2% DMPC or 2% DMPS were replaced by the corresponding NBD-labeled lipid, NDB-PC and NBD-PS, respectively. The lipid mixture was dried by rotary evaporation for 1.5 hours. The resulting film was rehydrated in buffer, which contains 10 mM HEPES, 150 mM NaCl, pH7.4 to form 1 mM liposomes. The rehydrated lipid was sonicated at 65°C for 20 minutes to produce small unilamellar vesicles (SUVs).

Mica was freshly cleaved and sealed with microscopy oil against a glass slide and sealed in an aluminum fluid cell with a Teflon O-Ring. The fluid cell was incubated for 5 minutes at 50°C with 400 μL HEPES buffer and 5 mM $CaCl_2$ to make the surface more hydrophilic prior to

the addition of 100 μL of the SUV suspension. After 10 minutes at room temperature, the fluid cell was flushed 3 times by adding 500 μL low salt buffer HP150 (25 mM HEPES, 25 mM PIPES, 150 mM NaCl, 1 mM DTT, 1 mM $MgCl_2$, pH 7.5) and by subsequently removing 500 μL to eliminate any excess SUVs in solution.

2.4 ACTIVITY ASSAYS

2.4.1 GTPase activity assay

The rates of GTP hydrolysis of purified Mgm1 were measured in HP500 buffer by a Malachite Green assay detecting released inorganic phosphate (Pi), which is a product of a GTP hydrolysis reaction. 50 μL of protein was added to 150 μL of reaction mix containing HP500 buffer, 5 mM $MgCl_2$ 7 mM KCl to obtain the final concentration of 0.25 μM, and incubated at 30 °C. The reaction starts when 1 mM GTP is added to the reaction mixture. A 20 μL aliquot was taken at each time point and was immediately quenched with 5 μL of 0.5 M EDTA, prior to the addition of 150 μL Malachite Green solution. Malachite Green color was allowed to develop for 1 minute and quenched with 25 μL of 34% citric acid prior to measuring of the absorbance at 650 nm. A standard curve with 0-100 μM Pi was used to convert absorbance measurements into Pi concentrations. All assays were conducted in 96-well plate format using a Molecular Devices plate reader.

2.4.2 Enzyme-linked immunosorbent assay

Lipid mixture was prepared to contain IM phospholipid composition as follows: 38% DMPC, 24% DMPE, 16% Liver PI, 16% TMCL, 4% DMPS, and 2% DMPA. 2 μg of total lipid was added to each well in a 96-well plate and allowed to coat overnight. 5% bovine serum albumin was added to each well and incubated for 1 hour to minimize non-specific binding of proteins to the wells. s-Mgm1 proteins were added at the concentrations indicated and incubated for 1 hour to allow for the binding to the coated lipids. Bound s-Mgm1 was detected by a mouse monoclonal anti-His antibody (BioShop) (1:1000 dilution), followed by horseradish peroxidase-

conjugated anti-mouse secondary antibody (Sigma) (1:5000 dilution). Color development was monitored at 655 nm using tetramethylbenzidine as a horseradish peroxidase substrate.

2.4.3 Lipid turbidity assay

The kinetic mode of a Thermo Scientific BioMate™ 3 UV-visible spectrophotometer was used to measure changes in absorbance at 350 nm (A350), which detects changes in particle size in real time. 10 μM IM liposomes were added to a 96-well plate, and its A350 absorbance was recorded as the baseline. s-Mgm1 proteins were added to 1 μM final concentration, and A350 reading was taken every 15 seconds for 30-60 minutes. Experiments were done in triplicates.

2.4.4 NBD/rhodamine lipid-mixing assay

Unlabeled liposomes were prepared from IM phospholipid composition as described above. Labeled liposomes were prepared as described above to also contain 0.8% NBD-PE and 0.8% rhodamine-PE in addition to phospholipid compositions in the IM mixture. In the lipid-mixing assay, labeled and unlabeled liposomes were mixed at the ratio of 1:9 to obtain the final concentration of 50 μM liposomes. The reaction mixtures contained 5 mM $MgCl_2$. s-Mgm1 was added to the final concentration of 0.125 μM. NBD signals were monitored by a spectrophotometer before and after protein was added. The percentage of lipid mixing is calculated by $100\times(I(t) - I(0))/(I(\infty) - I(0))$, where $I(0)$ and $I(\infty)$ are residual and maximal NBD signals, respectively. Maximal level of NBD signal $I(\infty)$ was obtained by lysing the liposomes with $C_{12}E_8$ detergent. The percentage of total lipid mixing was determined after 60 minutes.

2.4.5 HPTS/DPX content-mixing assay

Empty liposomes prepared from IM phospholipid composition as described above. The assay was done similarly to a previous study (Kreye, Malsam et al. 2008). HPTS (8-Hydroxypyrene-1,3,6-trisulfonic acid trisodium salt) and DPX (p-Xylene-bis-pyridinium bromide) loaded liposomes were prepared by rehydration lipid film in buffer containing 30 mM HPTS and 45

mM DPX. l-Mgm1 was reconstituted to both empty and HPTS/DPX-containing liposomes at equal molar concentrations by a quick dilution method as described above. Non-encapsulated HPTS and DPX were removed by dialysis. HPTS/DPX-containing liposomes were mixed with empty liposomes at the ratio of 1:9, respectively. 1 mM s-Mgm1, s-Mgm1 buffer, or 100 mM $CaCl_2$ was added, followed by the addition of 1 mM GTP. The reaction mixtures contained 5 mM $MgCl_2$. To eliminate the possibility of HPTS leakage, 45 mM DPX was included in the reaction mixture. The dequenching of the HPTS fluorescence was measured by excitation at 460 nm and emission at 520 nm. HPTS signal was measured over time for 30 minutes. % content mixing = $100\times[I(t)-I(0)]/ [I(\infty)-I(0)]$, where $I(0)$ and $I(\infty)$ are residual and maximal HPTS signal, respectively. Maximal signal was obtained by inducing content mixing with 100 mM $CaCl_2$.

2.5 CHROMATOGRAPHY

2.5.1 Size exclusion chromatography

Size exclusion chromatography was preformed on the Superdex 200 HR 10/30 column (GE Healthcare) in HP500 buffer. The column was calibrated with blue dextran, thyroglobulin (669 kDa), apoferritin (443 kDa), β-amylase (200 kDa), alcohol dehydrogenase (150 kDa), BSA (66 kDa), carbonic anhydrase (29 kDa), and cytochrome *c* (12.4 kDa). 250 µL of protein was injected at a flow rate of 0.5 mL/min, and 250 µL fractions were collected.

2.6 SPECTROSCOPY

2.6.1 Circular dichroism

Circular dichroism (CD) measurements were obtained using a Jasco J-810 instrument in a buffer containing 50 mM Tris 500 mM NaCl pH 7.5. Proteins were diluted to 0.2 mg/mL with the buffer and centrifuged at 13,200 rpm right before use. Protein solutions were allowed to

equilibrate for 5 minutes at each temperature prior to the ellipticity (millidegrees) being measured between 250 and 200 nm. Buffer alone was measured and subtracted from the protein samples. Values for mean residue ellipticity (θ_{mr}, in deg cm^2 $dmol^{-1}$) at each wavelength were obtained from the following equation: $\theta_m = \theta_{deg} M(cln_r)^{-1}$, where: θ_{deg} is the ellipticity (degrees), M is the molecular weight of the protein (grams per decimole), c is the protein concentration (grams per cubic centimeter), l is the path length (centimeters), and n_r is the number of residues in the protein.

2.7 MICROSCOPY

2.7.1 Negative stain electron microscopy

To visualized s-Mgm1 assembled liposomes, s-Mgm1 was diluted into the low salt buffer (HP150) as described above, and incubated with IM liposomes at 1:100 (protein:lipid) molar ratio at room temperature for 15 minutes. Nucleotides were added to the final concentration of 1mM and 5 mM $MgCl_2$ was added to certain experiments as indicated. Sample was prepared and visualized as previously described (Rubinstein 2007). The sample was blotted onto an EM grid and stained with 2% uranyl acetate. The samples were visualized using a Tecnai F20 electron microscope (FEI Co., Eindhoven, The Netherlands) equipped with a field emission gun and operating at 200 kV. Images were recorded at a magnification of 50,000x. Two-dimensional crystal analyses were performed by MRC imaging and 2dx programs as described previously (Crowther, Henderson et al. 1996, Gipson, Zeng et al. 2007).

2.7.2 Cryo-electron microscopy

Thin vitrified specimens were prepared at controlled temperatures and saturation and were examined at cryogenic temperatures as described previously (Danino, Bernheim-Groswasser et al. 2001). Images were recorded at low-dose conditions to minimize beam exposure and electron beam radiation damage on an Ultrascan 1000 cooled CCD camera (Gatan).

2.7.3 Epifluorescence microscopy

To monitor liposome deformation, a fluid cell was prepared by placing and sealing an O-Ring on a clean coverslip. 100 μM Liposome suspension was added to the fluid cell filled with buffer that contains 20 mM Tris-Cl, 150 mM NaCl, pH 7.4. Proteins were added to the fluid cell to the final concentration of 1 μM (1:100, protein:lipid molar ratio), and GTP/GDP was added to the final concentration of 1 mM in the absence of $MgCl_2$. An Olympus microscope equipped with Chroma ET-mCherry and ET-GFP filter sets, a Hamamatsu Orca-AG Cool Charge-Coupled Digital camera, and Volocity (Improvision, PerkinElmer) was used for image acquisition and analysis.

2.7.4 Confocal fluorescence microscopy

In a supported lipid bilayer experiment, imaging was conducted on an Olympus FluoView 300 confocal microscope equipped with an IX-70 inverted microscope using a PLAN-APO 60x 1.45 NA objective and a 488 nm laser. The bilayer was imaged once at 1x digital zoom, then every 15 seconds for 15 minutes at 10x. After the fourth frame, 25 μL of control buffer was added as a control or 25 μL of s-Mgm1 was added to obtain the final concentration of 0.4 μM. GTP was added to a final concentration of 1 mM and another time stack was created in the same fashion.

To obtain a three-dimensional reconstruction of an s-Mgm1-bound liposome, confocal fluorescence microscopy was used to collect thin sections of liposomes. An Olympus FluoView 300 confocal microscope, which comprises an IX-70 inverted microscope using a PLAN-APO 60x 1.45 NA objective, a 488 nm laser, and a 543 nm laser. FluoView software (Olympus) was used for image acquisition. A series of thin sections with 0.2 μm in separation was taken. ImageJ was used for image analysis and was used to perform three-dimensional reconstruction of liposomes (http://rsb.info.nih.gov).

2.7.5 Atomic force microscopy

Atomic force microscopy (AFM) images were obtained in a tapping mode using a Digital Instruments/Veeco/Bruker Bioscope scanning probe microscope with an E scanner and the Nanoscope IIIA controller using Nanoscope software (v5.30r3).

2.8 YEAST

2.8.1 *In vivo* complementation assay and imaging morphology

Mutant strains (BY4741 background strain) carrying test plasmids were generated by a plasmid shuffle method. *MGM1* gene in a pRS313 plasmid was a gift from Dr. Michael P. Yaffe. Point mutations were generated by QuickChange® site-directed mutagenesis (Stratagene). pRS313 Mgm1 plasmids were transformed into *mgm1Δ* strain that contains pRS316 WT Mgm1 plasmid and selected for by culturing in a synthetic complete medium lacking histidine. pRS316 WT Mgm1 plasmid was removed by culturing in the synthetic complete medium that contains 5-Fluoroorotic Acid (5-FOA). For imaging of mitochondrial morphology, yeast strains were expressing a mitochondrial targeted GFP, MTS-GFP.

Chapter 3

3 PHOSPHOLIPID ASSOCIATION IS ESSENTIAL FOR MGM1 FUNCTION IN MITOCHONDRIAL MEMBRANE FUSION

Published: Rujiviphat, J., G. Meglei, J. L. Rubinstein and G. A. McQuibban (2009). "Phospholipid association is essential for dynamin-related protein Mgm1 to function in mitochondrial membrane fusion." J Biol Chem **284**(42): 28682-28686.

Data attributions: Gabriela Meglei performed enzyme-linked immunosorbent assays. Dr. John L. Rubinstein performed two-dimensional crystal analyses. Dr. G. Angus McQuibban performed *in vivo* complementation assays and mitochondrial morphology analyses.

Acknowledgements: I thank Stephanie Bueler for assistance with electron microscopy.

3.1 SUMMARY

Mgm1 is a key component in mitochondrial membrane fusion and is required for maintaining mitochondrial dynamics and morphology. Meglei and McQuibban showed that the purified short isoform of Mgm1 (s-Mgm1) possesses GTPase activity, self-assembles into low-order oligomers, and interacts specifically with negatively charged phospholipids (Meglei and McQuibban 2009). Here, I demonstrate that s-Mgm1 binds to a mixture of phospholipids characteristic of the mitochondrial inner membrane. Binding to physiologically representative lipids results in ~6-fold stimulation of s-Mgm1 GTPase activity. s-Mgm1 point mutants that are defective in oligomerization, and lipid binding do not exhibit such stimulation and do not function *in vivo*. Electron microscopy and lipid turbidity assays demonstrate that s-Mgm1 promotes liposome interaction. Furthermore, s-Mgm1 assembles onto liposomes as oligomeric rings with 3-fold symmetry. The projection map of negatively stained s-Mgm1 shows six monomers, consistent with two stacked trimers. Taken together, I identify a possible lipid-binding domain in Mgm1 and suggest a model of how Mgm1 could promote the fusion of opposing mitochondrial inner membranes.

3.2 INTRODUCTION

Mitochondrial dynamics have been implicated in neurodegenerative diseases such as dominant optic atrophy and Parkinson's disease (Whitworth, Lee et al. 2008, Park, Kim et al. 2009). Mitochondrial morphology is regulated by balanced membrane fusion and fission reactions that are orchestrated by members of the highly conserved dynamin-related protein (DRP) family (Okamoto and Shaw 2005). DRPs are large GTPases that can self-assemble and promote membrane remodeling (Shaw and Nunnari 2002, Hoppins, Lackner et al. 2007). Meglei and McQuibban have shown previously that the dynamin-related protein Mgm1 has GTPase activity, self-assembles into low-order oligomers, and binds to negatively charged phospholipids (Meglei and McQuibban 2009). Mgm1 exists as two isoforms in the mitochondria; l-Mgm1 is anchored to the IM via a transmembrane domain, and s-Mgm1 is peripherally associated with the IM and also found in the IMS. s-Mgm1 results from the regulated cleavage by the mitochondrial rhomboid protease (McQuibban, Saurya et al. 2003, Herlan, Bornhovd et al. 2004). It was shown recently that both isoforms are essential but have distinct roles in mitochondrial

membrane fusion, whereby only s-Mgm1 requires its GTPase activity (Zick, Duvezin-Caubet et al. 2009). It is proposed that l-Mgm1 serves as a receptor for s-Mgm1 to mediate fusion of opposing membranes upon GTP hydrolysis. Here, I provide molecular data indicating that lipid binding of s-Mgm1 is required for proper membrane fusion. Furthermore, structural analysis of s-Mgm1 assembled onto liposomes suggests a model whereby stacked trimers of s-Mgm1 on opposing membranes would facilitate fusion.

3.3 RESULTS

3.3.1 Conserved lysines constitute a lipid-binding domain within s-Mgm1

s-Mgm1 interactions with single phospholipids were assayed by lipid overlay Western blotting (Meglei and McQuibban 2009). s-Mgm1 interacts with three negatively charged phospholipids: CL, PS, and PA. To further confirm and characterize the protein-lipid interactions, an enzyme-linked immunosorbent assay was conducted to quantitatively monitor the association of s-Mgm1 with a phospholipid mixture whose composition resembles the mitochondrial IM (Simbeni, Pon et al. 1991). Wild-type (WT) s-Mgm1 and several potential lipid-binding point mutants within the putative lipid-binding domain were tested for their interactions with IM lipid mixture.

Sequence alignment of 22 fungal sequences homologous to Mgm1 identified several conserved lysines: K544, K566, K724, K745, K795, and K804, which reside within the region between the middle domain and the GED (Meglei and McQuibban 2009). These positively charged lysine residues could serve as interaction motifs for the negatively charged phospholipids (**Figure 3.1, A**). K854 was also included in the analyses, as this residue is known to be required for s-Mgm1 protein oligomerization (Meglei and McQuibban 2009). Consistent with the previous report, K795A was severely compromised in lipid binding (**Figure 3.1, B**). Furthermore, K566A and K724A displayed a significant reduction in lipid binding compared with WT s-Mgm1 (**Figure 3.1, B**). In contrast, K544A, K745A, K804A, and K854A showed little difference in lipid binding compared with WT s-Mgm1 (**Figure 3.1, B**).

In addition, I conducted a spectroscopic turbidity assay (Connell, Scott et al. 2008). This assay measures the ability of Mgm1 not only to interact with liposomes but also to induce aggregation presumably based on *trans* interactions of Mgm1 on opposing liposomes. WT, K544A, K745A, and K854A were able to induce significant liposome aggregation, whereas K724A and K804A induced moderate liposome aggregation (**Figure 3.1, C**). K566A and K795A were completely devoid of this activity (**Figure 3.1, C**). To demonstrate that the mutant Mgm1 proteins did not undergo significant protein misfolding, I conducted size exclusion chromatography and circular dichroism (CD) analyses (**Figure 3.1, D and E**). The traces of K566A, K724A, and K795A overlapped with that of WT s-Mgm1 in both assays, indicating that these point mutants maintain proper folding and oligomerization properties. These results demonstrate that several conserved lysines in this region of s-Mgm1 are required to maintain proper lipid interaction. Given the position of this domain between the middle and GTPase effector domains of Mgm1, I propose that this region provides a lipid interaction interface similar to the PH domain in other dynamins (Praefcke and McMahon 2004).

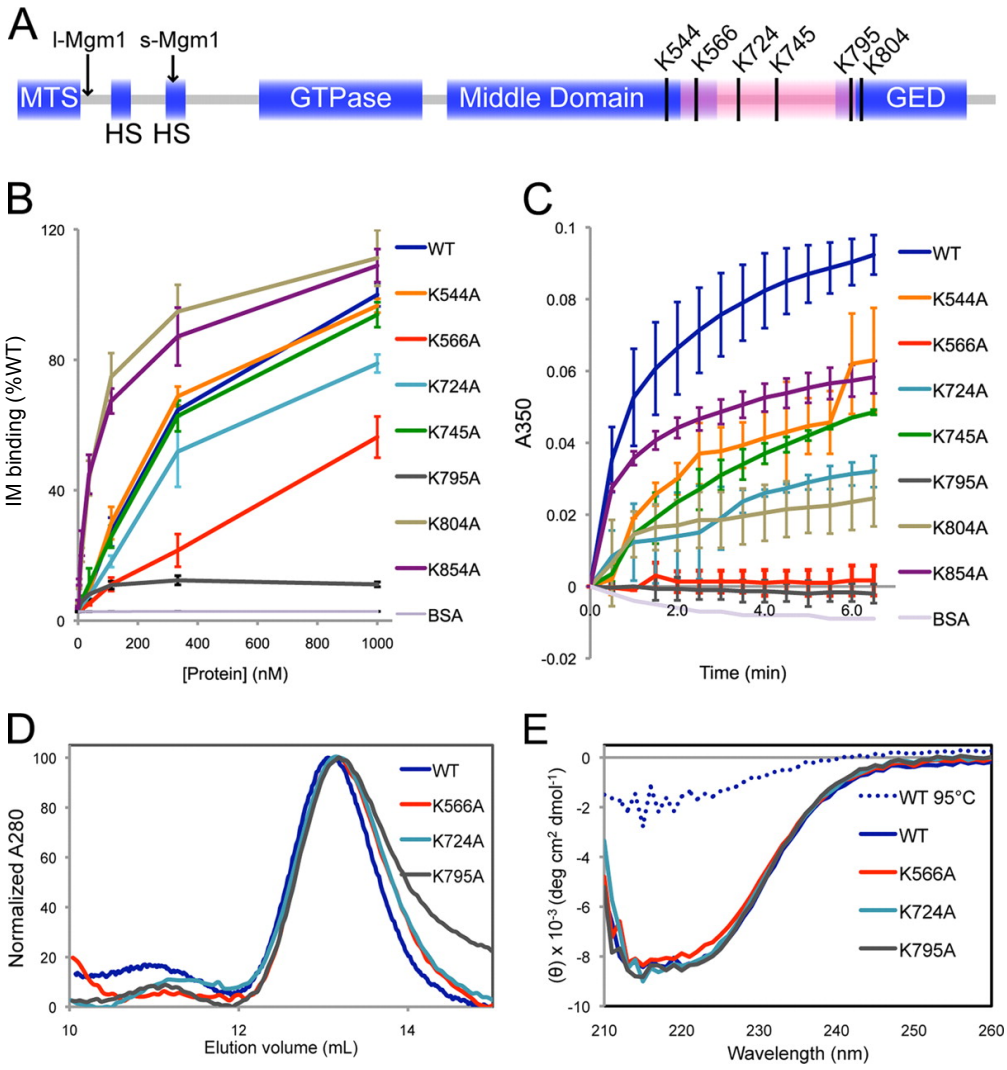

Figure 3.1. s-Mgm1 contains a lipid-binding domain that directly binds to lipids of the mitochondrial IM

(**A**) An Mgm1 schematic diagram illustrates the mitochondrial targeting sequence (MTS), hydrophobic segments (HS), GTPase domain, middle domain, and GTPase effector domain (GED). *Arrows* indicate the cleavage sites for processing into l-Mgm1 and s-Mgm1. The predicted lipid-binding domain is highlighted in *pink*, and the conserved lysines in this region are indicated. (**B**) The binding of s-Mgm1 and several lysine mutants to IM liposomes was assayed by an enzyme-linked immunosorbent assay. The amount of s-Mgm1 lysine mutants bound to the IM-coated wells was normalized to that of WT s-Mgm1 (% WT). BSA, bovine serum albumin. (**C**) Liposome aggregation induced by s-Mgm1 and lysine mutants was assayed by monitoring lipid turbidity at 350 nm. (**D**) WT s-Mgm1 and three representative lysine point mutants were subjected to size exclusion chromatography. (**E**) The results from CD spectroscopy of WT s-Mgm1 and three representative lysine mutants. WT s-Mgm1 after heat denaturation was included as a control for the unfolded state. IM liposomes were made from a mixture of phospholipids with the corresponding physiological concentrations: CL, 16%; PE, 24%; PA, 2%; PS, 4%; PC, 38%; and PI, 16%. deg, degrees. *Error bars* represent standard deviations. Source: Taken from Rujiviphat, Meglei et al. (2009).

3.3.2 s-Mgm1 GTPase activity is stimulated by phospholipids

Meglei and McQuibban previously characterized the GTPase activity of purified Mgm1, which was consistent with a basal level of hydrolysis found in other proteins in the dynamin superfamily (2009). Classical dynamins are known to undergo stimulated GTPase activity upon lipid-induced oligomerization (Praefcke and McMahon 2004). I therefore tested the ability of a variety of phospholipids to stimulate the activity of s-Mgm1. To test this, 1 μM s-Mgm1 was incubated with 300 μM liposomes in low salt buffer HP170 for 30 minutes prior to GTPase activity measurement by malachite green GTPase assay as previously described (Meglei and McQuibban 2009). Of the lipids tested, I found that PS stimulated the GTPase activity of s-Mgm1 by 55-fold, whereas PA- and CL-containing liposomes stimulated the GTPase activity by 14- and 9-fold, respectively (**Figure 3.2, A**). Importantly, these are the lipids that were previously reported to associate with s-Mgm1, and CL is physiologically relevant to the mitochondrial IM (Schlame and Hostetler 1997).

Furthermore, I tested whether a mixture of lipids representing the content of the mitochondrial IM could stimulate s-Mgm1 GTPase activity. The IM liposomes had the following content: 16% CL, 24% PE, 2% PA, 4% PS, 38% PC, and 16% PI. IM liposomes were able to stimulate the GTPase activity by 6-fold in a dose-dependent fashion (**Figure 3.2, A and B**). These results demonstrate that Mgm1 behaves similarly to other dynamin proteins and suggest that lipid interaction is mechanistically important for Mgm1 to function at the mitochondrial IM.

3.3.3 s-Mgm1 lipid binding is required for stimulated GTPase activity

Classical dynamin has a PH domain between the middle domain and the GED that mediates lipid association (Praefcke and McMahon 2004). Here, I identified several conserved lysines that contribute to lipid binding (**Figure 3.2, A and B**). I proposed that the region contains these lipid-binding lysines forms a lipid-binding module in Mgm1. I therefore investigated whether these mutants are impaired in IM liposome-stimulated GTP hydrolysis. The GTPase activities of K566A, K724A, K795A, and K854A were not stimulated in the presence of liposomes, whereas

K544A, K745A, and K804A exhibited IM-dependent stimulation of GTP hydrolysis (**Figure 3.2, C**). K854A does not undergo oligomerization (Meglei and McQuibban 2009) but maintains lipid interaction (**Figure 3.1, B**) and serves as a control for oligomerization-dependent stimulation (**Figure 3.2, C**). These data suggest that both phospholipid interaction and oligomerization are necessary for the stimulation of GTPase activity and that Mgm1 contains a lipid interaction domain similar to the PH domain in other dynamins.

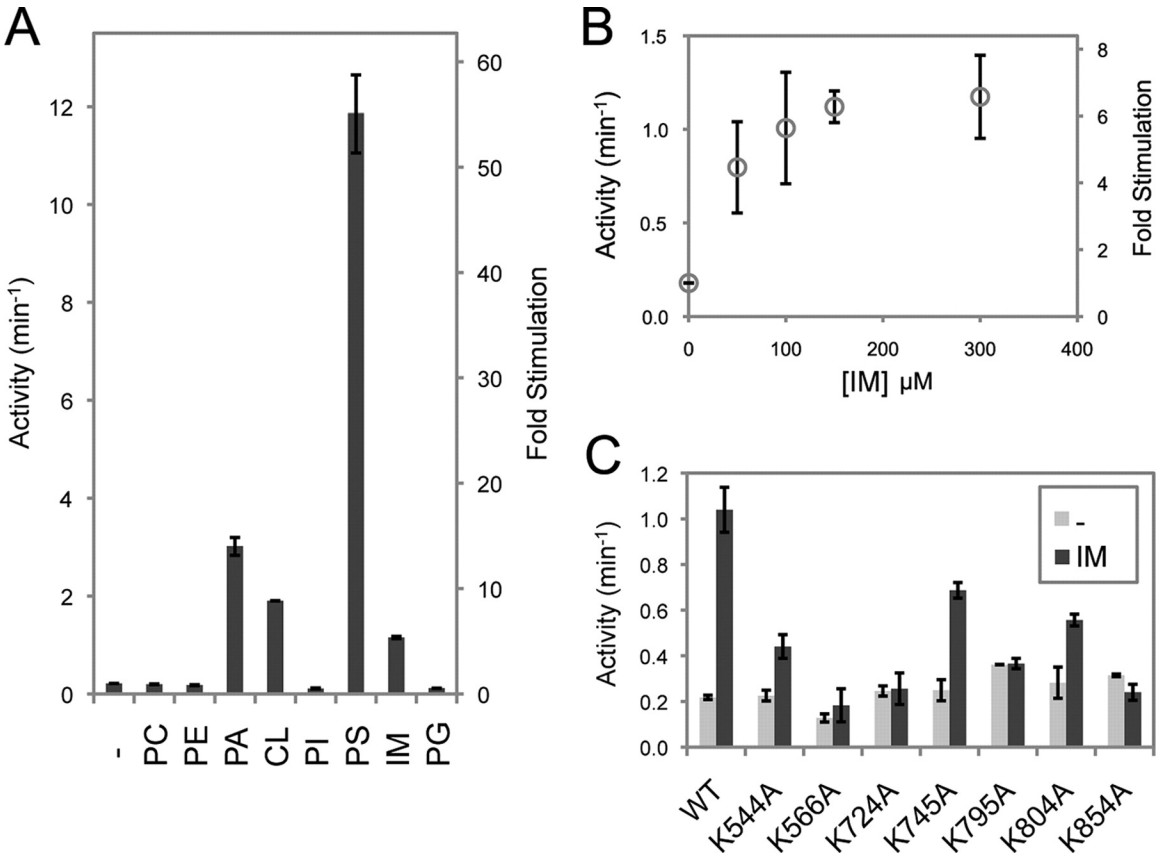

Figure 3.2. s-Mgm1 binding to lipids results in stimulated GTPase activity

(**A**) The GTPase activity of s-Mgm1 was assayed in the presence or absence of various phospholipid-containing liposomes (1:100, protein: lipid molar ratio). The fold stimulation was calculated in relation to the basal activity of s-Mgm1 in the absence of liposome. Phosphatidylglycerol (PG) is a negatively charged phospholipid but is not present in the mitochondrial IM and served as a control. PC, phosphatidylcholine; PE, phosphatidylethanolamine; PA, phosphatidic acid; CL, cardiolipin; PI, phosphatidylinositol; PS, phosphatidylserine. (**B**) The GTPase activity of s-Mgm1 in response to increasing concentrations of IM liposome was determined. (**C**) The GTPase activity of lysine point mutants in the putative lipid-binding domain of s-Mgm1 were tested in response to the presence of IM liposomes. All of the experiments were done in triplicate. *Error bars* represent standard deviations. Source: Taken from Rujiviphat, Meglei et al. (2009).

3.3.4 s-Mgm1 displays positive cooperativity in GTPase activity

Lipid-stimulated GTPase activities of other dynamins have been well studied, and the stimulation is known to be due to self-assembly of the dynamin onto liposomes (Mears and Hinshaw 2008). Meglei and McQuibban have investigated the effect of s-Mgm1 self-assembly on GTPase activity (2009). They showed that s-Mgm1 can self-assemble into low order

oligomers under high salt conditions (500 mM NaCl). Here, I determined the GTPase activity of WT s-Mgm1 and the oligomerization-defective mutant K854A at various protein concentrations under low salt (170 mM NaCl) conditions. I found that GTP hydrolysis of WT s-Mgm1 increased in a non-linear fashion compared with the oligomerization-defective mutant K854A (**Figure 3.3, A and B**). The sigmoidal curve in the activity plot indicates positive cooperativity at low concentrations of the WT. A sharp increase in WT GTPase activity was observed at protein concentrations of 0.2–0.4 μM. In contrast, I observed a slow increase in GTP hydrolysis for the K854A mutant. These data further support the idea that oligomerization of s-Mgm1 is essential for its GTPase activity and function.

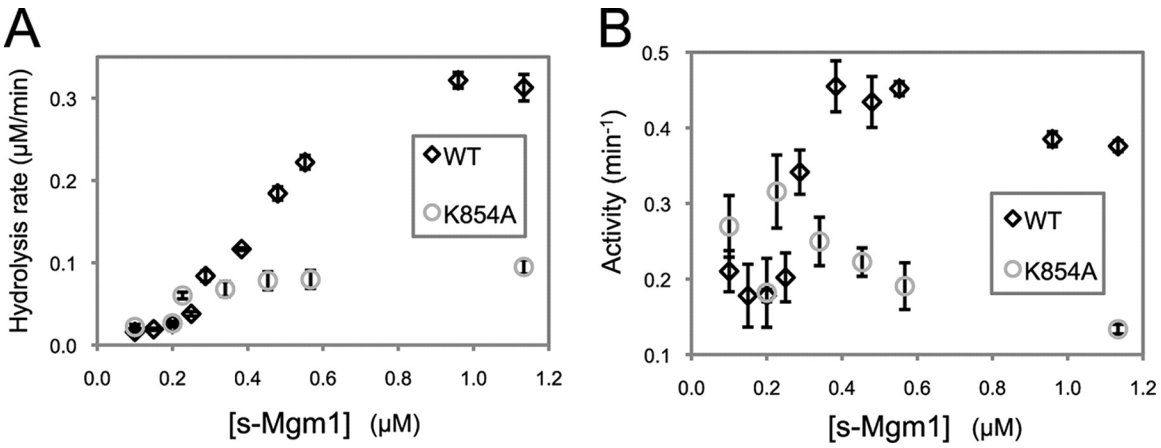

Figure 3.3 Oligomerization induces stimulated GTPase activity

The GTP hydrolysis of s-Mgm1 was determined as the concentration of WT s-Mgm1 or mutant K854A was increased. The same set of data was plotted as GTP hydrolysis rate (**A**) and specific activity (**B**). All of the experiments were done in triplicate. *Error bars* represent standard deviations. Source: Taken from Rujiviphat, Meglei et al. (2009).

3.3.5 *In vivo* complementation of s-Mgm1 requires lipid association

To further understand the biological role of Mgm1 lipid binding, complementation studies in yeast were conducted using a plasmid shuffle approach. K544A, K566A, K724A, K745A, K795A, and K804A were tested for the ability to restore normal growth and normal

mitochondrial morphology to cells lacking WT Mgm1. K566A and K795A could not complement mitochondrial morphology or growth (**Figure 3.4, A and C**). K544A and K724A displayed some rescue of mitochondrial morphology. K745A and K804A retained almost WT levels of mitochondrial morphology and growth (**Figure 3.4, A and C**). Importantly, all mutants were expressed at similar levels and produced equivalent amounts of both l-Mgm1 and s-Mgm1 (**Figure 3.4, D**). Consistently, the *in vivo* complementation ability of these point mutants correlates well with the *in vitro* ability of these mutants to interact with and be stimulated by IM lipids. Taken together, these data demonstrate that the lipid-binding activity of Mgm1 is required for this protein to function properly *in vivo* and provide compelling evidence that Mgm1 contains a lipid-binding domain.

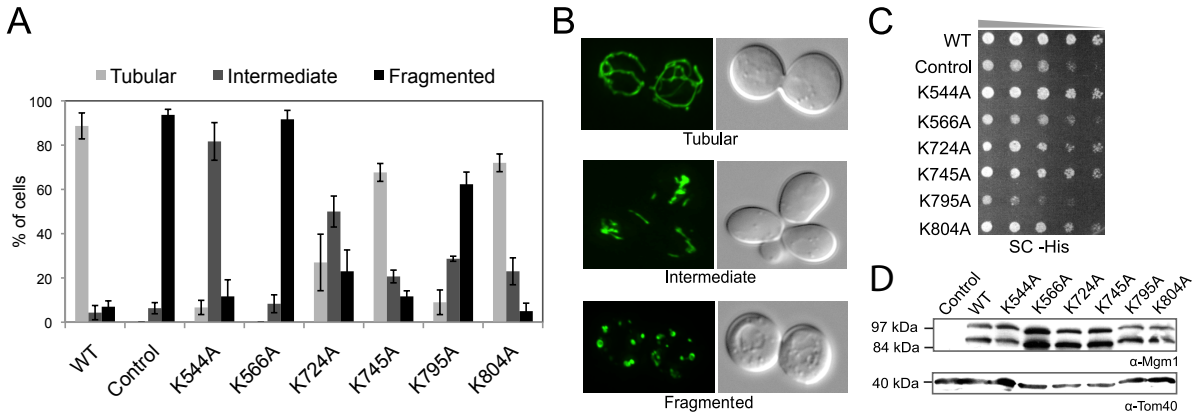

Figure 3.4. s-Mgm1 mutants defective in IM binding and stimulated GTPase activity have impaired function *in vivo*

(**A**) The mitochondrial morphology of complementation strains was scored by fluorescence microscopy of a mitochondria-targeted green fluorescent protein. 300 cells were counted for each mutant complementation experiment. (**B**) Representative micrographs of mitochondrial green fluorescent protein morphology that categorizes tubular (*upper panel*), intermediate (*middle panel*), and fragmented (*lower panel*) morphology. (**C**) Serial dilution onto synthetic complete medium (SC) demonstrated growth rates of lipid-binding mutants. (**D**) Western blot analysis of mutant strains demonstrated that Mgm1 was processed in all mutants tested (*upper panel*) and expressed to similar levels normalized to Tom40 levels (*lower panel*). Control represents no Mgm1 expressed. Source: Taken from Rujiviphat, Meglei et al. (2009).

3.3.6 s-Mgm1 causes aggregation of IM liposomes

The self-assembly of dynamins onto lipids and their ability to promote tubulation of liposomes have been thoroughly studied and visualized by electron microscopy (EM) (Mears and Hinshaw 2008). Therefore, I tested whether s-Mgm1 can induce tubulation of IM liposomes. Instead of tubulation, I observed that s-Mgm1 induced the assembly of liposomes into aggregates compared with a bovine serum albumin control (**Figure 3.5, A and B**). In agreement with the lipid binding studies above, I found that the lipid-binding mutant K795A could not induce liposome aggregation (**Figure 3.5, A**). In addition, I found that the oligomerization-defective mutant K854A was also impaired in lipid aggregation. The reduction in the level of liposome aggregation by K795A and K854A is consistent with the data from the liposome turbidity assay (**Figure 3.1, C**). These results indicate that both lipid binding and Mgm1 assembly into oligomers are required to induce liposome assembly.

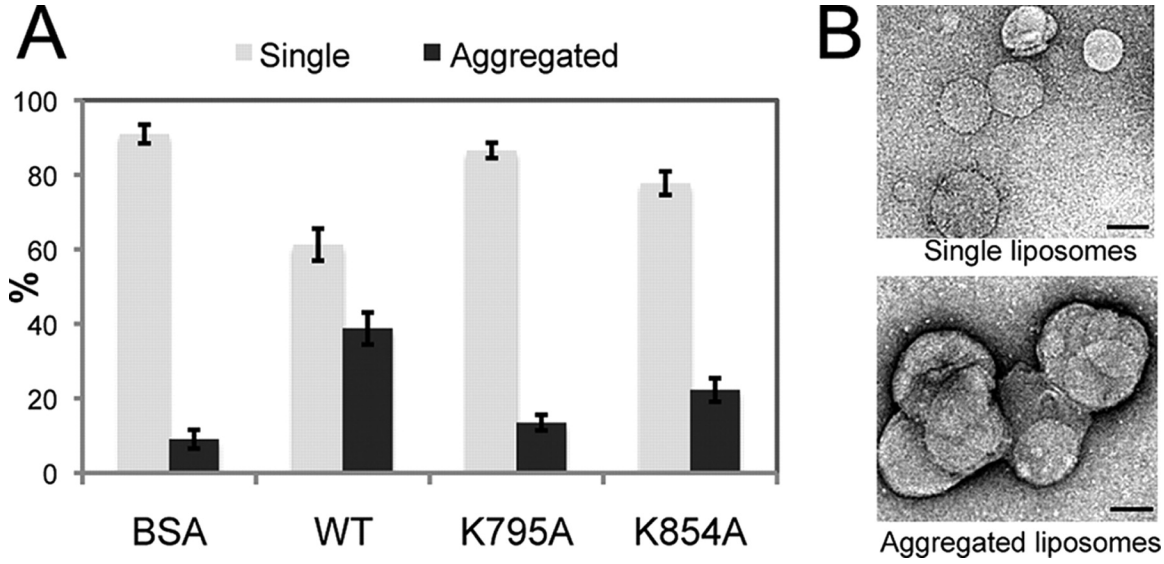

Figure 3.5. s-Mgm1 promotes liposome aggregation

(**A**) EM analysis was performed to visualize and quantify the extent of lipid aggregation induced by s-Mgm1. BSA, bovine serum albumin. (**B**) The liposomes were categorized into either single liposomes (*gray bars*) or large liposome aggregates (*black bars*). Scale bars represent 0.1 μm. All of the experiments were done in triplicate. *Error bars* represent standard deviations. Source: Taken from Rujiviphat, Meglei et al. (2009).

3.3.7 s-Mgm1 assembles onto IM liposomes and forms a two-dimensional crystalline array

Although s-Mgm1 on its own did not induce liposome tubulation, EM analysis revealed arrays of s-Mgm1 rings on IM liposomes (**Figure 3.6, A**). The arrays were composed of regions of ordered lattice. Processing of images with two-dimensional crystal analysis software (Gipson, Zeng et al. 2007) showed that well ordered regions contain a single lattice with p3 symmetry. To calculate an average projection of the stained s-Mgm1 oligomer, approximately 1000 images of oligomers were interactively selected from images of crystals and treated as unordered single particles. Oligomer images were rotationally and translationally aligned and averaged without assuming any symmetry. The resulting average revealed six densities arranged with clear 3-fold symmetry. The diameter of each unit density is approximately 50 Å, which is consistent with an 86-kDa s-Mgm1 monomer. A high signal-to-noise symmetrized average and contour map are shown (**Figure 3.6, B and C**). Given the clear difference in staining of the two different types of monomer in the hexamer, I propose that this reflects two s-Mgm1 trimers that have stacked on top of each other with a 60° rotational offset. Stacking of trimers could represent *trans* interactions of Mgm1 to tether membranes to promote mitochondrial IM fusion.

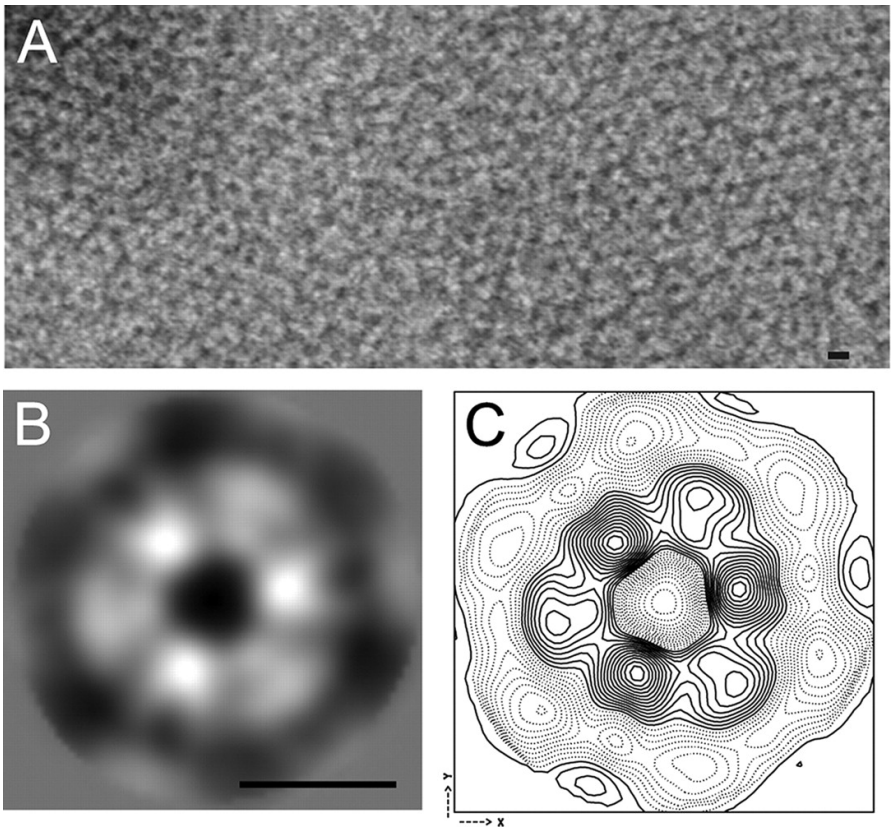

Figure 3.6. s-Mgm1 assembles onto IM liposomes as oligomeric rings

1 mg/mL (0.86 μM) of s-Mgm1 was incubated with 100 μM IM liposomes for 30 min. 4 μL of reaction mixture was absorbed on a glow-discharged carbon coated grid and stained with 2% uranyl acetate/. (**A**) Oligomeric rings of s-Mgm1 assembled onto IM liposomes. A small patch of an ordered array formed by s-Mgm1 is shown. (**B**) Averaged image of the s-Mgm1 particle that consists of six monomer densities. (**C**) Contour map of the s-Mgm1 hexamer. *Scale bars* represent 10 nm. Source: Taken from Rujiviphat, Meglei et al. (2009).

3.4 DISCUSSION

In this study, I provide data indicating that lipid binding of s-Mgm1 is required for proper membrane fusion. Furthermore, structural analysis of s-Mgm1 assembled onto liposomes suggests a model whereby stacked trimers of s-Mgm1 on opposing membranes facilitate IM fusion.

3.4.1 Mgm1-phospholipid associations

Lipid-binding activity is a hallmark activity of the dynamin superfamily proteins. Meglei and McQuibban previously demonstrated that s-Mgm1 interacts with negatively charged CL, PS, and PA individually by a lipid-overlay assay (2009). Here, I show that s-Mgm1 also interacts with these phospholipids in a bilayer context. Phospholipid interactions were demonstrated by two approaches: enzyme-linked immunosorbent assay and liposome recruitment. These methods are more physiologically relevant than the lipid overlay assay because they provide interactions between proteins and phospholipid head groups (Meglei and McQuibban 2009). In the enzyme-linked immunosorbent assay, Nunc-Immuno™ polysterene PolySorp® plate was used to investigate s-Mgm1-lipid interactions. PolySorp® treated surface provides high affinity to hydrophobic molecules. Therefore, lipids were bound to the plate by their fatty acid chains exposing their head groups to the solution for s-Mgm1 binding, which resembles s-Mgm1's association with the IM *in vivo*. Similarly, liposomes also allow protein-lipid head group interactions and provide a bilayer system with a phospholipid composition characteristic of mitochondrial IM.

By an enzyme-linked immunosorbent assay, s-Mgm1 was shown to interact with a lipid mixture, which has phospholipid composition characteristic of the IM, in a dose-dependent manner (**Figure 3.1, B**). Consistently, s-Mgm1 was readily recruited to IM liposomes, and s-Mgm1-assembled liposomes were visualized by negative stain EM (**Figure 3.6, A)**. This Mgm1-IM association was also confirmed by a recent study (DeVay, Dominguez-Ramirez et al. 2009). DeVay et al. showed that s-Mgm1 had a preference for liposomes with IM composition containing 20% CL (IMC 20%CL) rather than with liposomes with OM composition 6% CL (OMC 6%CL). They also showed that this interaction is specific to CL because s-Mgm1-liposome association was drastically reduced when CL was removed from the IMC (IMC 0%CL). l-Mgm1 also preferentially inserted into IMC 20%CL but not IMC 0%CL liposomes. Therefore, the absence of CL would abolish most of Mgm1-IM association. However, in the cell, IM also contains high protein contents that may influence Mgm1 function. It is conceivable that, in addition to CL, certain IM proteins may play a role in Mgm1-membrane association. Together, these results along with the previous findings (DeVay, Dominguez-Ramirez et al. 2009, Meglei and McQuibban 2009) demonstrate that Mgm1 associates with the IM and the

affinity could be via Mgm1 specific interactions with certain negatively charged phospholipids, especially CL.

3.4.2 s-Mgm1 GTP hydrolysis is stimulated by lipid binding and s-Mgm1 oligomerization

In addition to s-Mgm1-lipid association, I characterized the oligomerization properties of s-Mgm1. s-Mgm1 oligomerization was observed by negative stain EM (**Figure 3.6**). In a liposome binding experiment, s-Mgm1 was readily recruited to the liposomes as hexameric rings. Even though s-Mgm1's monomeric size, which is predicted to be approximately 5 nm in diameter, was not resolved by negative stain EM, the s-Mgm1 hexameric ring was observed to have a diameter of approximately 20 nm. These hexameric rings were clearly observed on liposomes but not in the solution, suggesting that s-Mgm1 may form hexameric rings only when it assembles onto liposomes, and that lipid binding could promote s-Mgm1 oligomerization.

s-Mgm1 oligomerization was previously observed (Meglei and McQuibban 2009). Here, I show the positive cooperativity of s-Mgm1 GTPase activity, suggesting that oligomerization could be essential for s-Mgm1 GTPase activity (**Figure 3.3, A and B**). In addition, DeVay et al. and Zick et al. showed that s-Mgm1 and l-Mgm1 interact in homo- and heterotypic manners, and that the l-Mgm1 simulates the GTPase activity of s-Mgm1 (DeVay, Dominguez-Ramirez et al. 2009, Zick, Duvezin-Caubet et al. 2009).

Classical dynamins interact with PI via their positively charged residues in their PH domain. A single PH domain has low affinity for PI, whereas protein oligomerization induces strong membrane association (Praefcke and McMahon 2004). The switch from low to high affinity for phospholipids upon protein oligomerization could serve as a tight control for GTPase activation, suggesting that stimulated GTPase activity relies on both protein-lipid interactions and protein oligomerization. Consistently, in this study, I show that s-Mgm1 phospholipid association and oligomerization stimulates the GTPase activity of s-Mgm1. The lipid-binding-dependent stimulation of GTPase activity was also observed by DeVay et al. (DeVay, Dominguez-Ramirez et al. 2009). The basal GTPase activity of OPA1, which is the human homologue of Mgm1, is also enhanced by its association with CL-containing liposomes (Ban,

Heymann et al. 2010). Interestingly, this stimulation is abolished in a disease allele mutant, which is defective in lipid binding. Together, these findings support the notion that the lipid-binding activity and lipid-dependent stimulation of GTP hydrolysis are crucial for Mgm1 function.

DeVay et al. and I showed that the basal level of s-Mgm1 GTPase activity was little to none (DeVay, Dominguez-Ramirez et al. 2009). Therefore, GTPase stimulation may act as a crucial regulatory step for Mgm1 function. Unlike other GTPases, proteins in the dynamin superfamily do not require a GTP exchange factor (GEF) to allow GTP binding, which in turn activates the GTPase activity. Instead, Mgm1-lipid association and Mgm1 oligomerization may be crucial to promote GTP binding and hydrolysis to drive membrane fusion.

3.4.3 A possible lipid-binding domain of Mgm1

Although DRPs do not possess a PH domain, several DRPs associate with negatively charged phospholipids in a similar region as the PH domain, which is between the middle domain and the GED. As discussed above, s-Mgm1 also binds to certain negatively charged phospholipids and IM liposomes. Three conserved lysine residues are shown here to be crucial for the GTPase activity of s-Mgm1 *in vitro* and Mgm1 function *in vivo*. These three residues, K566, K724, and K795, span the region between the middle domain (amino acids 438-undefined) and the GED (amino acids 801-902). An atomic model structure for s-Mgm1 was recently proposed by a combination of homology and threading modeling and structure docking into a three-dimensional reconstruction (DeVay, Dominguez-Ramirez et al. 2009). In this structure, the region between the middle domain and the GED forms two helices that face the membrane. Therefore, the mutagenesis studies presented here along with the model structure of Mgm1 suggest that s-Mgm1 has a lipid-binding region, which is between the middle domain and the GED similar to the PH domain of dynamin. Moreover, it is possible that this region represents a functional lipid-binding domain unique to Mgm1 since this region has no homology to other known lipid-binding domain (Meglei and McQuibban 2009).

3.4.4 A possible role of s-Mgm1 in the tethering step of IM fusion

The first step of a membrane fusion event is to tether opposing membranes. The membranes have to be docked and stabilized for the membrane fusion process to occur. Several membrane fusion molecules like Fzo1 and atlastins are already anchored to membranes, and their *trans* interactions bring the membranes close to one another. Here, I show that s-Mgm1 associates and assembles onto IM-like membranes. Moreover, I show that s-Mgm1 oligomerization and *trans* interaction tethers IM liposomes, which are highly negatively charged. Therefore, these data suggest that s-Mgm1-lipid interaction and s-Mgm1 *trans* interaction are strong enough to stabilize opposing membranes together in close proximity. These interactions are independent of GTP, suggesting that although GTP binding and hydrolysis are important for the lipid-mixing step, it is not required for the tethering step in Mgm1-mediated IM fusion.

A two-dimensional crystal analysis reveals that membrane-bound s-Mgm1 oligomerizes as a hexameric ring that contains two different kinds of monomers (**Figure 3.6**). The difference could be explained by proposing that the monomers are on two different planes, suggesting that the hexameric ring could be two trimeric rings stacked together (**Figure 3.7**). Each trimer could be on the opposing membranes, and the stacking of two trimers could be the mechanism of how s-Mgm1 tethers opposing membranes together. Similarly, DeVay et al. also observed uniform organization of s-Mgm1 on CL-containing liposomes (DeVay, Dominguez-Ramirez et al. 2009). The authors performed two-dimensional crystallization and showed a trimer of densities. Each density can be separated into dimers, resulting in a hexameric ring-like structure similarly to the hexameric structure observed in this study. Therefore, the hexameric structure of s-Mgm1 could be essential for s-Mgm1 function in the tethering step of IM fusion.

Although future studies are still required to fully understand the exact mechanism of Mgm1-mediated membrane fusion, these data highlight the importance of Mgm1-phospholipid association to maintain mitochondrial dynamics.

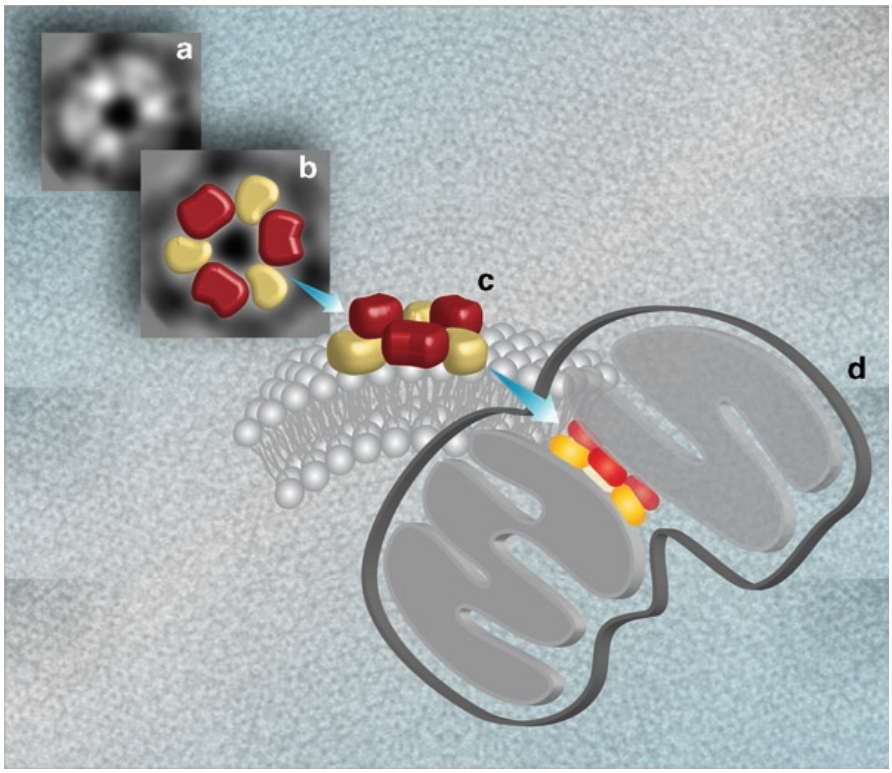

Figure 3.7. Model of s-Mgm1 mechanistic actions during the tethering step of mitochondrial IM fusion

Images from the *top left* to the *bottom right* corner show an averaged image of s-Mgm1 oligomeric rings to a proposed model of Mgm1-mediated mitochondrial fusion. The background pattern shows s-Mgm1 assembled onto liposomes as oligomeric rings. An averaged image of the s-Mgm1 oligomer consists of six monomer densities (**A**). These six monomers can be interpreted as two stacks of trimers shown in *red* and *yellow* (**B**). These stacking trimers could be how s-Mgm1 tethers two opposing membranes to mediate membrane fusion (**C** and **D**). Source: Taken from Chan, Rujiviphat et al. (2011).

Chapter 4

4 MEMBRANE TETHERING AND GTP-DEPENDENT CONFORMATIONAL CHANGES DRIVE MGM1-MEDIATED MITOCHONDRIAL FUSION

Published: Abutbul-Ionita, I., J. Rujiviphat, I. Nir, G. A. McQuibban and D. Danino (2012). "Membrane tethering and nucleotide-dependent conformational changes drive mitochondrial genome maintenance (Mgm1) protein-mediated membrane fusion." J Biol Chem **287**(44): 36634-36638.

Data attribution: Inbal Abutbul-Ionita performed cryo-electron microscopy experiments.

Acknowledgements: I thank Dr. John L. Rubinstein, Stephanie Bueler and Dr. Lindsay Baker for assistance with electron microscopy analysis and two-dimensional crystal analysis. I thank Dr. Alan Davidson and Dr. David Isenman for assistance with circular dichroism analysis.

4.1 SUMMARY

Cellular membrane-remodeling events such as mitochondrial dynamics, vesicle budding, and cell division rely on the large GTPases of the dynamin superfamily. Dynamins have long been characterized as fission molecules; however, how they mediate membrane fusion is largely unknown. Here, by cryo-electron microscopy and *in vitro* liposome fusion assays, I show how the mitochondrial dynamin Mgm1 may mediate membrane fusion. Cryo-EM images demonstrate that the Mgm1 complex is able to tether opposing membranes to a gap of ~15 nm, which is the size of mitochondrial cristae folds. I further show that the Mgm1 oligomer undergoes a dramatic GTP-dependent conformational change, suggesting that s-Mgm1 interactions could overcome repelling forces at fusion sites and that ultrastructural changes could promote the fusion of opposing membranes. Together, these findings provide mechanistic details of the two known *in vivo* functions of Mgm1, membrane fusion and cristae maintenance, and more generally shed light onto how dynamins may function as fusion proteins.

4.2 INTRODUCTION

Members of the dynamin superfamily are conserved in yeast, plants, and higher eukaryotes including humans. They share sequence homology, structural motifs, biochemical characteristics, and the ability to self-assemble into ordered structures and interact with cellular membranes. They are implicated in diverse fundamental cellular membrane binding processes such as membrane fission and membrane fusion, plant cell plate formation, and chloroplast biogenesis (Danino and Hinshaw 2001, Praefcke and McMahon 2004). A key question is, therefore, whether they all share a common mechanism of action. The mechanism of how dynamins mediate fission is largely evidenced from *in vitro* structural studies indicating membrane tubulation upon protein self-assembly and formation of highly ordered helical structures composed of repeated T-shaped dimers (Sweitzer and Hinshaw 1998, Takei, Haucke et al. 1998, Stowell, Marks et al. 1999, Yoon, Pitts et al. 2001, Danino, Moon et al. 2004, Mears, Ray et al. 2007, Ban, Heymann et al. 2010, von der Malsburg, Abutbul-Ionita et al. 2011). The protein molecules dimerize via their G domain interface, and the dimers self-assemble into helical structures via the stalk (middle domain and GTPase effector domain (GED)) interface (Low, Sachse et al. 2009, Chappie, Mears et al. 2011, Faelber, Posor et al. 2011, Ford, Jenni et

al. 2011). Cryogenic-electron microscopy (cryo-EM) of dynamin and of Dnm1 showed constriction of the lipid tubes in the presence of GTP and non-hydrolyzable analogues that is proposed to facilitate mitochondrial fission (Zhang and Hinshaw 2001, Danino, Moon et al. 2004, Mears, Ray et al. 2007, Mears, Lackner et al. 2011). In contrast to the detailed knowledge of the role of dynamin proteins in fission, it is unclear how the dynamin-related proteins (DRPs) promote mitochondrial fusion.

Mgm1 is a yeast DRP that has two important functions in the cell: mitochondrial membrane fusion and the formation and maintenance of cristae structures. The mechanism of action of the protein has yet to be determined, but requires two isoforms, an inner membrane-bound l-Mgm1 and an intermembrane space s-Mgm1; both isoforms contain a lipid-binding domain that is required for their *in vivo* function (DeVay, Dominguez-Ramirez et al. 2009, Rujiviphat, Meglei et al. 2009). The isoforms are proposed to have distinct roles due to the differences in activity and localization (DeVay, Dominguez-Ramirez et al. 2009). Recent studies showed that l-Mgm1 preferentially localizes to the CM, and a functional GTPase domain is only required for s-Mgm1 function (DeVay, Dominguez-Ramirez et al. 2009, Zick, Duvezin-Caubet et al. 2009). Therefore, l-Mgm1 is proposed to serve a structural role, and s-Mgm1 is thought to use the energy of GTP binding and hydrolysis to drive the fusion reaction. In this study, I focus on the possible mechanistic actions that s-Mgm1 may have by employing *in vitro* biochemical assays with purified proteins and liposomes as a model mitochondrial membrane. I demonstrate that s-Mgm1 can both tether membranes to likely support inner membrane cristae structures and also undergo a striking GTP-dependent conformational change that could promote the fusion of opposing membranes.

4.3 RESULTS

4.3.1 s-Mgm1 assembles onto the surface of liposomes and forms protein bridges to promote membrane tethering

Using liposomes reflecting IM lipid composition, I demonstrated by negative stain EM that s-Mgm1 assembled onto liposomes and promoted liposome aggregation (Rujiviphat, Meglei et al.

2009) (Chapter 3). Here, I extend and refine the characterization of s-Mgm1-membrane associations. Cryo-EM analysis showed that s-Mgm1 self-assembled onto both PS liposomes (**Figure 4.1, C-E**) and IM liposomes (**Figure 4.1, F**). Strikingly, images reveal liposome tethering by s-Mgm1 (**Figure 4.1, C, D and F**) through protein assembly onto both of the opposing membranes, creating protein bridges with a characteristic tethering distance of ~15 nm (**Figure 4.1, D and F, insets**). Interestingly, s-Mgm1 assembled onto liposomes independently of the presence of CL.

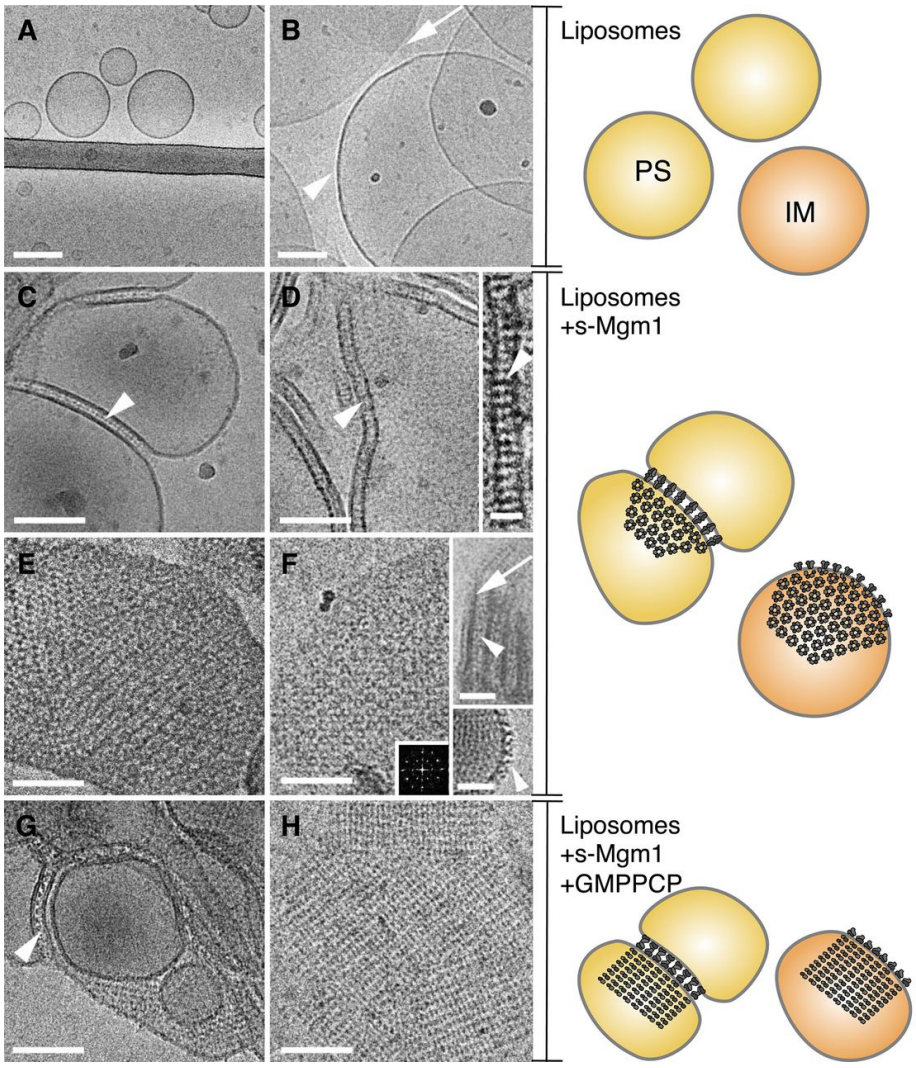

Figure 4.1. s-Mgm1 assembles onto and tethers liposomes

(**A** and **B**) Cryo-EM images of PS and IM liposomes, respectively. *Arrowhead* in **B** points to round liposome, and *arrow* points to the border of flat IM membrane. (**C** and **D**) Cryo-EM images show tethered PS liposomes and protein bridges (*arrowheads*). (**E** and **F**) Cryo-EM images show a crystalline protein array on PS (**E**) and IM (**F**) liposomes. The diffraction spots in (**F**) show the three-fold lattice symmetry. *Arrowhead* and *arrows* (**E, upper inset**) mark protein bridges and lipid bilayer. *Lower inset* shows T-shaped s-Mgm1 structures (*arrowhead*) on the outer liposome surface. (**G** and **H**) Cryo-EM images of crystalline arrays of s-Mgm1 in the presence of GMPPCP on PS (**G**) and IM (**H**) liposomes. *Scale bars* represent 100 nm (**A**–**H**), 25 nm (**inset in D**), and 50 nm (**insets in F**). Schematics on the *right* summarize the observations from the cryo-EM images on the *left*. *Yellow* and *orange circles* represent PS and IM liposomes, respectively. At the periphery of the liposomes, a pair of *light* and *dark gray structures* represents the side view of an s-Mgm1 dimer. The ring of *light* and *dark gray structures* represents the top view of s-Mgm1 oligomers. Upon the addition of GMPPCP (from *middle* to *bottom panels*), the hexameric array of s-Mgm1 reorganizes into a square array. Source: Taken from Abutbul-Ionita, Rujiviphat et al. (2012).

Additionally, a highly ordered crystalline array of s-Mgm1 was frequently observed on the liposome surfaces (**Figure 4.1, E and F**), and occasionally, perimeter structures resembling the T-shaped dimer of dynamin (**Figure 4.1, F inset**). Crystalline assembly was more evident on IM liposomes due to the high content (16%) of CL, which has an inherent tendency to flatten as compared with PS liposomes (**Figure 4.1, A and B**). In other words, by visualizing PS liposomes, most liposomes have spherical shape, while more liposomes with flatten structures with larger surface area and less curvature were observed in the case of IM liposomes. Like dynamin, DRPs, including Dnm1 and optic atrophy 1 (OPA1, the mammalian orthologue of Mgm1), form protein-lipid tubes (Yoon, Pitts et al. 2001, Ingerman, Perkins et al. 2005, Zick, Duvezin-Caubet et al. 2009, Ban, Heymann et al. 2010, Mears, Lackner et al. 2011). s-Mgm1 also occasionally transformed liposomes into protein-decorated tubes (**Figure 4.2**). The majority of s-Mgm1 structures were tethered lipid bilayers and protein-lipid flat crystals, which agrees well with the suggested *in vivo* functions of this protein within mitochondria.

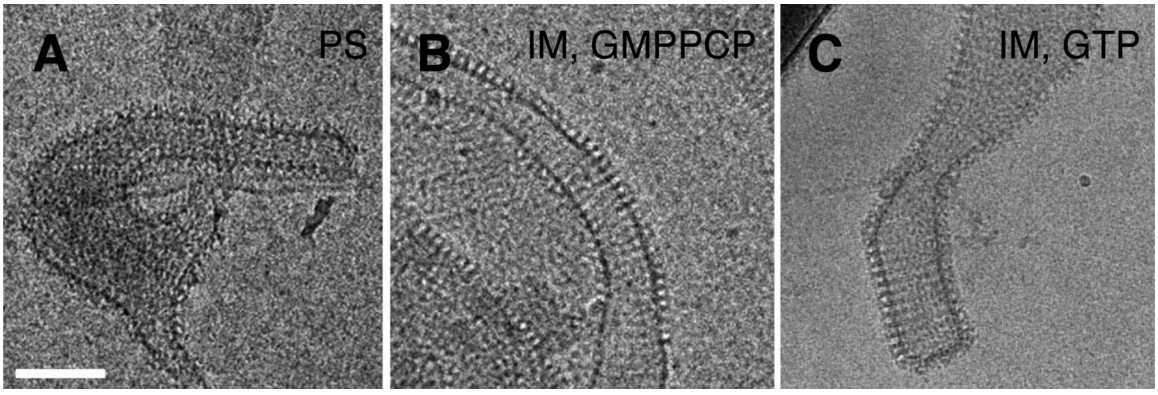

Figure 4.2. s-Mgm1 can transform liposomes into protein-decorated tubes

Tubes are created with both PS (**A**) and IM (**B** and **C**) liposomes, without and with nucleotides as indicated. s-Mgm1 and lipid concentrations were 0.7 and 0.45 mg/ml respectively. *Scale bar* represents 100 nm. Source: Taken from Abutbul-Ionita, Rujiviphat et al. (2012).

4.3.2 s-Mgm1 lipid-bound oligomers undergo a nucleotide-dependent conformational transition

Nucleotide-dependent conformational changes have been observed in several dynamin proteins (Zhang and Hinshaw 2001, Danino, Moon et al. 2004, Mears, Lackner et al. 2011). Here, I investigate whether s-Mgm1 undergoes such structural transitions. EM images as well as two-dimensional crystallization analysis of the lattices by Fourier transformation and image processing showed a hexameric (flower-like) (Avinoam, Fridman et al. 2011) three-fold symmetry lattice **(Figure 4.1, F**, and **Figure 4.3, A and B**, *left panels*), consistent with two previous studies (DeVay, Dominguez-Ramirez et al. 2009, Rujiviphat, Meglei et al. 2009). A structural transition in the crystalline array to a square lattice was observed by the addition of 1 mM GTP and/or its non-hydrolyzable analogue GMPPCP (**Figure 4.1, G and H**, and **Figure 4.3, A and B**, *right panels*) after allowing s-Mgm1 to bind to liposomes. The constriction in the planar packing of the protein-lipid lattice was clearly evident in both the EM images and the projection maps (**Figure 3.6, B**).

Quantitative analysis of the structural transition from hexameric to square lattice suggested a GTP-bound state because it was observed with GMPPCP and GTP (**Figure 4.3, D**). To test this, I found that the GTPase mutants S224A and T244A predominantly created the hexameric lattice, demonstrating that they retain the basal ability to assemble onto the lipid bilayer (**Figure 4.3, C and E**). However, they could not undergo this GTP-dependent structural transition and displayed the same hexameric lattice with and without nucleotides (**Figure 3, E**), further demonstrating that nucleotide binding and/or hydrolysis is the driving force behind the lattice transformation. Therefore, these data suggest that s-Mgm1 membrane-assembled oligomers undergo a structural transition that is dependent on GTP.

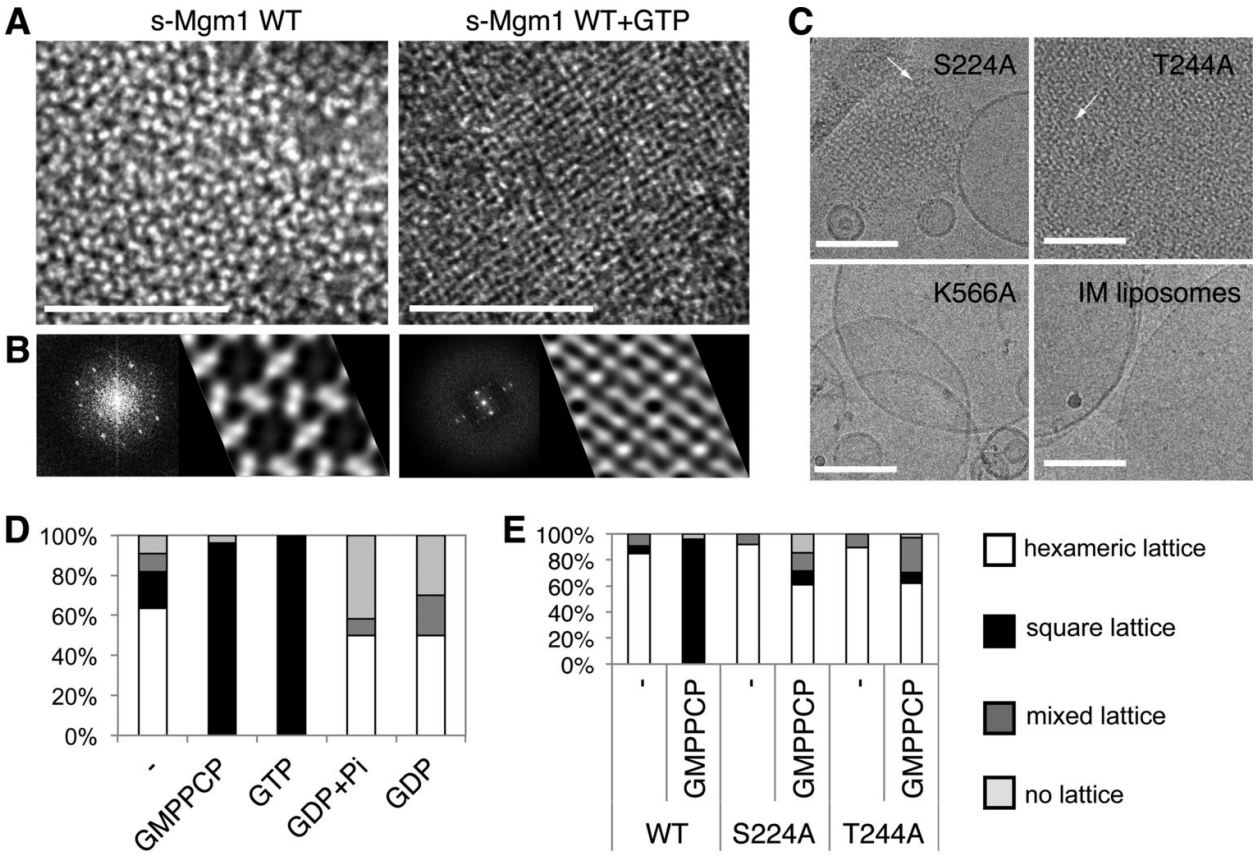

Figure 4.3. s-Mgm1 oligomeric arrays undergo a nucleotide-dependent structural transition that enhances s-Mgm1 membrane fusion activity

(**A**) EM images of s-Mgm1 arrays on IM liposomes in the presence (*right*) and absence (*left*) of GTP. *Scale bar* represents 100 nm. (**B**) Corresponding two-dimensional crystal analysis on protein crystalline arrays. Two-dimensional Fourier transform analysis and projection maps show the average patterns of s-Mgm1 arrays. (**C**) Cryo-EM images of GTPase mutants, S224A and T244A, and a lipid-binding mutant K566A. *Upper panels*: cryo-EM images of ordered protein arrays on IM liposome formed by S224A (*left*) and T244A (*right*). *Arrows* mark hexameric arrays. *Lower panels*: K566A does not assemble onto liposomes nor alter their morphology (compare *left* and *right images*). *Scale bar* represents 100 nm. (**D**) Quantification of the nucleotide-dependent structural transition as categorized into four lattices, hexameric, square, mixed, or none. s-Mgm1-bound IM liposomes were incubated with buffer containing no nucleotide or 2 mM nucleotide as indicated. Source: Adapted from Abutbul-Ionita, Rujiviphat et al. (2012).

4.3.3 s-Mgm1 secondary structures may undergo conformational changes

The structural transition could be due to oligomer rearrangement or structural change in s-Mgm1. To directly assess the conformational change of s-Mgm1, I performed circular dichroism (CD) spectroscopy analysis (**Figure 4.4**) of s-Mgm1 alone in solution and after three subsequent additions: IM liposomes, IM liposomes with GTP, and IM liposomes with GTP and $MgCl_2$. A change in the spectra was observed in presence of both liposomes and GTP, indicative of gross changes in the secondary structure. However, the change was reversed back upon $MgCl_2$ addition, which catalyzes GTP hydrolysis. Fitting the experimental data with theoretical spectra (Perez-Iratxeta and Andrade-Navarro 2008), I found that the fraction of alpha helical structure was reduced in the presence of GTP (**Figure 4.4**, *left panel*). Changes were not detected with the S224A or T244A mutants (**Figure 4.4**, *middle and right panel*). Therefore, these data suggest that s-Mgm1 may undergo a conformational change in its secondary structure that is dependent on GTP binding. This conformational change could contribute to the change in membrane-bound s-Mgm1 lattice. Moreover, this change could be the conformation of s-Mgm1 in GTP bound state.

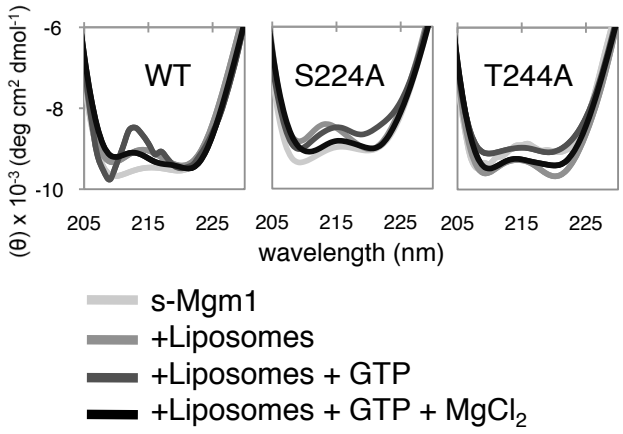

Figure 4.4. GTP binding may alter s-Mgm1 secondary structure.

Circular dichroism spectroscopy profiles of wild-type s-Mgm1, S224A, and T244A mutants. The traces show the zoom in of sample scans between 200 and 240 cm^{-1} wavelength. Each trace is the average of five scans and the signals were subtracted from the scans of buffer alone, with IM liposomes, with GTP, and with $MgCl_2$. A structural transition of wild-type s-Mgm1 assembled onto the membrane in GTP presence. The GTPase mutants S224A and T244A do not undergo a similar transition.

4.3.4 GTP enhances the lipid-mixing activity of s-Mgm1

To investigate the functional significance of the GTP-dependent structural transitions, I monitored potential s-Mgm1 membrane fusion activity using a well-characterized NBD/rhodamine lipid-mixing assay (Fitzgerald 1992, Marsden, Tomatsu et al. 2011). I showed that s-Mgm1 promoted IM lipid mixing in a dose-dependent manner independently of nucleotide (**Figure 4.5, A**). Furthermore, I confirmed that this lipid-mixing activity was dependent on the lipid binding activity as the lipid-binding mutant K566A was significantly impaired in lipid-mixing activity (**Figure 4.5, A**). Importantly, no spontaneous mixing of liposomes was found using BSA as control (**Figure 4.5, A**). Further, by dithionite treatment of liposomes, I found that the lipid mixing I was monitoring was that of the outer leaflet as s-Mgm1 does not induce lipid mixing of the inner leaflet of the liposome bilayer (**Figure 4.5, B**).

Although nucleotide was not absolutely required for s-Mgm1-mediated lipid mixing shown in this NBD/rhodamine lipid-mixing assay, the addition of GTP enhances the rate and amount of this lipid mixing. After IM liposome fusion was induced by the addition of s-Mgm1 for 3 minutes, 1 mM GTP was added (indicated in **Figure 4.5, C** by an *arrow*). In comparison with the sample that has only added buffer (*gray diamond*), the initial rate of fusion and the total lipid mixing was higher by the addition of GTP (*black square*) (**Figure 4.5, C**). I repeated the experiments with the nucleotide mutants S224A and T244A and monitored the total lipid mixing after 60 minutes of reaction. Importantly, GTP was unable to stimulate the basal rate of lipid mixing with the nucleotide mutants S224A and T244A as compared with WT s-Mgm1 (**Figure 4.5, D**). Therefore, these data suggest that GTP binding and hydrolysis enhance liposome fusion likely by inducing conformational changes, as I have demonstrated by the cryo-EM images.

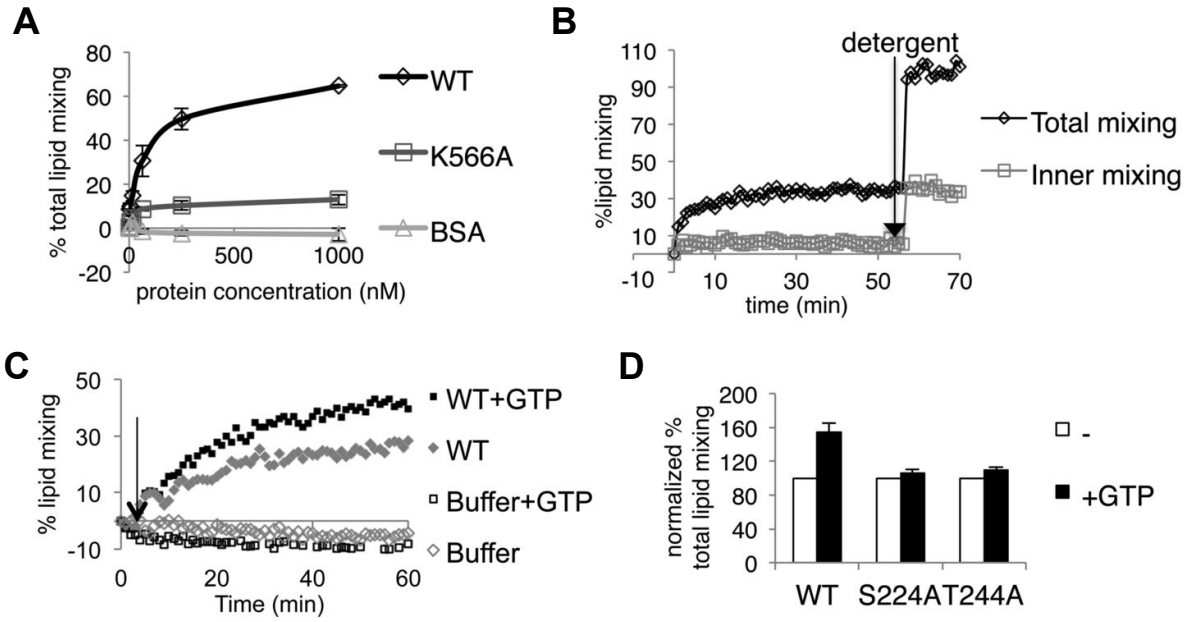

Figure 4.5. s-Mgm1 promotes lipid mixing of IM liposomes that is enhanced by nucleotide

(**A**) NBD/rhodamine assay showing the lipid-mixing activity of Mgm1. Wild-type s-Mgm1 caused lipid mixing in a concentration-dependent manner, while the lipid-mixing activity of the lipid-binding mutant K566A was significantly impaired. No activity is found for the control (bovine serum albumin, BSA). (**B**) The lipid mixing of the inner leaflet only by s-Mgm1 was monitored by dithionite treatment. Lipsomes were incubated with 1 mM dithionite for 10 min prior to the addition of s-Mgm1. s-Mgm1 lipid mixing activity was monitored by the fusion of dithionite-treated and untreated labelled liposomes indicative of the mixing of the inner leaflet phospholipids only and total phospholipids, respectively. Detergent was added to determine the maximal NBD signals. (**C**) GTP enhances Mgm1 lipid mixing activity. *Arrow* points to the 3-minute point after the fusion has been initiated. GTP (1 mM) increased the total lipid mixing by wild-type s-Mgm1 (0.125 μM). 5mM $MgCl_2$ was included in the reaction mixture. (**D**) The bar graph shows that GTP addition increased total lipid mixing induced by wild-type s-Mgm1 but not by the GTPase mutants S224A and T244A. Three separate experiments were performed. Basal levels of lipid mixing were normalized to 100%. The *error bars* represent standard deviations. Source: Adapted from Abutbul-Ionita, Rujiviphat et al. (2012).

4.4 DISCUSSION

In this study, I show that s-Mgm1 tethers membranes, a process important to promote IM fusion and to support inner membrane cristae structures. s-Mgm1 also undergoes a striking GTP-dependent conformational change that could promote the fusion of opposing membranes.

4.4.1 Possible morphology and *trans* interactions of s-Mgm1 to tether membranes

Although it is widely accepted that pro-fusion proteins interact in *trans* to tether membranes, this proposal has been mainly based on indirect observations. Immuno-gold labeling experiments detect a pool of Mgm1 molecules on opposing membranes of tethered IMs (Meeusen, DeVay et al. 2006). Cryo-EM images of Soluble NSF Attachment Protein Receptor (SNARE) proteins loaded vesicles showed that the fusing vesicles are docked with a gap (Diao, Grob et al. 2012). The gap had high electron density, suggesting that SNARE proteins reside within the gap to tether vesicles. In contrast to these indirect observations, the cryo-EM images in this study show that single s-Mgm1 molecules align on both sides of the tethered PS liposomes, providing a direct visualization of protein *trans* interaction during a membrane-tethering step in a membrane fusion process (**Figure 4.1**). This morphology of protein assembly is consistent both with the size of an s-Mgm1 dimer (DeVay, Dominguez-Ramirez et al. 2009) and with the biological function of Mgm1 in mediating membrane fusion and possibly mitochondrial cristae maintenance. These data suggest that s-Mgm1 homo-complexes may act in *trans* like a zipper to tether the two membranes together to stabilize IM folds and possibly facilitate fusion. Identifying this unique tethering activity of Mgm1 may explain the mechanistic requirement for Mgm1 in maintaining proper inner membrane cristae topology, a vital *in vivo* function for this protein.

4.4.2 Possible GTP-dependent structural transitions of s-Mgm1 to promote phospholipid mixing and fusion of bilayers

Although nucleotide-dependent conformational changes of Mgm1 have not previously been reported, several lines of evidence have demonstrated that nucleotide binding induces

transformations that promote the activity of other dynamin family members. Atlastin, a dynamin-like GTPase involved in endoplasmic reticulum morphology and fusion, has also been shown to tether membranes (Orso, Pendin et al. 2009). Further, atlastin nucleotide-bound states suggest conformational changes upon GTPase activity (Bian, Klemm et al. 2011). Thus, these data may suggest a new yet conserved mechanism for DRP-mediated fusion. Indeed, in this study, I directly show that Mgm1 membrane-bound oligomers undergo a GTP-dependent conformational change. Indeed, a complete rearrangement of the s-Mgm1 lattice was observed. In the presence of GTP, a more condensed and organized lattice was observed. The transition from loosely packed flower-like lattice to highly order square lattice could constrict the membrane, and it is possible that this membrane stress or constriction could promote membrane fusion. Therefore, I propose a model where this structural transition promotes a possible membrane deformation that may facilitate mitochondrial IM fusion (**Figure 4.6**).

4.4.3 A proposed mechanism of Mgm1 function

Although the GTP-induced structural transition is reminiscent of dynamins, the mechanical forces that would be transferred to the membrane would likely be quite distinct, suggesting a key mechanistic difference in how these related proteins function. Dynamin and s-Mgm1 GTPase activity is highly stimulated in the presence of lipid (Sever, Damke et al. 2000, Marks, Stowell et al. 2001, DeVay, Dominguez-Ramirez et al. 2009, Rujiviphat, Meglei et al. 2009, He, Yu et al. 2010), suggesting that these proteins use the hydrolysis energy to apply force on the membrane while performing their biological activities: membrane fusion by s-Mgm1 and membrane fission by dynamin. However, the difference in biological activities reflects the unique structures they form *in vivo* and *in vitro*. Dynamin shapes liposomes *in vitro* into helical tubes, with a diameter similar to that of endocytic buds. GTP hydrolysis induces conformational changes that generate force, which constricts and twists the underlying membrane, decreasing the distance between the bilayers as a step toward fission (Zhang and Hinshaw 2001, Danino, Moon et al. 2004, Roux, Uyhazi et al. 2006, Lenz, Morlot et al. 2009, Chappie, Mears et al. 2011, Ford, Jenni et al. 2011) (**Figure 4.6**). These data point to Mgm1 as an unconventional dynamin-like protein, uniquely acting to bridge the bilayers of opposing membranes and anchor them at a fixed distance, to support mitochondrial inner membrane cristae structures and to promote the fusion of opposing

membranes. In addition, I propose that the GTP-dependent conformational transitions and that GTP hydrolysis could constrict or deform the membrane to promote membrane fusion (**Figure 4.6**).

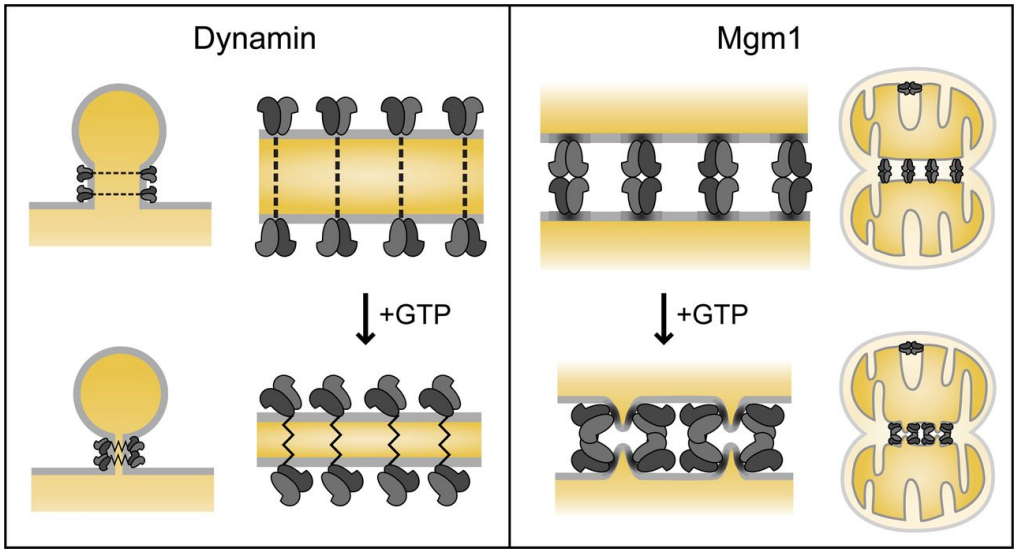

Figure 4.6. Model of Mgm1 structural transitions during mitochondrial IM fusion

A model depicting the function of dynamin in fission (*left*), and s-Mgm1 in fusion (*right*). Both dynamin and Mgm1 shape membranes *in vivo* and *in vitro*. Dynamin dimers assemble into a helical collar, which upon GTPase activity constrict the underlying membrane to mediate fission. I propose that s-Mgm1 forms a homo-oligomeric complex in *trans* to create protein bridges and ordered lattices that tether opposing membranes to support mitochondrial inner membrane cristae structures and to also undergo a GTP-induced transition to promote fusion. Source: Taken from Abutbul-Ionita, Rujiviphat et al. (2012).

Given that Mgm1/OPA1 is an important human disease gene, understanding its biophysical properties will direct future studies to reveal mechanisms of disease. Specifically, identifying and characterizing the protein/protein interfaces that both stabilize the lattice work and allow for the gross nucleotide-dependent conformational changes will further reveal its *in vivo* function. In addition, future studies will need to incorporate the long isoform of Mgm1 to fully understand the breadth of the *in vivo* activities of Mgm1. These studies will help uncover the mechanistic roles of other membrane-fusing proteins in the cell and the unique biophysical properties required to regulate membrane dynamics.

Chapter 5

5 MGM1 ALTERS MEMBRANE TOPOLOGY AND PROMOTES LOCAL MEMBRANE BENDING

Manuscript in preparation: Rujiviphat J., M.K. Wong, A. Won, Y.L. Shih, C.M.Yip, G.A. McQuibban (2013). "Mgm1 alters membrane topology and promotes local membrane bending" submitted to Journal of Molecular Biology, October, 2013.

Data attribution: Michael K. Wong performed initial supported lipid bilayer experiments. Dr. Amy Won performed giant unilamellar vesicle electroformation. Dr. Christopher M. Yip performed atomic force microscopy analysis.

Acknowledgements: I thank Dr. Yu-ling Shih for assistance with fluorescence microscopy analysis. I thank Dr. Carol Froese for purified human Sept5 and Dr. Helena Friesen for purified Drosophila amphiphysin proteins.

5.1 SUMMARY

Large GTPases of the dynamin superfamily promote membrane fusion and division, which are crucial for intracellular trafficking and organellar dynamics. To promote membrane scission, dynamin proteins polymerize, wrap around, and constrict the membrane. However, the mechanism underlying their role in membrane fusion remains unclear. I have shown that the mitochondrial dynamin-related protein Mgm1 mediates fusion by first tethering opposing membranes and then by undergoing a nucleotide-dependent structural transition (Abutbul-Ionita, Rujiviphat et al. 2012) (Chapter 4). However, it is still unclear how Mgm1 directly affects the membrane to drive the fusion of tethered membranes. Here, I show that Mgm1 association with the membrane alters membrane topology and promotes local membrane bending. I also demonstrate that Mgm1 creates membrane ruffles with tubular structures on both supported lipid bilayers and liposomes. These data suggest that Mgm1-membrane interactions could direct a mechanical force onto the membrane to overcome the hydrophilic repulsion of the phospholipid head groups and initiate the fusion reaction. Together, these data point to a possible mechanism of how Mgm1 acts on the mitochondrial inner membrane to cause mitochondrial fusion and shed light on how proteins in the dynamin superfamily function as fusion molecules.

5.2 INTRODUCTION

In the cell, membranes are dynamic structures that undergo complex rearrangement during processes such as cell division, vesicle budding, and organelle restructuring. Mitochondria are double membrane-bound organelles that continually fuse and divide. Mitochondria serve as the power plant of the cell, generating most of the cellular supply of chemical energy in the form of adenosine triphosphate (ATP). Mitochondria are also major sites for cell signaling and regulation; for instance, cytochrome *c* is released from the mitochondria to activate apoptosis, the process of programmed cell death (Kroemer, Dallaporta et al. 1998, Westermann 2010, Kulikov, Shilov et al. 2012). These important mitochondrial functions rely on a proper balance in the rates of mitochondrial fusion and fission. Imbalance in mitochondrial dynamics causes mitochondrial misshape and dysfunction as evidenced by a reduction in energy production and uncontrolled cell death (Westermann 2010). Disruption in mitochondrial morphology and function has been linked to several neurodegenerative diseases, including Parkinson's disease

(Exner, Lutz et al. 2012). In addition, mitochondrial inheritance, genome maintenance, and a quality control pathway termed mitophagy require precise regulation in mitochondrial fusion and fission (Nunnari, Marshall et al. 1997, Chan 2012, Youle and van der Bliek 2012). Therefore, proper regulation of mitochondrial dynamics is crucial for both organellar and cellular integrity. To maintain mitochondrial dynamics, the opposing forces of mitochondrial fusion and fission require distinct protein machineries. The key components driving mitochondrial fusion and fission belong to the same protein superfamily called dynamin.

The dynamin superfamily is composed of classical dynamin and dynamin-related proteins (DRPs), which are large GTPases that undergo GTP cycling and act as mechanoenzymes to mediate intracellular membrane-remodeling events such as vesicle budding and organelle fusion and fission (Praefcke and McMahon 2004, Ferguson and De Camilli 2012). These events require core domains of the dynamin superfamily: a GTPase domain, a middle domain, and a GTP effector domain (GED) (Praefcke and McMahon 2004). Crystal structures show that the head region (which consists of the GTPase domain) and the stalk region (which consists of the middle domain and the GED) can self-interact to promote oligomerization and polymerization into highly ordered helical structures (Chappie, Acharya et al. 2010, Haller, Gao et al. 2010, Faelber, Posor et al. 2011, Ford, Jenni et al. 2011, Ferguson and De Camilli 2012). The foot region (which is between the middle domain and the GED) is typically composed of a pleckstrin-homology (PH) domain that interacts with lipids (Ferguson and De Camilli 2012). To cause fission, dynamin binds to the membrane, polymerizes, and constricts the membrane upon GTP-induced rearrangement of the head and stalk regions (Ford, Jenni et al. 2011). Membrane tubulation, constriction, and scission have been observed by electron microscopy analyses (Chen, Zhang et al. 2004, Danino, Moon et al. 2004, Chappie, Mears et al. 2011). While this model of dynamin-mediated membrane fission is widely accepted, it is still unclear how members of the DRP subfamily promote membrane fusion.

In humans, while dynamin-related protein 1 (DRP1) mediates the scission of both the outer and inner mitochondrial membranes, mitofusins (MFN1 and MFN2) and optic atrophy 1 (OPA1) mediate outer and inner mitochondrial membrane fusion, respectively. Mutations in these DRPs cause neurodegenerative diseases, underscoring the importance of mitochondrial dynamics maintenance in cell health (Delettre, Lenaers et al. 2000, Zhao, Alvarado et al. 2001, Zuchner, Mersiyanova et al. 2004). Membrane tethering and nucleotide-dependent structural

changes are thought to be important processes for other membrane fusion proteins, as in the case of atlastin-mediated membrane fusion of the endoplasmic reticulum (Moss, Daga et al. 2011, Byrnes, Singh et al. 2013). Likewise, mitofusins mediate fusion of the outer mitochondrial membrane by tethering membranes via their coiled-coil domains, which is followed by GTP binding and GTP hydrolysis (Escobar-Henriques and Anton 2013). In the case of OPA1, very little is known about how it mediates inner mitochondrial membrane fusion. Mgm1 is the yeast homologue of OPA1 and has two isoforms, s-Mgm1 and l-Mgm1. Both isoforms are crucial for inner mitochondrial membrane fusion. l-Mgm1 is anchored to the inner membrane while s-Mgm1 resides in the intermembrane space. Since l-Mgm1 does not require a functional GTPase domain to function, it is proposed that l-Mgm1 serves a structural role while s-Mgm1 acts as the mechanoenzyme in the fusion reaction (Zick, Duvezin-Caubet et al. 2009). To address these questions, I focused on the mechanistic actions of s-Mgm1 in this study.

Meglei and McQuibban have shown that s-Mgm1 has GTPase activity and binds to specific phospholipids, which is similar to other dynamin-related proteins (2009). Although a soluble isoform of OPA1 has been shown to tubulate liposomes similar to other DRPs, the majority of s-Mgm1 only assembles onto the membrane as a crystalline array (DeVay, Dominguez-Ramirez et al. 2009, Rujiviphat, Meglei et al. 2009, Ban, Heymann et al. 2010). I have demonstrated that, similar to atlastin and mitofusins, s-Mgm1 tethers membranes and undergoes a striking GTP-dependent structural transition that may be the mechanism to promote membrane fusion (Abutbul-Ionita, Rujiviphat et al. 2012) (Chapter 4). Since the fundamental difference between pro-fusion dynamins and pro-fission dynamins is that pro-fusion dynamins are anchored to the membrane, it is plausible that the transmembrane domains of mitofusin, atlastin, and l-Mgm1 are essential for destabilizing the phospholipid bilayer to facilitate fusion. However, it is still unclear how s-Mgm1, which is only peripherally associated with the membrane, could act directly on the membrane to drive the fusion of tethered membranes. In this study, I apply real-time confocal fluorescence microscopy and scanning probe microscopy to characterize how s-Mgm1 promotes membrane fusion *in vitro* by using model membrane substrates. Here, I show that s-Mgm1 binds to the membrane, alters membrane topology, and promotes local membrane bending, which could serve as crucial steps in orchestrating membrane fusion. This work provides insights into the mechanism of Mgm1 in mediating mitochondrial

membrane fusion and more generally how members of the dynamin superfamily function as pro-fusion molecules.

5.3 RESULTS

5.3.1 s-Mgm1 promotes lateral lipid movement and lipid clustering

Having shown that phospholipid interaction stimulates the GTP hydrolysis rate of s-Mgm1 (Rujiviphat, Meglei et al. 2009) (Chapter 3), I propose that lipid interaction could be essential for Mgm1's activity and Mgm1-mediated membrane fusion. The energy from the GTP hydrolysis could be necessary to destabilize membrane to initiate membrane fusion. For two bilayers to fuse, significant energy is required to overcome the electrostatic repulsion of the phospholipid head groups upon membrane tethering, and to overcome the energy barriers associated with membrane curvature and fusion pore formation (Martens and McMahon 2008). I have shown that Mgm1 self-interacts in *trans*, which overcomes membrane repulsion, to tether opposing membranes (Abutbul-Ionita, Rujiviphat et al. 2012) (Chapter 4). However, it is still unclear how s-Mgm1 mediates the fusion of tethered membranes to initiate fusion. Using a supported lipid bilayer (SLB) system, I specifically asked whether s-Mgm1 could alter the topology of the phospholipid bilayer to promote membrane curvature and fusion pore formation, which are necessary for membrane fusion to occur.

To observe changes in phospholipid organization within a bilayer, I fluorescently labeled SLBs and used confocal fluorescence microscopy to monitor morphological changes in the SLB. I used a lipid mixture with a composition similar to that of the yeast mitochondrial IM to form the SLB. The SLB was fluorescently labeled by including 2% NBD-PS in the lipid mixture. Phospholipids in the SLB separated into at least two different phases that were apparent as areas with or without NBD-PS signal (**Figure 5.1, A**). This phase separation suggests that NBD-PS preferentially localizes to certain domains. The SLB structure is stable over time, even after the addition of buffer and GTP (**Figure 5.1, B**). After the addition and incubation of s-Mgm1 with the SLB for 15 minutes, I observed the formation of bright fluorescent clusters and the subsequent formation of fibre-like structures (**Figure 5.1, C**). These images suggest that the

presence of s-Mgm1 can alter SLB morphology. To confirm that the formation of these lipid clusters and fibre-like structures is due to s-Mgm1-lipid interaction, I incubated the SLB with K795A, which is defective in lipid binding (Rujiviphat, Meglei et al. 2009). No lipid clustering or fibre-like structure formation was observed upon incubation with K795A and GTP (**Figure 5.1, D**). To confirm that these changes were specifically due to s-Mgm1-phospholipid interactions, instead of NBD-PS, I labeled the SLB with NBD-PC, which is an s-Mgm1 non-interacting phospholipid. Consistently, I did not observe any significant changes in the NBD-PC-labeled SLB (**Figure 5.2**). Therefore, these controls show that the lipid clustering and fibre-like structure formation are dependent on the association of s-Mgm1 with certain negatively charged phospholipids.

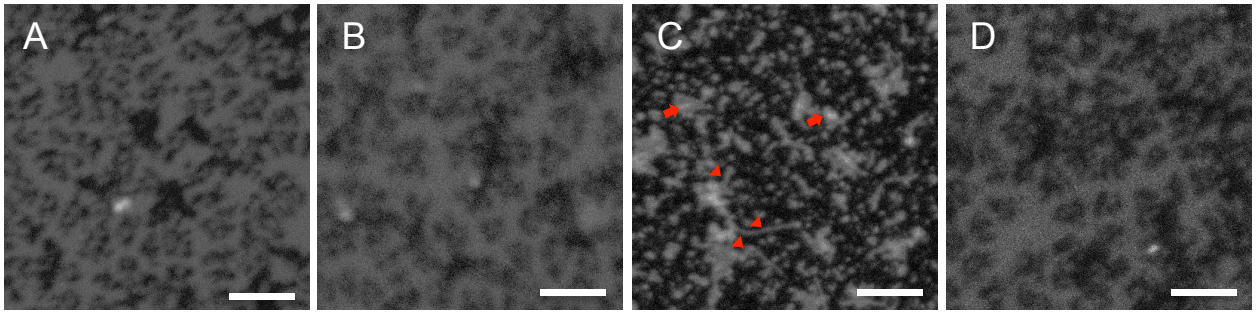

Figure 5.1. s-Mgm1 lipid-binding activity causes phospholipid clustering and fibre-like structure formation

Representative confocal images show the fluorescence signal of the SLB that is labeled with NBD-PS before and after 15-minute incubation with buffer only, with wild-type s-Mgm1, or with K795A. 1 mM GTP was included in all conditions. SLB was formed by fusing 250 μM SUV IM liposomes onto a mica surface and excess liposomes were removed from the fluid cell (**A**) Phase separation was observed in the NBD-PS-labeled SLB that contained IM lipid composition. (**B**) After the addition of buffer, no change in SLB structure or NBD-PS signal was observed. (**C**) The addition of 0.4 μM wild-type s-Mgm1 caused the formation of stable bright clusters (*arrows*) and fibre-like structures (*arrowheads*). (**D**) The addition of 0.4 μM K795A, which is defective in lipid binding, did not cause changes in the SLB. *Scale bars* represent 5 μm.

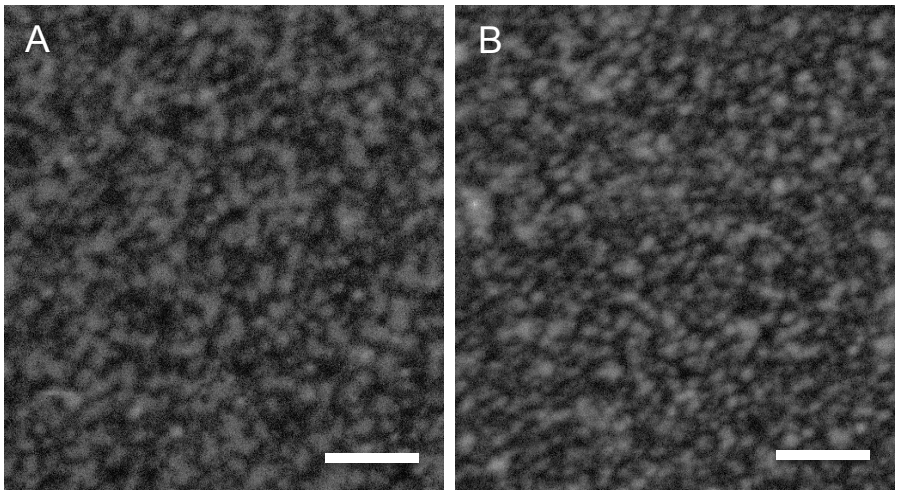

Figure 5.2. s-Mgm1 does not cause clustering of NBD-PC

Representative confocal images show the fluorescence signals of the NDB-PC-labeled SLB that contains IM composition before and after a 15-minute incubation with s-Mgm1. 2% NBD-PC was included in the IM mixture. (**A**) Phase separation was observed in the SLB. (**B**) No change in SLB structure and the NBD-PC signal was observed after the addition s-Mgm1. *Scale bars* represent 5 μm.

To monitor these phospholipid movements in real time, time-lapse images were acquired at 15-second intervals upon the addition of s-Mgm1 and GTP. After the addition of s-Mgm1, I observed an immediate rearrangement of fluorescent lipids into bright clusters ranging from ~0.4 to ~1.5 μm in diameter (**Figure 5.3, A**). While these clusters were widespread, the overall underlying phase-separated structure of the bilayer remained unchanged. These bright clusters then nucleated and grew into ~200 nm wide fibre-like structures at a rate of ~0.4 μm/min for 14-15 minutes. The addition of GTP catalyzed the immediate and complete transformation of the underlying bilayer into bright clusters (**Figure 5.3, B**). The underlying structure of the bilayer observed prior to s-Mgm1 addition was no longer present. Notably, the fibre-like structures seen prior to GTP addition were not affected by the addition of nucleotide. These data suggest that GTP can further promote lipid clustering and fibre-like structure formation, possibly indicating its mechanistic role in completing the fusion reaction. Together, these results suggest that s-Mgm1 can interact with certain phospholipids to induce their lateral movements to form lipid clusters and fibre-like structures, which may be necessary for membrane fusion to occur.

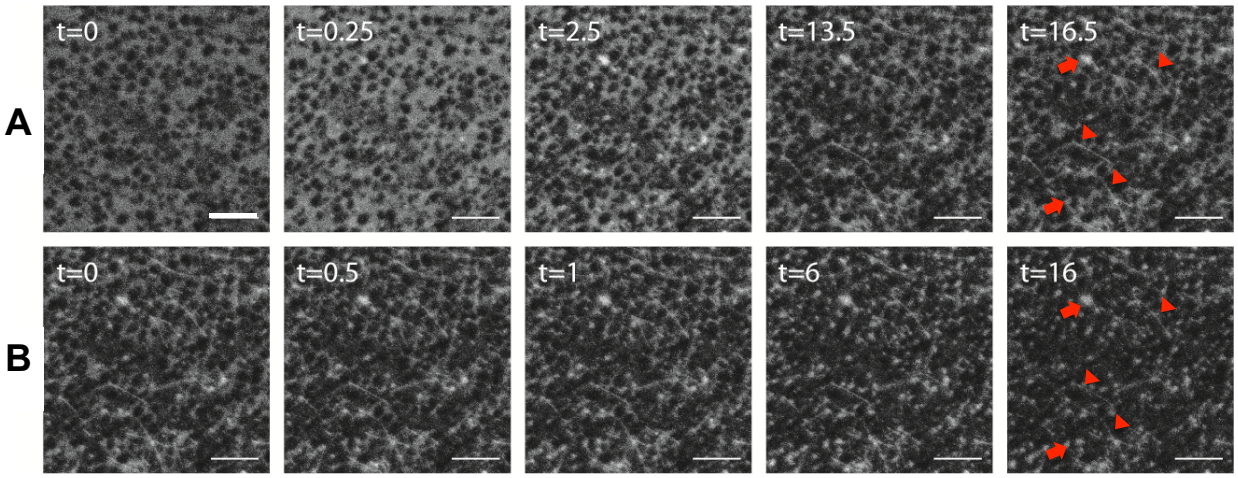

Figure 5.3. s-Mgm1 promotes immediate phospholipid lateral lipid movement and clustering and fibre-like structure formation

Confocal time-lapse images show fluorescence signal of the initial bilayer and after addition of s-Mgm1 and GTP. (**A**) The addition of 0.4 μM s-Mgm1 caused the formation of stable bright clusters (*arrows*) and fibre-like structures (*arrowheads*). (**B**) The addition of 1 mM GTP caused the remodeling of the underlying bilayer into bright clusters while fibres remained stable. Time is in minutes. *Scale bars* represent 5 μm.

5.3.2 s-Mgm1 alters membrane topology

Atomic force microscopy (AFM) was used to further characterize the s-Mgm1-induced fibre-like structure on the SLB. The SLB was formed to contain the IM lipid mixture by a process similar to that described above. The AFM tapping mode of imaging was used to monitor membrane topology upon the sequential addition of s-Mgm1 and GTP. As expected, fused IM liposomes resulted in the SLB with a phase-separated topography, in which the gel phase extending ~2.2 to ~2.5 nm above the surrounding fluid phase domains (**Figure 5.4, A**). The addition of s-Mgm1 catalyzed the immediate formation of fibre-like structures that were ~40 to ~250 nm in width and ~30 to ~115 nm in height (**Figure 5.4, B**). The size of these fibre-like structures was in the same range as those observed in the confocal experiments (**Figure 5.1 and Figure 5.3**). Upon the addition of GTP, the underlying bilayer structure became less contiguous and more uneven, showing a height difference of ~10 to ~15 nm (**Figure 5.4, C**). In addition, the membrane roughness upon GTP binding coincided with the disappearance of the underlying structure observed in fluorescently labeled SLB. These data further support the notion that s-Mgm1 can

disrupt the membrane to promote membrane roughness and the growth of fibre-like structures by binding and acting on the membrane. Such activity is enhanced in the presence of GTP.

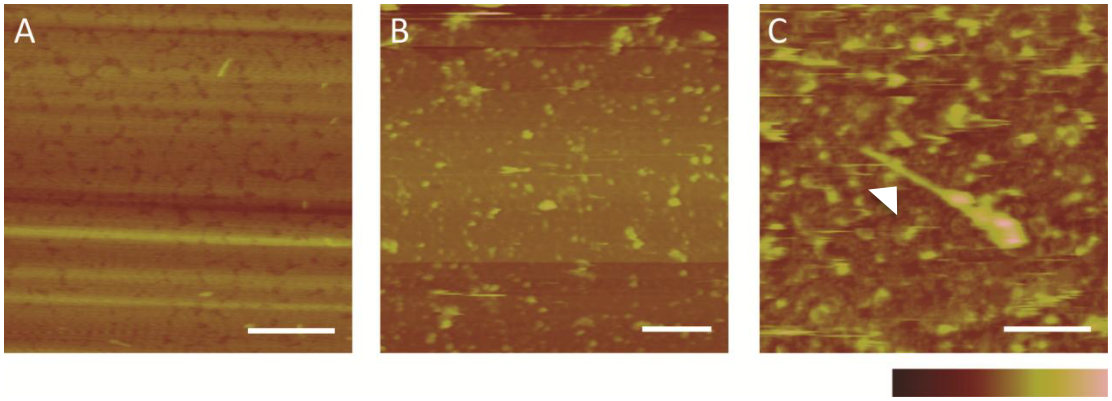

Figure 5.4. s-Mgm1 alters the topology of the supported lipid bilayer

Representative AFM images show the topology of the SLB before and after the addition of s-Mgm1 and GTP. (**A**) The SLB was made with a phospholipid composition similar to that found in the inner mitochondrial membrane. (**B**) The addition of 0.4 μM s-Mgm1 caused membrane roughness. (**C**) Fibre-like structure formation (*arrowheads*) and additional membrane roughness was observed upon the addition of 1 mM GTP. *Scale bars* represent (A) 2.5 μm, (B) 1 μm, (C) 2.5 μm. The *gradient* represents the height scale from low to high: (A) 0 to 50 nm, (B) and (C) 0 to 100 nm.

5.3.3 s-Mgm1 deforms liposomes

Next, I asked whether s-Mgm1 could also alter the morphology of liposomes. To do this, I used fluorescence microscopy to monitor changes in liposome morphology before and after the addition of s-Mgm1. For these experiments, I used liposomes comprised of a mixture of CL, PS, and PA, which were previously shown to stimulate the GTPase activity of s-Mgm1 (Rujiviphat, Meglei et al. 2009) (Chapter 3). The liposomes were labeled with Texas Red®-DHPE for imaging. Liposomes with the diameters of 5-30 μm were formed by electroformation and rehydration methods (**Figure 5.5, A**).

Membrane-remodeling proteins have been shown to alter the surface morphology of liposomes locally and tubulate liposomes globally (Shih, Huang et al. 2011, von der Malsburg,

Abutbul-Ionita et al. 2011). After incubating the liposomes with s-Mgm1 for 60 minutes, I observed roughness on the liposomes, indicating local membrane bending but not global liposome tubulation (**Figure 5.5, B**). Liposome tubulation is a common activity of membrane-remodeling proteins. Amphiphysin is a known membrane-remodeling protein and was used as a positive control to demonstrate liposome tubulation (**Figure 5.5, C**). On the other hand, Sept5, which is only active when it is in the complex with other Septin proteins, caused liposome tethering but did not cause any liposome tubulation or local membrane bending. Therefore, Sept5 served as a negative control (**Figure 5.5, D**). Collectively, these results suggest that s-Mgm1 could induce local membrane bending.

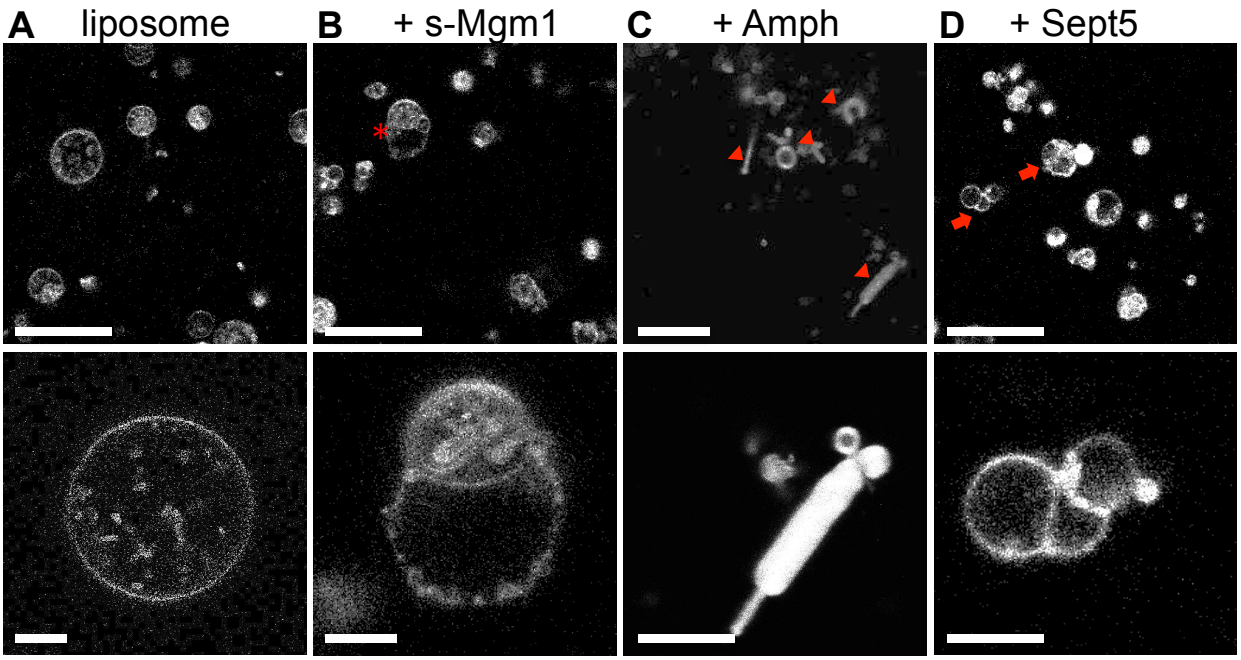

Figure 5.5. s-Mgm1 deforms liposomes

Representative fluorescence microscopy images in wide field (*upper panels*) and zoom-in (*lower panels*) show the morphology of liposomes upon incubation with s-Mgm1, Amphiphysin, and Septin5. (**A**) Texas Red®-DHPE-labeled liposomes appeared round in a fluid cell containing 50 mM Tris, 150 mM NaCl, 300 mM glucose, pH 7.4. (**B**) s-Mgm1 caused liposome deformation (*asterisks*). (**C**) The addition of Drosophila Amphiphysin (Amph) caused liposome tubulation (*arrowheads*). (**D**) The incubation with human Septin5 (Sept5) promoted liposome tethering (*arrows*) but not liposome surface deformation. *Scale bars* represent 25 μm (*upper panels*) and 5 μm (*lower panels*).

5.3.4 s-Mgm1 promotes local membrane bending

Next, I used confocal microscopy to further characterize s-Mgm1-mediated local membrane bending by monitoring both liposomes and s-Mgm1. Liposomes, which contain CL, PS, and PA, were fluorescently labeled with Texas Red®-DHPE; s-Mgm1 was fluorescently labeled with a thiol-reactive Alexa Fluor® 488 probe. The GTPase activity of Alexa Fluor® 488-labeled s-Mgm1 was comparable to that of the unlabeled s-Mgm1, confirming that the probe did not alter the GTPase activity of s-Mgm1 (**Figure 5.6**). Labeled s-Mgm1 was incubated with labeled liposome in a fluid cell and monitored after a 15-minute incubation. WT s-Mgm1 and S224A were found to co-localize with liposomes, suggesting that they were recruited and assembled onto liposomes (**Figure 5.7, A and B**), similar to previous observations by electron microscopy (Abutbul-Ionita, Rujiviphat et al. 2012). Consistently, K795A, which is defective in lipid binding, aggregated out of the solution (**Figure 5.7, C**). These data confirm the previous finding that s-Mgm1 interacts with phospholipids and assembles onto liposomes and provides a basis to monitor nucleotide effects.

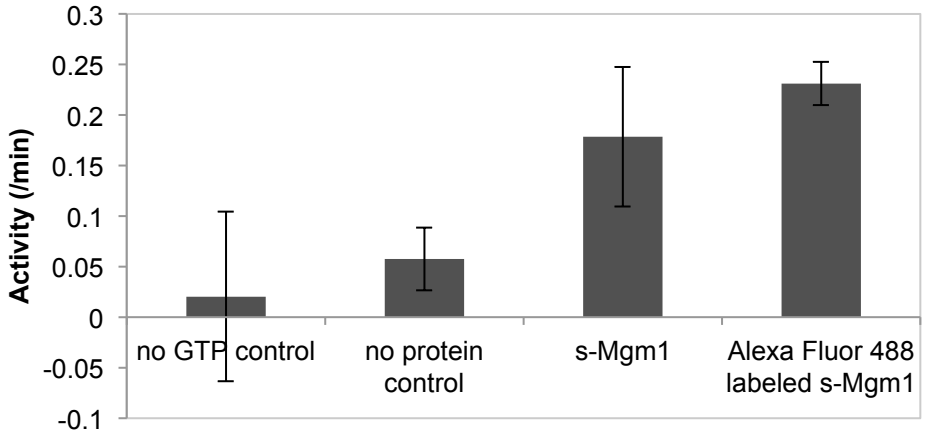

Figure 5.6. The GTPase activity of s-Mgm1 is not altered by thiol-reactive fluorescence probe labeling

The GTPase activity of unlabelled and Alexa Fluor® 488-labeled s-Mgm1 were assayed by a malachite green assay detecting released inorganic phosphate (see section **2.4.1**). The samples lack GTP or protein serve as negative controls. All of the experiments were done in triplicate. *Error bars* represent standard deviations.

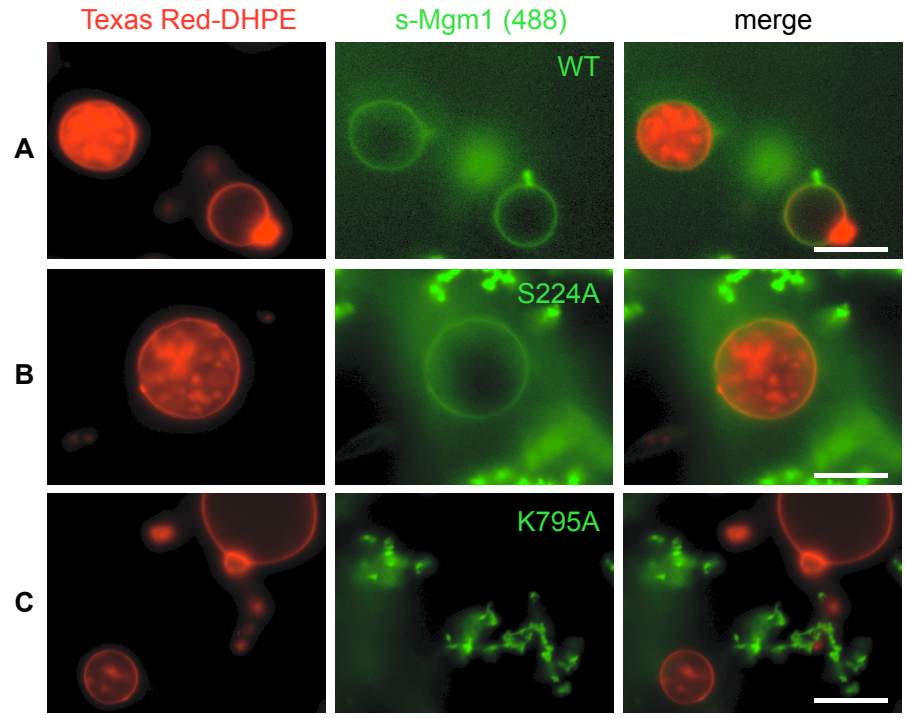

Figure 5.7. s-Mgm1 requires a functional lipid-binding domain to bind to liposomes

Representative fluorescence microscopy images show liposomes in fluid cells after a 15-minute incubation with WT s-Mgm1 or mutants. (**A**) s-Mgm1 was found at the periphery of the liposomes. (**B**) Similar to the WT s-Mgm1, the S224A mutant was recruited onto liposomes. (**C**) K795A mutant did not bind to liposomes, but instead formed aggregates. *Scale bars* represent 5 μm.

By monitoring s-Mgm1 recruitment to liposomes over time, I found that liposomes became deformed after ~16 minutes of s-Mgm1 incubation (**Figure 5.8**), suggesting that s-Mgm1 association with liposomes could lead to liposome deformation. Importantly, incubation with the K795A mutant did not cause any liposome deformation, supporting the notion that liposome deformation is dependent on s-Mgm1 lipid-binding activity (**Figure 5.9**).

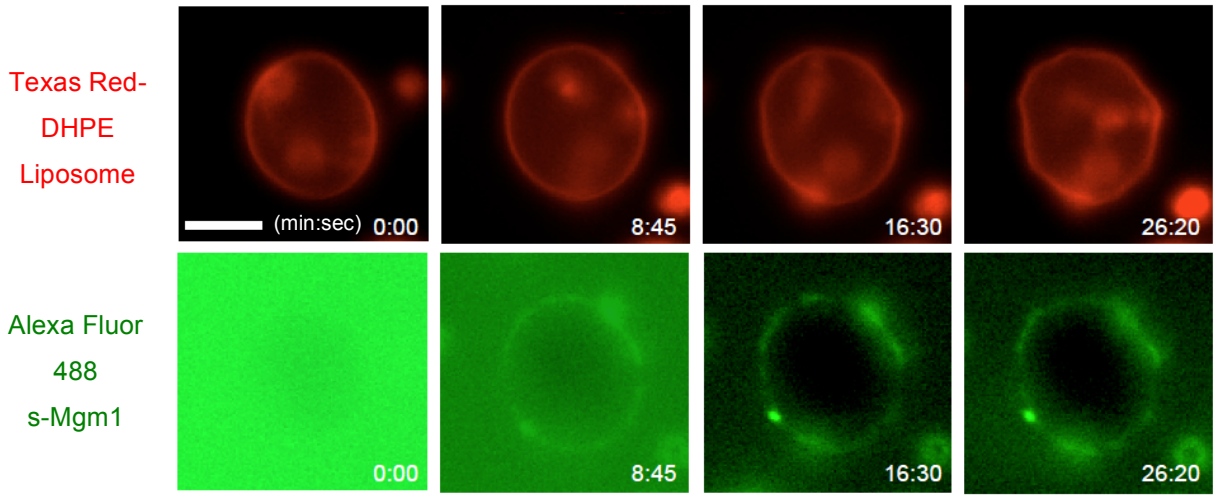

Figure 5.8. s-Mgm1 binds to liposomes and causes local membrane bending

Fluorescence microscopy time-lapse images show s-Mgm1 binding to a liposome over time. s-Mgm1 was added at time zero and images were taken every 5 seconds with alternating ET-mCherry and ET-GFP filters to detect liposomes and s-Mgm1, respectively. Liposome deformation occurred after 16.5 minutes. *Scale bar* represents 3 μm.

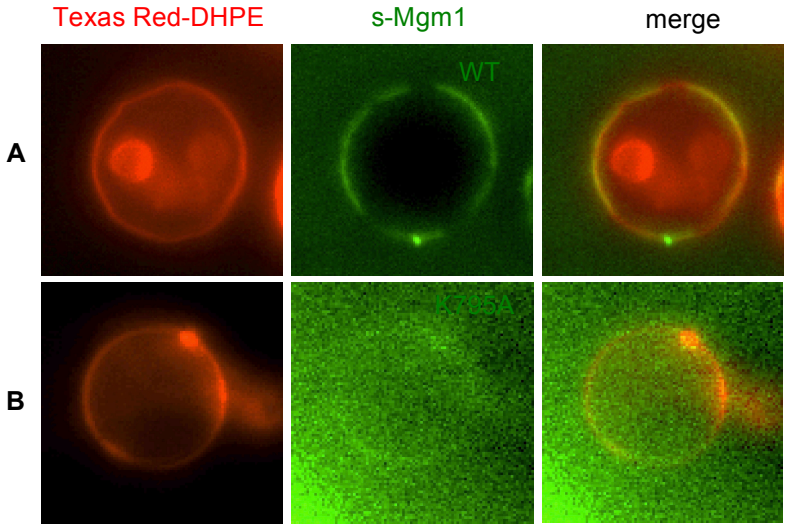

Figure 5.9. Lipid-binding mutant K795A does not promote local membrane bending

Representative fluorescence microscopy images show liposomes in fluid cells after a 30-minute incubation with WT s-Mgm1 and K795A mutant. (**A**) WT s-Mgm1 was recruited onto the liposomes and the liposome deformation was subsequently observed. (**B**) K795A did not bind to the liposomes and the liposome morphology was not altered. *Scale bar* represents 3 μm.

5.3.5 GTP binding enhances Mgm1-mediated local membrane bending

Since GTP promotes conformational changes in s-Mgm1, I investigated whether GTP would stimulate the local membrane-bending activity of s-Mgm1. The addition of GTP to s-Mgm1-bound liposomes resulted in local membrane bending within 5 minutes (**Figure 5.10, A)**, in comparison to 16 minutes in the absence of GTP (**Figure 5.8**). Consistently, this enhancement in liposome deformation was not observed in the case of S224A, which is a mutant defective of GTP binding, suggesting that the enhancement in liposome deformation could be due to GTP binding (**Figure 5.10, B**). I confirmed that the presence of GTP or GDP alone without membrane-bound s-Mgm1 did not cause local membrane bending (**Figure 5.11, A**). Moreover, this enhancement is specific to GTP not GDP (**Figure 5.11, B**). By taking time-lapse images every 5 seconds, I observed that local membrane bending was initiated at 120 seconds after the addition of GTP (**Figure 5.11, C**). Therefore, these results suggest that GTP binding enhances the local membrane-bending activity of s-Mgm1.

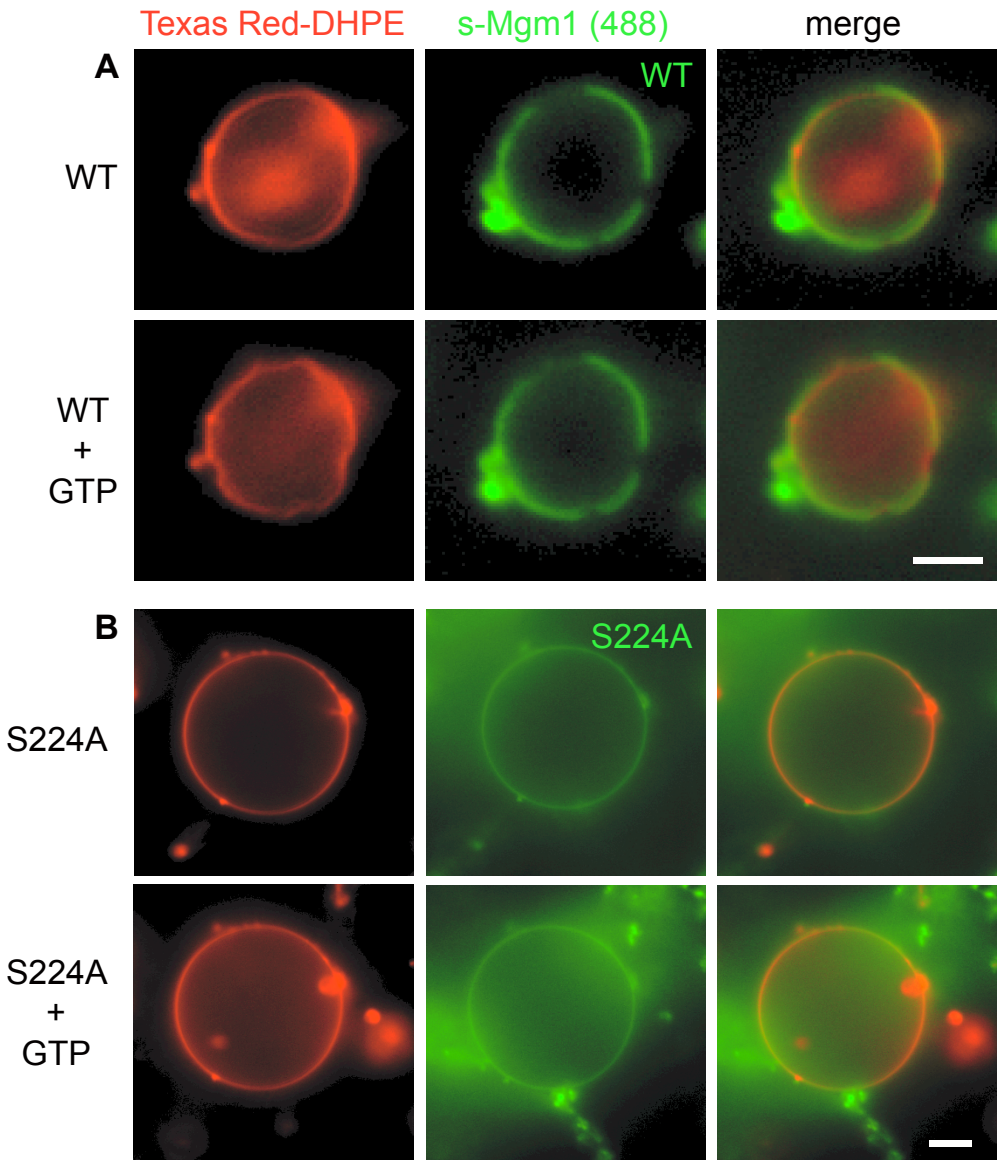

Figure 5.10. GTP binding enhances local membrane bending by s-Mgm1

Fluorescence microscopy images show s-Mgm1-bound liposomes before and after the addition of 1 mM GTP. (**A**) GTP enhanced the local membrane bending of WT-assembled liposomes. (**B**) No change in membrane topology was observed after the addition of 1 mM GTP to the liposome pre-incubated with S224A mutant. *Scale bar* represents 3 μm.

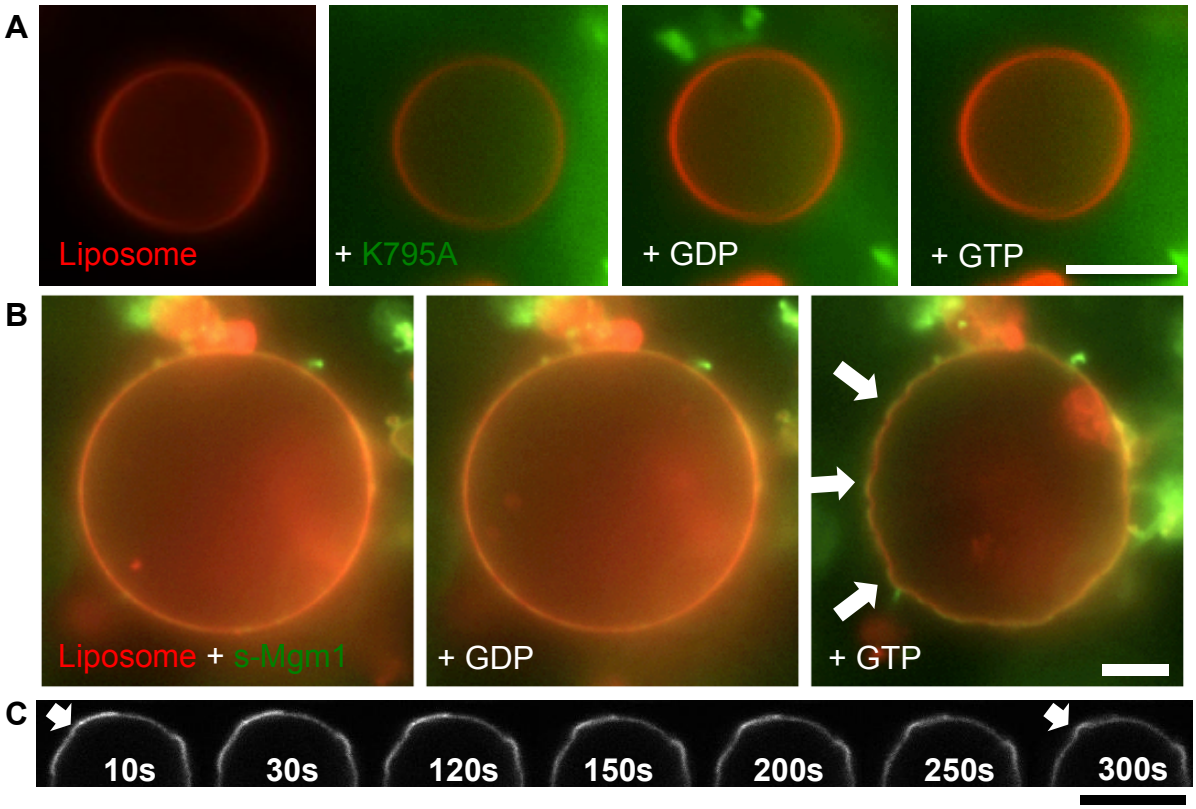

Figure 5.11. The enhancement in membrane bending is specific to GTP but not GDP

(**A**) Local membrane bending did not spontaneously occur due to the presence of protein or nucleotide. The panels (*left to right*) show fluorescence images of a liposome in the fluid cell, after incubation with K795A, GDP, and GTP, respectively. (**B**) Fluorescence microscopy two-channel merged images show s-Mgm1 bound liposome before (*left panel*) and after the addition of GDP (*middle panel*) and GTP (*right panel*). Areas with local membrane bending (*arrows*) were observed after the addition of 1 mM GTP. (**C**) Time-lapse images of a liposome section show s-Mgm1 concentrated at the bent areas of the membrane (*arrow*). The addition of 1 mM GTP was time zero. *Scale bars* represent 5 μm.

I further investigated how GTP binding promotes local membrane bending of s-Mgm1-bound liposomes in three dimensions and in real time. After incubating s-Mgm1 with liposomes, I monitored the changes in s-Mgm1 intensity on the liposomes by confocal fluorescence microscopy. I observed that s-Mgm1 segregated and concentrated at points coinciding with points where the membrane was bent (**Figure 5.11, C** and **Figure 5.12**). Three-dimensional reconstruction from stacking sections of images shows fibre-like structures similar to those observed by AFM images (**Figure 5.12, B**). These data suggest that s-Mgm1 could promote local membrane bending into a fibre-like structure, and that the membrane bending activity of s-

Mgm1 is enhanced upon GTP binding.

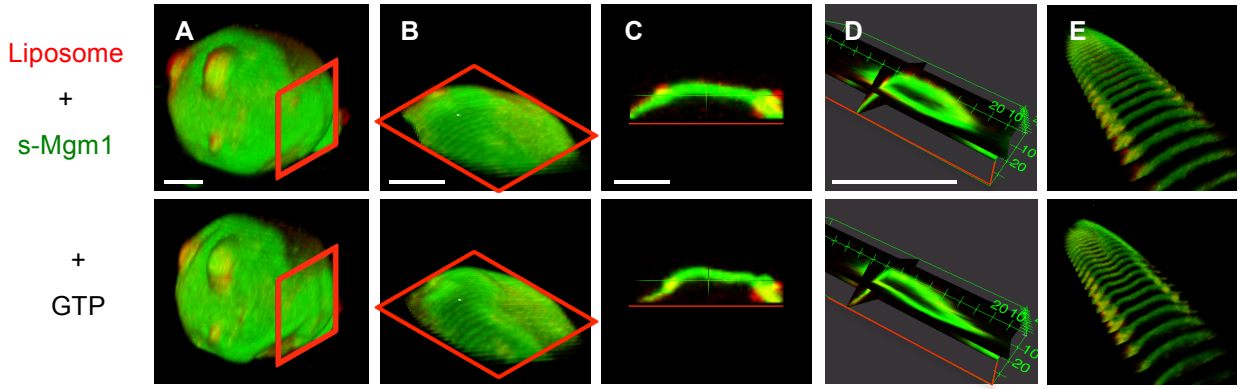

Figure 5.12. s-Mgm1 segregates to promote local membrane bending upon GTP binding

A series of confocal images shows the change in morphology of the s-Mgm1-bound liposome before (*upper panels*) and after (*lower panels*) the addition of GTP (**A-E**). (**A**) Stacks of confocal images with 0.2 µm separation were used to build three-dimensional reconstructions. The *red box* indicates the area of interest where local membrane bending was observed. (**B**) The reconstructions show the zoom-in top view of the area of interest. (**C**) The mid-section of the area of interest shows that membrane curvature was induced. (**D**) The orthoslides show dimensions of the curvature. Each tick on the axes represents 10 pixels, which is equivalent to 0.78 µm. (**E**) Alignment of the series of confocal images highlights the curvature that is observed in each image plane. *Scale bar* represents 3 µm.

5.3.6 GTP promotes liposome fusion in the presence of both s-Mgm1 and l-Mgm1

To confirm that the s-Mgm1-dependent local membrane bending and GTP-dependent stimulation lead to membrane fusion, I monitored liposome fusion by a content-mixing assay using fluorescence microscopy. Mitochondrial IM fusion *in vivo* requires s-Mgm1 as well as l-Mgm1, which is another isoform that anchors to the inner mitochondrial membrane. Therefore, I incorporated l-Mgm1 in the assays by reconstituting purified l-Mgm1 into IM liposomes (**Figure 5.13, A and B**). I confirmed that liposome-reconstituted l-Mgm1 was active. l-Mgm1 itself has no GTPase activity but it can stimulate the GTP hydrolysis rate of s-Mgm1 activity, as previously reported (DeVay, Dominguez-Ramirez et al. 2009) (**Figure 5.13, C**).

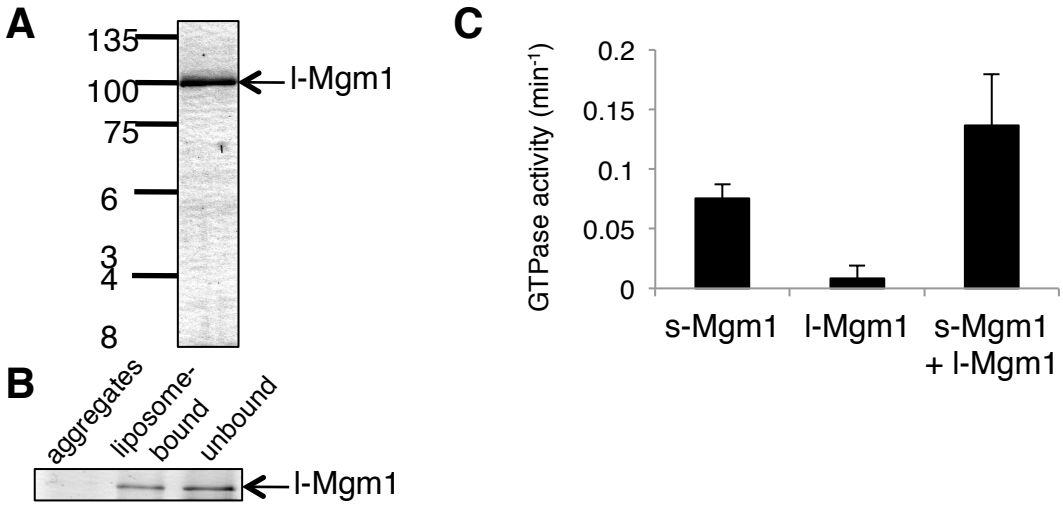

Figure 5.13. l-Mgm1 is reconstituted into IM liposomes and stimulates s-Mgm1 activity

(**A**) l-Mgm1 expression and purification. l-Mgm1 is expressed in *E.coli* and purified by Ni-NTA and size exclusion chromatography. Purified fractions are subject to SDS-PAGE and silver stain analysis. The *arrow* points to the purified l-Mgm1. (**B**) l-Mgm1 reconstitution into liposomes. Detergent-bound l-Mgm1 was exchanged and reconstituted into IM liposomes by the quick dilution method. Liposome-bound l-Mgm1 was purified by centrifugation. Unbound l-Mgm1 aggregates were discarded by low-speed centrifugation. High-speed ultracentrifugation separated liposome-bound and unbound l-Mgm1, indicated by *arrow*. (**C**) s-Mgm1 GTP hydrolysis was stimulated in the presence of l-Mgm1.

Using a HPTS/DPX content-mixing assay, in the presence of both s-Mgm1 and l-Mgm1, GTP promotes liposome content mixing, which is indicative of liposome fusion (**Figure 5.14, A**). By fluorescence microscopy, I also observed liposome deformation upon the addition of GTP (**Figure 5.14, B**). Moreover, I was able to detect liposome fusion occurring within 30 seconds (**Figure 5.14, C**). Without l-Mgm1, I observed only liposome tethering and deformation, but not fusion. Therefore, these data further support the notion that s-Mgm1 causes local membrane bending, which could be a necessary step to initiate fusion. GTP could enhance this membrane bending activity of s-Mgm1 and could promote IM fusion in the presence of l-Mgm1.

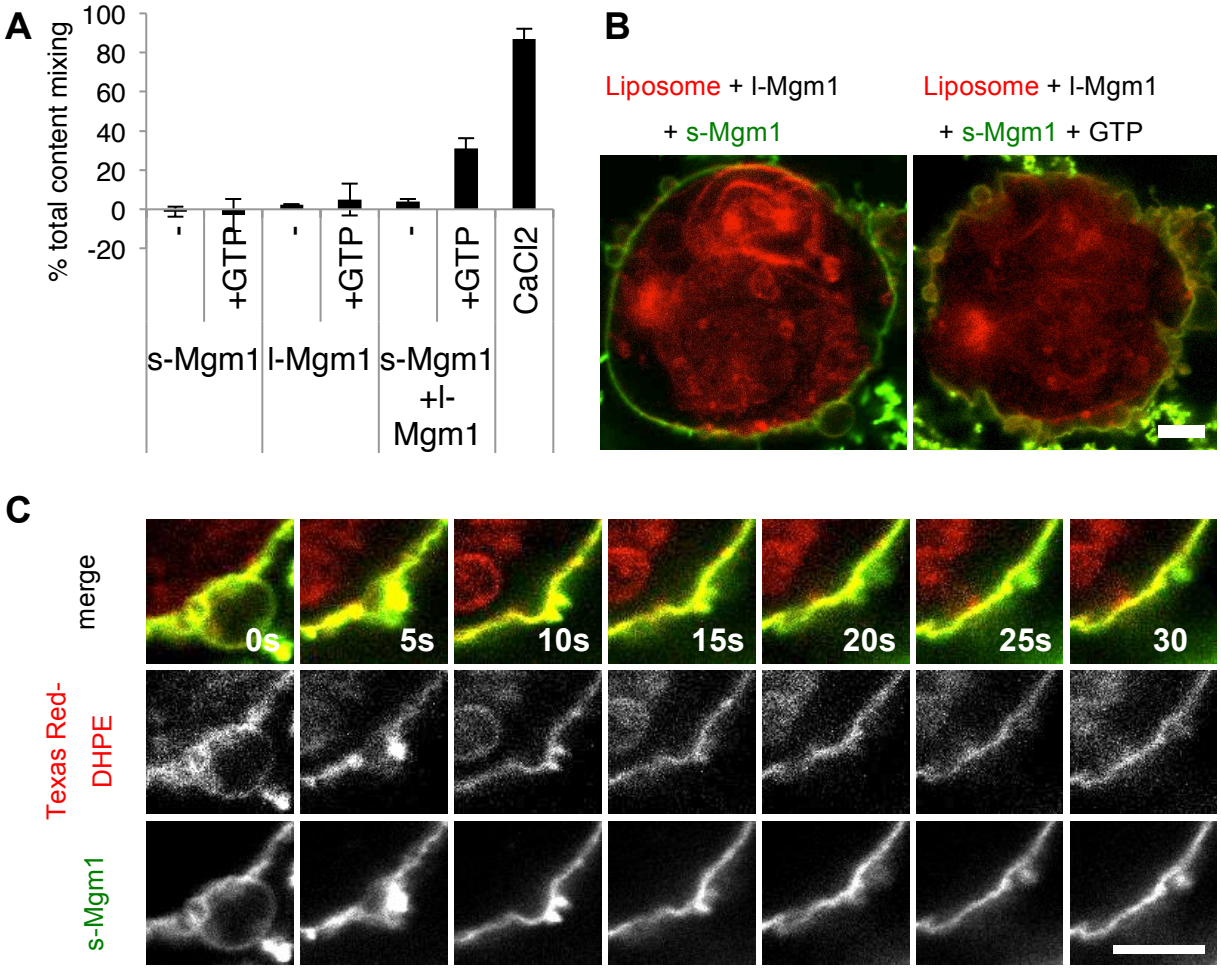

Figure 5.14. GTP promotes s-Mgm1-dependent liposome deformation and membrane fusion

Liposome fusion assay and fluorescence microscopy images show liposome fusion. (**A**) Liposome content-mixing assay demonstrated that membrane fusion was induced only when all s-Mgm1, l-Mgm1, and GTP were present. $CaCl_2$ was used as a positive control to induce fusion of the liposomes. (**B**) s-Mgm1 was found to be recruited around the liposomes, and liposome tethering was observed. GTP was added and incubated for 30 minutes. Liposome deformation and local membrane bending were observed. (**C**) Time-lapse images showed a small liposome fusing to a large liposome upon GTP addition. The addition of GTP was time zero. *Scale bar* represents 5 μm.

5.4 DISCUSSION

Proteins in the dynamin superfamily play a crucial role in intracellular communication and the maintenance of organellar dynamics by allowing membranes to fuse and divide (Praefcke and McMahon 2004). Dynamin wraps around and constricts membranes to cause membrane scission. However, it is unclear how pro-fusion dynamin-related proteins promote membrane fusion. I have shown that s-Mgm1 self-oligomerizes to tether opposing membranes and undergoes a nucleotide-dependent structural transition that may promote fusion (Abutbul-Ionita, Rujiviphat et al. 2012). However, it is unknown how Mgm1 directly affects the membrane to initiate membrane fusion. In this study, I demonstrated that s-Mgm1 clusters phospholipids, alters membrane topology, and promotes local membrane bending. These activities of s-Mgm1 provide mechanistic insight into how Mgm1 mediates mitochondrial IM fusion.

5.4.1 Lipid clustering activity of s-Mgm1 may be important for IM fusion

Here, I report that s-Mgm1 causes certain phospholipids to move laterally and cluster within SLBs. The aggregation of specific phospholipids, especially non-bilayer-forming phospholipids, could be essential for promoting membrane fusion. s-Mgm1 preferentially binds to CL, PS, and PA, which are non-bilayer-promoting phospholipids (Meglei and McQuibban 2009). As shown by confocal microscopy, the clustering of these phospholipids can lead to phase separation in the IM (**Figure 5.1**). Changes in local lipid composition can trigger phase separation and lipid tension that may facilitate membrane fusion. It has been proposed that dynamin clusters PI(4,5P)2, and the lipid clustering is proposed to create line tension at the interface between different lipid phases (Bethoney, King et al. 2009). This line tension is believed to cause the fusion of adjacent lipid bulk, which in turn pinches off vesicles. Therefore, a possible effector role of s-Mgm1-lipid interactions is to cluster certain phospholipids that would destabilize the membrane at the future fusion sites to promote membrane fusion.

5.4.2 s-Mgm1 is a membrane-remodeling protein

The clustering of non-bilayer-forming phospholipids like CL and PA may promote the alteration in membrane topology. In this study, I showed that s-Mgm1 may cause membrane topological changes: (1) membrane ruffling, (2) local membrane bending, and (3) fibre-like structure formation, which together could lead to membrane fusion. The unevenness in the membrane, which was observed by AFM, could represent substantial membrane deformation (**Figure 5.4**). Local convex areas of IM liposomes have higher concentrations of s-Mgm1, suggesting the role of s-Mgm1 membrane assembly in the promotion of local membrane bending (**Figure 5.11**). Fibre-like structures are an elongation of local membrane bending along an extended area, which was observed by three-dimensional reconstruction of deformed liposomes and on SLBs (**Figure 5.1**, **Figure 5.3**, and **Figure 5.12**). Together, these data support the notion that s-Mgm1 is a membrane-remodeling protein that can alter membrane topology to promote fusion.

5.4.3 A possible fusion initiation step of s-Mgm1-mediated IM fusion

It is interesting to note that s-Mgm1 can form fibre-like structures on the membrane. These structures could represent the topology of the membrane at the fusion site. The average width or crosswise diameter of the fibre-like structure was measured to be ~200 nm by confocal fluorescence microscopy but only ~45 nm by AFM. This discrepancy is likely due to the diffraction limit of 200-300 nm of confocal microscopy (Huang, Babcock et al. 2010). I have shown that s-Mgm1 makes a protein bridge between two opposing membranes with a tethering gap of ~15 nm (Abutbul-Ionita, Rujiviphat et al. 2012) (Chapter 4). Remarkably, this is comparable to the height of the fibre-like structure resolved by AFM, suggesting that tethered membranes could make physical contact upon induced membrane bending. Although image distortion reduces the accuracy of these measurements, the numbers are well within the range required to cause membrane contact. A similar model has been proposed in SNARE-mediated membrane fusion (Ungermann and Langosch 2005, Martens and McMahon 2008). Therefore, the local membrane bending observed in this study could represent the s-Mgm1-induced membrane topology required to initiate membrane fusion.

5.4.4 A possible role of s-Mgm1 in the lipid-mixing step of IM fusion

On the basis of the data presented in this study, I propose a model in which s-Mgm1 disrupts the membrane to promote lipid mixing of the fusing bilayers, driving membrane fusion (**Figure 5.15**). Upon membrane tethering, assemblies of s-Mgm1 move toward each other, bringing the s-Mgm1-interacting phospholipids to the fusion sites. The clustering of certain non-bilayer phospholipids such as CL promotes phase separation and membrane bending, which is enhanced upon Mgm1's GTP binding and structural transition. Next, membrane bending can promote the formation of fibre-like structures on the membrane. The fibre-like structures of opposing membranes could lead to membrane contact and promote the mixing of phospholipids at the contact sites. In addition, membrane curvature causes membrane stress, which further destabilizes the membrane. At this point, membrane fusion becomes energetically favorable because stresses that are generated by membrane repulsion and membrane curvature would be released upon the completion of membrane fusion. A similar model that relies on membrane curvature and membrane contact has been proposed in SNARE-mediated membrane fusion (Ungermann and Langosch 2005).

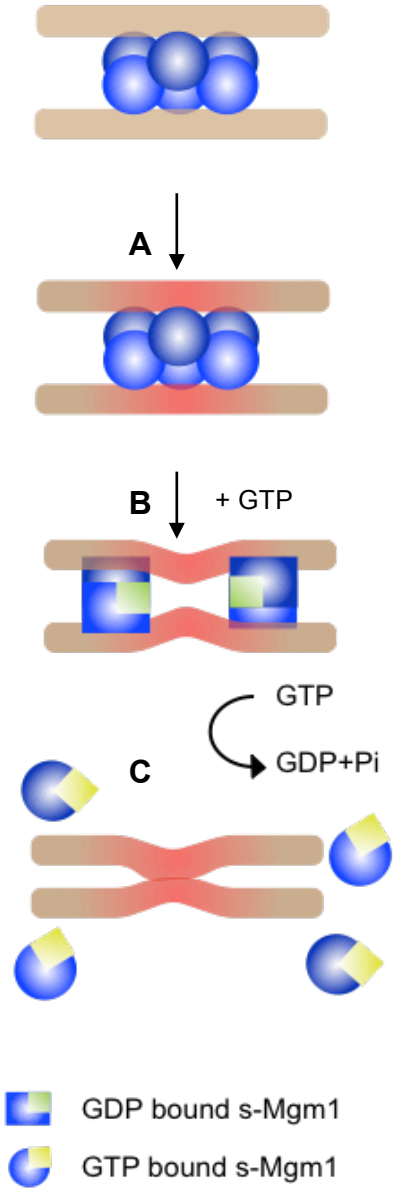

Figure 5.15. Model of s-Mgm1 mechanistic actions in the lipid-mixing step of mitochondrial IM fusion

In the proposed tethering step, s-Mgm1 hexamer tethers the two membranes. (**A**) s-Mgm1-lipid interactions drive the clustering of anionic non-bilayer phospholipids at the fusion site in the membrane, indicated by *red* highlight. (**B**) GTP binding promotes s-Mgm1 structural changes and local membrane bending. (**C**) GTP hydrolysis may lead to the dissociation of s-Mgm1, allowing membranes to fuse.

5.4.5 A possible role of l-Mgm1 in IM fusion

Mitochondrial fusion requires both s-Mgm1, which resides in the IMS, and l-Mgm1, which is anchored to the IM, respectively. It has been proposed that the two isoforms have distinct roles: while l-Mgm1 provides structural support, s-Mgm1 plays a mechanistic role (Zick, Duvezin-Caubet et al. 2009). This proposal is based on the difference in their localization and the lack of GTPase activity of l-Mgm1. l-Mgm1, which is anchored to the mitochondrial IM, is mostly found in the CM rather than the IBM, suggesting that l-Mgm1 moves laterally from the CM to future fusion sites in the IBM to allow for s-Mgm1 recruitment during mitochondrial fusion. A functional GTPase domain is not required for l-Mgm1 function *in vivo* (DeVay, Dominguez-Ramirez et al. 2009, Zick, Duvezin-Caubet et al. 2009). Expressing WT s-Mgm1 with S224A l-Mgm1, which has a mutation in the GTPase domain, can rescue *mgm1Δ* phenotypes. Moreover, purified l-Mgm1 cannot hydrolyze GTP *in vitro* but stimulates the GTPase activity of s-Mgm1 (DeVay, Dominguez-Ramirez et al. 2009). Consistently, in this study, I also show that l-Mgm1 does not have GTPase activity but it is active in the liposome because it enhances the GTP hydrolysis rate of s-Mgm1 (**Figure 5.14**). Although s-Mgm1 and GTP can promote hemifusion of liposomes (**Figure 4.5**), the fusion of both leaflets of the two bilayers requires the presence of l-Mgm1, suggesting that l-Mgm1 is required in a later step of IM fusion (**Figure 5.14**). Although membrane contact could promote the mixing of phospholipids in the outer leaflet in a hemifusion intermediate, l-Mgm1 is needed to complete IM fusion. Since l-Mgm1 differs from s-Mgm1 only in that l-Mgm1 has a transmembrane segment, it is possible that the insertion of l-Mgm1 into the membrane is crucial for IM fusion. Therefore, these data suggest that in addition to serving as a docking site for s-Mgm1 recruitment, l-Mgm1 membrane insertion may help destabilize the membrane and thereby promote IM fusion.

In sum, I showed that lipid clustering and local membrane bending could be a mechanism of how s-Mgm1 promotes mitochondrial IM fusion. This mode of action is similar to that of SNARE proteins, which also promote membrane fusion via membrane bending and a hemifusion intermediate. This characteristic may also be common among other dynamin-related proteins involved in membrane fusion. Therefore, these findings provide us with a better understanding of the molecular mechanism of s-Mgm1 in promoting mitochondrial fusion and shed light on how dynamin-related proteins function as a fusion molecule.

Chapter 6

6 GENERAL DISCUSSION AND FUTURE DIRECTIONS

6.1 SUMMARY

Given the debilitating effect that mitochondrial dysfunction has on human health, it is important to understand mitochondrial dynamics, which are crucial for the maintenance of mitochondrial function, genome, morphology, and overall organelle and cell health. Although the mechanisms and regulation of mitochondrial fission are largely elucidated, less is known about mitochondrial fusion. Mgm1 is a key protein that mediates mitochondrial IM fusion in yeast. However, it is still unclear how Mgm1 functions to promote IM fusion. To investigate how Mgm1 promotes membrane fusion, I conducted several biochemical assays and microscopy experiments to: (1) further characterize Mgm1 domain architecture and function, (2) determine the structure of Mgm1, and (3) investigate Mgm1 activities involved in IM fusion. To this end, I have revealed a possible lipid-binding domain of Mgm1, demonstrated that phospholipid is an essential characteristic of Mgm1 function, and proposed a possible effector role of lipid binding in clustering certain phospholipids to the sites of fusion. Furthermore, I have shown that Mgm1 oligomerizes into a hexameric structure that undergoes conformational changes. I proposed that this oligomeric structure and structural transitions initiate membrane fusion. Lastly, I have demonstrated that Mgm1 exhibits membrane-remodeling activities that could be necessary for the tethering and lipid-mixing steps in a membrane fusion event.

6.2 MGM1 DOMAIN ARCHITECTURE AND FUNCTION

In addition to the GTPase domain, the middle domain, and the GED, in this thesis work, I show that the region between the middle domain and the GED could constitute a unique lipid-binding domain in Mgm1. To reveal the possible existence of an Mgm1 lipid-binding domain, I demonstrated lipid-binding activity *in vitro*, its significance *in vivo*, its tentative domain

boundary, and its possible effector role in Mgm1-mediated fusion. Despite these findings, the following questions remain: (1) Is lipid-binding activity required for l-Mgm1 function? (2) What are the effector roles of lipid binding? (3) Is this proposed region a true lipid-binding domain, and what is the domain boundary?

6.2.1 Requirement for lipid-binding activity

Mutations in the lipid-binding domain of both s-Mgm1 and l-Mgm1 affect Mgm1 function *in vivo*. I demonstrated that lipid binding is important for s-Mgm1 function because it stimulates s-Mgm1 GTPase activity. However, it is unclear whether lipid-binding activity is required for l-Mgm1 function. To test this, one could employ a recently designed *in vivo* complementation assay that can separately introduce mutations in s-Mgm1 and l-Mgm1 (Zick, Duvezin-Caubet et al. 2009). In this assay, s-Mgm1 and l-Mgm1 can be expressed from two different plasmids: l*-Mgm1 (ΔRCR) and s*-Mgm1 (ΔTM) expressing plasmids (**Figure 6.1**). Deletion in the rhomboid cleavage region (RCR) prevents s-Mgm1 processing, which then results in the production of l-Mgm1 only. Removing the first transmembrane (TM) segment forces the Mgm1 precursor to tether to the IM via the second TM, which contains the RCR, allowing for the processing into s-Mgm1 only (**Figure 6.1**). One can perform an *in vivo* complementation assay by co-expressing s*-Mgm1 WT with l*-Mgm1 K566A/K724A/K795A or s*-Mgm1 K566A/K724A/K795A with l*-Mgm1 in an *mgm1Δ* strain, and then determining their phenotypes, including mitochondrial morphology and mitochondrial genome presence. *mgm1Δ* yeast have fragmented mitochondria and mitochondrial genome loss. Co-expressing s*-Mgm1 WT with l*-Mgm1 WT would serve as a positive control, whereas co-expressing s*-Mgm1 K566A/K724A/K795A with l*-Mgm1 K566A/K724A/K795A would serve as a negative control. If lipid-binding activity is crucial for l-Mgm1 function, the *mgm1Δ* strain co-expressing the pair of s*-Mgm1 WT with l*-Mgm1 K566A/K724A/K795A would have phenotypes similar to that of *mgm1Δ*. If the lipid-binding activity is required for functional l-Mgm1, which is already anchored to the membrane, l-Mgm1-lipid interactions may not be necessary for membrane recruitment but may be crucial for other steps during Mgm1-mediated IM fusion.

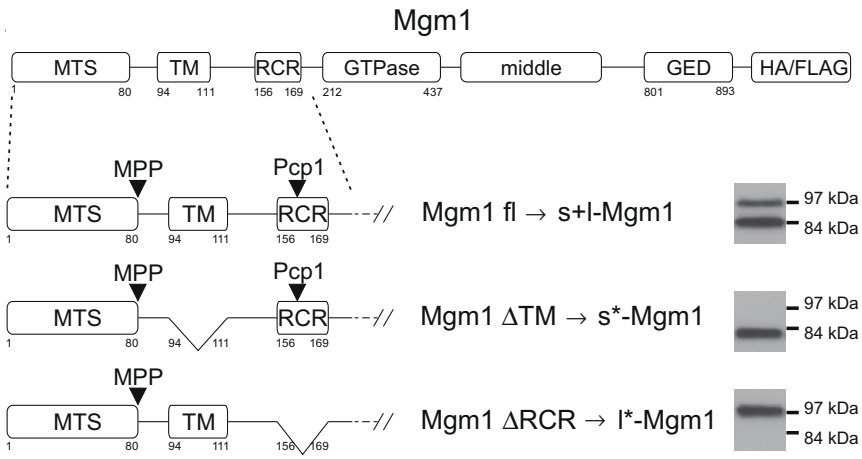

Figure 6.1. Schematic representation of Mgm1 and Mgm1 variants used to generate l*-Mgm1 and s*-Mgm1

Deletion of the first transmembrane segment (TM, aa 94-111) results in the production of s-Mgm1 only. Deletion of the rhomboid cleavage region (RCR) results in the production of l-Mgm1 only. Source: Adapted from Herlan, Bornhovd et al. (2004).

6.2.2 Possible effector roles of lipid-binding activity

The effector roles of lipid-binding activity of Mgm1 could be as the following: (1) to target proteins to the membrane; (2) to modify protein structure, which in turn affects its function; and/or (3) to modify membrane structure, which in turn promotes IM fusion.

First, I demonstrated that s-Mgm1-lipid interactions recruits s-Mgm1 to liposomes in the absence of l-Mgm1, suggesting that specific s-Mgm1-lipid interactions can alone target Mgm1 to the membrane. However, the heterotypic interaction of s-Mgm1 with l-Mgm1 can also play a role in s-Mgm1 targeting (Zick, Duvezin-Caubet et al. 2009). Therefore, it is unclear whether s-Mgm1 is targeted to the membrane via the interaction with phospholipids or with l-Mgm1. Even though s-Mgm1 is recruited to the IM via interaction with l-Mgm1, l-Mgm1 may first localize to future membrane fusion sites via interaction with certain phospholipids. Therefore, future studies are required to investigate whether lipid-binding activity plays a role in Mgm1 targeting. Immuno-EM and subcellular fractionation experiments can be conducted to investigate Mgm1 membrane targeting and localization *in vivo.* To investigate the importance of the lipid-binding domain in l-Mgm1 localization, one can conduct a quantitative immuno-EM experiment with an

l-Mgm1 specific antibody as previously described (Zick, Duvezin-Caubet et al. 2009). l-Mgm1 is thought to move from the CM to IBM during IM fusion (Zick, Duvezin-Caubet et al. 2009). If the lipid-binding domain of l-Mgm1 is necessary for l-Mgm1 targeting to the IBM, one would expect to observe less l-Mgm1 localized to the IBM in a lipid-binding mutant than in wild-type yeast. To investigate the membrane recruitment of s-Mgm1, a subcellular fractionation experiment can be conducted where mitochondria can be cross-linked and lysed, and the membrane fraction can be separated from non-membrane fraction by ultracentrifugation. The amount of IM associated s-Mgm1 (membrane fraction) and s-Mgm1 in the IMS (non-membrane fraction) can be determined by western blot analysis. If the lipid-binding domain of s-Mgm1 is necessary for s-Mgm1 targeting to the IM, one would expect to observe a lower level of s-Mgm1 in the membrane fraction in a lipid-binding mutant than in wild-type yeast.

Second, lipid interactions may be able to modify s-Mgm1 tertiary structure to promote s-Mgm1 oligomerization into hexameric rings. Since s-Mgm1 hexameric rings were not observed in solution either by EM or by size exclusion chromatography, it is possible that hexamerization happens only in the presence of lipids. Lipid interaction drastically enhances GTPase activity of s-Mgm1, suggesting that s-Mgm1 structure may be modified to allow for a higher rate of GTP hydrolysis. It would be worthwhile to further address the possibility that lipid interaction may modify Mgm1 structure by structural studies such as X-ray crystallography (see section **6.3**).

Lastly, instead of affecting protein structure, Mgm1-lipid interactions may affect the topology of IM. I showed that s-Mgm1-lipid interactions alter membrane topology by promoting local membrane bending, which can be enhanced by GTP. In addition, GTP also promotes the fusion of s-Mgm1 and l-Mgm1 bound liposomes. Therefore, s-Mgm1-lipid interaction may be a requirement to induce local membrane bending in order to promote membrane fusion. To investigate these potential steps in IM fusion, a total internal reflection fluorescence microscopy experiment can be conducted to monitor membrane topology changes in a millisecond timescale (see section **6.4**).

6.2.3 Possible unique lipid-binding domain of Mgm1

Mutagenesis experiments reveal that K566, K724, and K795 are crucial residues for Mgm1 interactions with negatively charged phospholipids. Therefore, I propose that the region from amino acid 566 to 795 could represent a lipid-binding domain of Mgm1. To further confirm this, one can investigate whether this 566-795 polypeptide folds into a functional domain and determine the domain structure. To characterize the lipid-binding domain of Mgm1, a plasmid expressing a polypeptide containing amino acids 566 to 795 of Mgm1 and a 6xHis tag can be generated. The 6xHis tagged polypeptide can be expressed and purified as previously done (Rujiviphat, Meglei et al. 2009) (Chapter 3). A series of sequence modifications including adding hydrophilic residues at the N- and C-terminal tails or mutating some residues may be necessary to obtain the optimal protein expression and stability. Once the expression and the stability of Mgm1 truncations are optimized, far-UV circular dichroism spectroscopy can be performed to investigate secondary structure as previously described (Rujiviphat, Meglei et al. 2009) (Chapter 3). An atomic model of Mgm1 reveals two helices, which reside between the middle domain and the GED, facing the membrane. Therefore, the two characteristic minima at 208 and 220 nm are expected if the 566-795 polypeptide is properly folded into a protein domain. To determine whether it is a functional domain, the lipid-binding activity can next be tested by the enzyme-linked immunosorbent assay as well as the liposome recruitment assay, as previously done (Rujiviphat, Meglei et al. 2009) (Chapter 3). Conducting these assays on a series of truncations will also determine the boundary of the lipid-binding domain. Alternatively, information on domain boundary could also be illustrated by structural determination studies, including spectroscopy experiments and X-ray crystallography.

6.3 MGM1 STRUCTURE

Although the crystal structure of either Mgm1 or its human homologue OPA1 has not been determined, there are atomic model structures of Mgm1 and the GTPase domain of OPA1. In addition, in this thesis, I characterized s-Mgm1 oligomeric structures and its structural transitions by electron microscopy (Rujiviphat, Meglei et al. 2009, Abutbul-Ionita, Rujiviphat et al. 2012) (Chapters 3 and 4). The oligomeric structures further confirm the hypothesis that Mgm1 interacts in *cis* and in *trans*. The two-dimensional crystal structures and cryo-EM images

suggest that the size of the Mgm1 monomer is approximately 5 nm, which is consistent with the predicted size of an 86 kDa globular protein (**Figure 3.6** and **Figure 4.1**). DeVay et al. also presented a similar two-dimensional crystal structure and proposed an atomic model of Mgm1 (DeVay, Dominguez-Ramirez et al. 2009). Together, these findings provide a basis for future structural characterization. Solving Mgm1 monomeric and oligomeric structures is important to understand how Mgm1 assembles onto the membrane to promote IM fusion.

Determining the crystal structure of Mgm1 could reveal structural details of the Mgm1-Mgm1 and Mgm1-lipid interaction surfaces, which are essential to fully understand Mgm1 mechanistic actions. I have attempted to crystallize s-Mgm1 by screening with 288 different conditions, and by optimizing with a range of pH and precipitant concentrations. In addition, I have tried a lipidic-mesophase method to crystallize s-Mgm1 (Caffrey and Cherezov 2009) using two different lipid mixtures and in 384 conditions. However, to date, I have not yet been able to obtain a suitable s-Mgm1 crystal for x-ray diffraction. One of the major problems I encountered was protein aggregation, which could be due to the fact that Mgm1 oligomerizes, and that purified s-Mgm1 is not stable under low salt concentration. Point mutations or truncations can be introduced to abolish protein oligomerization and may eliminate the protein aggregation problem and promote protein crystallization.

Co-crystallization of s-Mgm1 with interacting lipids and with l-Mgm1 would provide answers to how s-Mgm1 interacts with the IM and how s-Mgm1 forms a complex with l-Mgm1, respectively. To pursue this, one can conduct a traditional approach of detergent solubilized protein or lipidic phase crystallization (Johansson, Wohri et al. 2009). One would expect to observe the interacting surface between the membrane and the proposed lipid-binding domain, which exposes the lysine residues to the membrane. It is also interesting to observe l-Mgm1 and s-Mgm1 interactions to form the Mgm1 complex. Since amino acid sequence of l-Mgm1 is identical to that of s-Mgm1 except for the additional amino acids 60-161 in the N-terminus of l-Mgm1, the l-Mgm1/s-Mgm1 complex may have a structure similar to that of s-Mgm1 dimer, which was previously shown in the model structure of s-Mgm1 (DeVay, Dominguez-Ramirez et al. 2009).

In addition, I demonstrated Mgm1 conformational changes by EM and by circular dichroism. Although these results confirm that structural changes occur during GTP binding, it

is still unknown what are the atomic changes. The crystal structures of Mgm1 in different nucleotide-bound forms would directly demonstrate these changes. For instance, recent crystal structures of GDP-bound, GDP•AlF_4^--bound and GppNHp-bound forms of atlastin show that atlastin conformational changes may be crucial to promote membrane fusion (Byrnes, Singh et al. 2013). The author proposed that GTP binding and GTP hydrolysis promotes conformational changes and the dimerization of GTPase and middle domains, respectively. Moreover, phosphate release promotes the disassembly of the dimer. Together, the structural information on Mgm1 interaction surfaces and structural transitions during GTP cycle will provide mechanistic details of how Mgm1 mediates IM fusion.

6.4 A MODEL OF MGM1-MEDIATED IM FUSION

Membrane fusion requires two planar bilayers to come together. The membranes also have to undergo rearrangement into a non-bilayer structure for joining and mixing lipids from the opposing monolayers. Cellular membrane fusion requires the help from pro-fusion proteins, and therefore involves more steps and regulation to promote the two main actions: membrane tethering and lipid mixing. Findings from this thesis and other recent studies led me to propose that, to mediate membrane fusion, Mgm1 may (1) localize to the fusion site, (2) tether the opposing membranes, (3) initiate the joining of the opposing monolayers, (4) move away from the fusion site to promote membrane contact, (5) complete the bilayer fusion, and (6) release and recycle itself back for the next round of IM fusion (**Figure 6.2**).

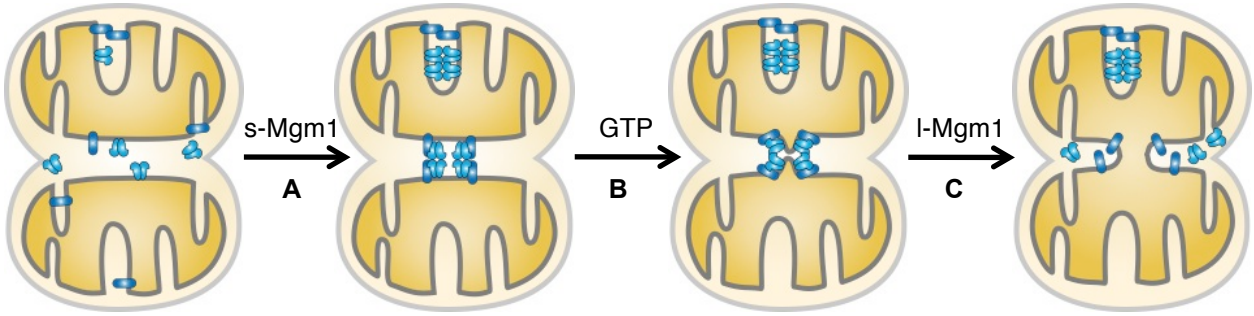

Figure 6.2. Model of Mgm1-mediated IM fusion

I propose that following mitochondrial outer membrane fusion, s-Mgm1 (*light blue*) and l-Mgm1 (*dark blue*) assemble into pre-fusion complexes to mediate inner membrane fusion (**A**). GTP binding induces a conformational change to induce the fusion of the mitochondrial inner membrane (**B**) followed by resolution of the s-Mgm1 and l-Mgm1 complexes (**C**).

As illustrated in **Figure 6.2**, to localize to the fusion site, l-Mgm1 first moves laterally to the fusion site. l-Mgm1 may be able to recognize the fusion site by localizing to a particular membrane domain that is concentrated with Mgm1-interacting phospholipids. Then, s-Mgm1 can be recruited to the membrane by interacting with l-Mgm1 and/or by interacting with phospholipids. Upon membrane recruitment, s-Mgm1 may oligomerize in *cis* and in *trans* to tether fusing membranes. GTP binding may cause conformational changes of s-Mgm1 to promote membrane curvature, which in turn initiates membrane fusion via a hemifusion intermediate. Lastly, the insertion of the l-Mgm1 hydrophobic segment may help destabilize the bilayer and promote lipid mixing to complete the fusion. The two remaining questions to this model are (1) how Mgm1 dissociates from the fusion site to allow membranes to make contact and fuse, and (2) how s-Mgm1 releases from the membrane and recycles back to the IMS to mediate the next round of IM fusion.

EM images obtained in this thesis work demonstrated that s-Mgm1 tightly assembles with one another, raising the question of how s-Mgm1 would resolve from the fusion site to allow for membrane contact. It is possible that s-Mgm1 oligomeric transitions into tighter arrays would constrict the membrane enough to allow the membrane the make contact, without the necessary protein clearance, as illustrated in **Figure 6.2**. However, more data are required to

support this notion. Total internal reflection fluorescence (TIRF) microscopy can be a method of choice to detect small changes in the bilayer as well as to monitor vesicle fusion. In a TIRF experiment, a small region of fluorescently labeled bilayer can be excited by an evanescent wave. Since the evanescent electromagnetic field decays exponentially, only particles within ~100 nm will be illuminated. In addition, the farther away the particles are, the lower the level of signal that can be detected. Therefore, one would expect a decrease in fluorescence signal in the areas where membranes that have positive curvatures. Simultaneous vesicle fusion can also be detected by labeling the fusing vesicles with a different fluorescence probe. On the basis of the proposed model, one would expect to observe a decrease in membrane fluorescence signal due to membrane disruption, following by an increase in vesicle fluorescence signal upon vesicle fusion. Therefore, this proposed experiment will address the possibility that s-Mgm1 structural rearrangement can constrict membrane to promote membrane fusion.

Second, to determine whether Mgm1 is degraded or recycled back to mediate the next round of IM fusion, one can investigate the Mgm1 turnover rate. Fzo1 is degraded in the last step of OM fusion and, thus, is quickly turned over (Anton, Fres et al. 2011). To determine whether Mgm1 also gets degraded upon IM fusion, I performed a cycloheximide chase assay, where protein synthesis is inhibited. Interestingly, I observed that the Mgm1 protein level is stable over a period of at least 12 hours. The low level of protein turnover suggests that, unlike Fzo1, Mgm1 does not degrade upon IM fusion but gets recycled back for the next round of IM fusion. In the presence of GDP+Pi, which represents the condition following GTP hydrolysis, I observed a reduction of liposomes with lattice (from >90% to ~60%) (**Figure 4.3**). The lack of lattice could be due to the lack of protein. Therefore, it is possible that s-Mgm1 is released from the IM upon GTP hydrolysis (**Figure 5.15**). To test this possibility, liposome co-sedimentation or co-flotation experiments can be conducted, as previously described (DeVay, Dominguez-Ramirez et al. 2009, Ban, Heymann et al. 2010), to quantitatively determine the recruitment of s-Mgm1 to liposomes in the presence of different nucleotides. If Mgm1 were recycled upon IM fusion, one would expect to observe less s-Mgm1 in the liposome co-sedimentation/co-floatation fraction in the presence of GDP+Pi than in the presence of a GTP non-hydrolyzable analog. This result would further support the proposed model regarding Mgm1-membrane disassembly (**Figure 5.15**).

6.5 REGULATION OF MGM1-MEDIATED IM FUSION

On the basis of the findings in this thesis work and the proposed model, multiple mechanistic steps are involved in Mgm1-mediated IM fusion, and each step could be differently regulated. The only known regulation of Mgm1 function is the control of the ratio of s-Mgm1 and l-Mgm1. Since no more than 20% of the liposomes were fused in the content-mixing assay in the presence of s-Mgm1 and l-Mgm1 (**Figure 5.14, A**), there could be other factors influencing IM fusion. For instance, Ugo1 may play a role in the lipid-mixing step of IM fusion (Hoppins, Horner et al. 2009). Therefore, including Ugo1 in the content-mixing assay may stimulate the liposome fusion rate.

In addition to Ugo1, Mgm1-mediated IM fusion may involve other proteins. To identify additional players in IM fusion, one can conduct an affinity purification screen to identify physical interacting partners of Mgm1 complex. Tandem affinity purification (TAP) could be a method of choice. I constructed a plasmid expressing full-length Mgm1 with a TAP tag, which consists of a calmodulin-binding peptide and Protein A, allowing for a two-step purification of Mgm1 complex and Mgm1 interacting partners. I confirmed that the fusion protein does not alter Mgm1 expression, processing, or function. TAP-tagged Mgm1 is expressed at the endogenous level, is localized to mitochondria, and is processed in to TAP-tagged l-Mgm1 and s-Mgm1 at an equal molar ratio. The strain expressing TAP-tagged Mgm1 maintains its normal growth rate and mitochondrial morphology and function, suggesting that the TAP tag does not affect Mgm1 function. Moreover, preliminary data showed that TAP-tagged Mgm1 interacts with Fzo1 as expected. Therefore, tandem affinity purification is a suitable method to identify new players or regulators that function with Mgm1 to mediate IM fusion.

6.6 CONCLUSION

In this thesis, I provide insights into the molecular mechanism of how Mgm1 mediates mitochondrial IM fusion by showing that phospholipid associations, membrane tethering, structural changes, and membrane deformation are essential activities of s-Mgm1. I also show that l-Mgm1 is required at the later stage of IM fusion, and I propose a model of how the two isoforms work together to mediate IM fusion. The proposed model will lay a path to the

understanding of how each mechanistic step can be regulated. It will also help identify additional proteins that may play a role in regulating IM fusion and in maintaining the balance of mitochondrial fusion and fission. Disrupted balance in mitochondrial dynamics has been implicated in several neurodegenerative diseases. Therefore, the advancements made in this thesis work would contribute to the understanding of the mechanism of Mgm1 function, the mechanism of mitochondrial fusion, the mechanism of pro-fusion dynamin-related proteins, and the link between mitochondrial dynamics and neurodegenerative diseases.

References

Abutbul-Ionita, I., J. Rujiviphat, I. Nir, G. A. McQuibban and D. Danino (2012). "Membrane tethering and nucleotide-dependent conformational changes drive mitochondrial genome maintenance (Mgm1) protein-mediated membrane fusion." J Biol Chem **287**(44): 36634-36638.

Anderson, S., A. T. Bankier, B. G. Barrell, M. H. de Bruijn, A. R. Coulson, J. Drouin, I. C. Eperon, D. P. Nierlich, B. A. Roe, F. Sanger, P. H. Schreier, A. J. Smith, R. Staden and I. G. Young (1981). "Sequence and organization of the human mitochondrial genome." Nature **290**(5806): 457-465.

Andersson, S. G. and C. G. Kurland (1999). "Origins of mitochondria and hydrogenosomes." Curr Opin Microbiol **2**(5): 535-541.

Andersson, S. G., A. Zomorodipour, J. O. Andersson, T. Sicheritz-Ponten, U. C. Alsmark, R. M. Podowski, A. K. Naslund, A. S. Eriksson, H. H. Winkler and C. G. Kurland (1998). "The genome sequence of Rickettsia prowazekii and the origin of mitochondria." Nature **396**(6707): 133-140.

Anton, F., G. Dittmar, T. Langer and M. Escobar-Henriques (2013). "Two deubiquitylases act on mitofusin and regulate mitochondrial fusion along independent pathways." Mol Cell **49**(3): 487-498.

Anton, F., J. M. Fres, A. Schauss, B. Pinson, G. J. Praefcke, T. Langer and M. Escobar-Henriques (2011). "Ugo1 and Mdm30 act sequentially during Fzo1-mediated mitochondrial outer membrane fusion." J Cell Sci **124**(Pt 7): 1126-1135.

Avinoam, O., K. Fridman, C. Valansi, I. Abutbul, T. Zeev-Ben-Mordehai, U. E. Maurer, A. Sapir, D. Danino, K. Grunewald, J. M. White and B. Podbilewicz (2011). "Conserved eukaryotic fusogens can fuse viral envelopes to cells." Science **332**(6029): 589-592.

Backues, S. K. and S. Y. Bednarek (2010). "Arabidopsis dynamin-related protein 1A polymers bind, but do not tubulate, liposomes." Biochem Biophys Res Commun **393**(4): 734-739.

Ban, T., J. A. Heymann, Z. Song, J. E. Hinshaw and D. C. Chan (2010). "OPA1 disease alleles causing dominant optic atrophy have defects in cardiolipin-stimulated GTP hydrolysis and membrane tubulation." Hum Mol Genet **19**(11): 2113-2122.

Baryshnikova, A., M. Costanzo, S. Dixon, F. J. Vizeacoumar, C. L. Myers, B. Andrews and C. Boone (2010). "Synthetic genetic array (SGA) analysis in Saccharomyces cerevisiae and Schizosaccharomyces pombe." Methods Enzymol **470**: 145-179.

Berger, K. H. and M. P. Yaffe (1998). "Prohibitin family members interact genetically with mitochondrial inheritance components in Saccharomyces cerevisiae." Mol Cell Biol **18**(7): 4043-4052.

Bethoney, K. A., M. C. King, J. E. Hinshaw, E. M. Ostap and M. A. Lemmon (2009). "A possible effector role for the pleckstrin homology (PH) domain of dynamin." Proc Natl Acad Sci U S A **106**(32): 13359-13364.

Bian, X., R. W. Klemm, T. Y. Liu, M. Zhang, S. Sun, X. Sui, X. Liu, T. A. Rapoport and J. Hu (2011). "Structures of the atlastin GTPase provide insight into homotypic fusion of endoplasmic reticulum membranes." Proc Natl Acad Sci U S A **108**(10): 3976-3981.

Bleazard, W., J. M. McCaffery, E. J. King, S. Bale, A. Mozdy, Q. Tieu, J. Nunnari and J. M. Shaw (1999). "The dynamin-related GTPase Dnm1 regulates mitochondrial fission in yeast." Nat Cell Biol **1**(5): 298-304.

Bourne, H. R., D. A. Sanders and F. McCormick (1991). "The GTPase superfamily: conserved structure and molecular mechanism." Nature **349**(6305): 117-127.

Burgess, S. M., M. Delannoy and R. E. Jensen (1994). "MMM1 encodes a mitochondrial outer membrane protein essential for establishing and maintaining the structure of yeast mitochondria." J Cell Biol **126**(6): 1375-1391.

Burmann, F., N. Ebert, S. van Baarle and M. Bramkamp (2011). "A bacterial dynamin-like protein mediating nucleotide-independent membrane fusion." Mol Microbiol **79**(5): 1294-1304.

Byrnes, L. J., A. Singh, K. Szeto, N. M. Benvin, J. P. O'Donnell, W. R. Zipfel and H. Sondermann (2013). "Structural basis for conformational switching and GTP loading of the large G protein atlastin." EMBO J **32**(3): 369-384.

Byrnes, L. J. and H. Sondermann (2011). "Structural basis for the nucleotide-dependent dimerization of the large G protein atlastin-1/SPG3A." Proc Natl Acad Sci U S A **108**(6): 2216-2221.

Caffrey, M. and V. Cherezov (2009). "Crystallizing membrane proteins using lipidic mesophases." Nat Protoc **4**(5): 706-731.

Carr, J. F. and J. E. Hinshaw (1997). "Dynamin assembles into spirals under physiological salt conditions upon the addition of GDP and gamma-phosphate analogues." J Biol Chem **272**(44): 28030-28035.

Cerveny, K. L., S. L. Studer, R. E. Jensen and H. Sesaki (2007). "Yeast mitochondrial division and distribution require the cortical num1 protein." Dev Cell **12**(3): 363-375.

Chacinska, A., C. M. Koehler, D. Milenkovic, T. Lithgow and N. Pfanner (2009). "Importing mitochondrial proteins: machineries and mechanisms." Cell **138**(4): 628-644.

Chan, D. C. (2006). "Mitochondria: dynamic organelles in disease, aging, and development." Cell **125**(7): 1241-1252.

Chan, D. C. (2012). "Fusion and fission: interlinked processes critical for mitochondrial health." Annu Rev Genet **46**: 265-287.

Chan, E. Y. and G. A. McQuibban (2012). "Phosphatidylserine decarboxylase 1 (Psd1) promotes mitochondrial fusion by regulating the biophysical properties of the mitochondrial membrane and alternative topogenesis of mitochondrial genome maintenance protein 1 (Mgm1)." J Biol Chem **287**(48): 40131-40139.

Chappie, J. S., S. Acharya, M. Leonard, S. L. Schmid and F. Dyda (2010). "G domain dimerization controls dynamin's assembly-stimulated GTPase activity." Nature **465**(7297): 435-440.

Chappie, J. S., J. A. Mears, S. Fang, M. Leonard, S. L. Schmid, R. A. Milligan, J. E. Hinshaw and F. Dyda (2011). "A pseudoatomic model of the dynamin polymer identifies a hydrolysis-dependent powerstroke." Cell **147**(1): 209-222.

Chen, C. H., S. L. Howng, S. L. Hwang, C. K. Chou, C. H. Liao and Y. R. Hong (2000). "Differential expression of four human dynamin-like protein variants in brain tumors." DNA Cell Biol **19**(3): 189-194.

Chen, H. and D. C. Chan (2005). "Emerging functions of mammalian mitochondrial fusion and fission." Hum Mol Genet **14 Spec No. 2**: R283-289.

Chen, H., S. A. Detmer, A. J. Ewald, E. E. Griffin, S. E. Fraser and D. C. Chan (2003). "Mitofusins Mfn1 and Mfn2 coordinately regulate mitochondrial fusion and are essential for embryonic development." J Cell Biol **160**(2): 189-200.

Chen, Y. and G. W. Dorn, 2nd (2013). "PINK1-phosphorylated mitofusin 2 is a Parkin receptor for culling damaged mitochondria." Science **340**(6131): 471-475.

Chen, Y. J., P. Zhang, E. H. Egelman and J. E. Hinshaw (2004). "The stalk region of dynamin drives the constriction of dynamin tubes." Nat Struct Mol Biol **11**(6): 574-575.

Chernomordik, L. V. and M. M. Kozlov (2008). "Mechanics of membrane fusion." Nat Struct Mol Biol **15**(7): 675-683.

Choi, S. Y., P. Huang, G. M. Jenkins, D. C. Chan, J. Schiller and M. A. Frohman (2006). "A common lipid links Mfn-mediated mitochondrial fusion and SNARE-regulated exocytosis." Nat Cell Biol **8**(11): 1255-1262.

Cohen, M. M., E. A. Amiott, A. R. Day, G. P. Leboucher, E. N. Pryce, M. H. Glickman, J. M. McCaffery, J. M. Shaw and A. M. Weissman (2011). "Sequential requirements for the GTPase domain of the mitofusin Fzo1 and the ubiquitin ligase SCFMdm30 in mitochondrial outer membrane fusion." J Cell Sci **124**(Pt 9): 1403-1410.

Cohen, M. M., G. P. Leboucher, N. Livnat-Levanon, M. H. Glickman and A. M. Weissman (2008). "Ubiquitin-proteasome-dependent degradation of a mitofusin, a critical regulator of mitochondrial fusion." Mol Biol Cell **19**(6): 2457-2464.

Connell, E., P. Scott and B. Davletov (2008). "Real-time assay for monitoring membrane association of lipid-binding domains." Anal Biochem **377**(1): 83-88.

Coonrod, E. M., M. A. Karren and J. M. Shaw (2007). "Ugo1p is a multipass transmembrane protein with a single carrier domain required for mitochondrial fusion." Traffic **8**(5): 500-511.

Crowther, R. A., R. Henderson and J. M. Smith (1996). "MRC image processing programs." J Struct Biol **116**(1): 9-16.

Danino, D., A. Bernheim-Groswasser and Y. Talmon (2001). "Digital cryogenic transmission electron microscopy: an advanced tool for direct imaging of complex fluids." Colloids and Surfaces A: Physicochemical and Engineering Aspects **183–185**(0): 113-122.

Danino, D. and J. E. Hinshaw (2001). "Dynamin family of mechanoenzymes." Curr Opin Cell Biol **13**(4): 454-460.

Danino, D., K. H. Moon and J. E. Hinshaw (2004). "Rapid constriction of lipid bilayers by the mechanochemical enzyme dynamin." J Struct Biol **147**(3): 259-267.

Davies, V. J., A. J. Hollins, M. J. Piechota, W. Yip, J. R. Davies, K. E. White, P. P. Nicols, M. E. Boulton and M. Votruba (2007). "Opa1 deficiency in a mouse model of autosomal dominant optic atrophy impairs mitochondrial morphology, optic nerve structure and visual function." Hum Mol Genet **16**(11): 1307-1318.

Delettre, C., G. Lenaers, J. M. Griffoin, N. Gigarel, C. Lorenzo, P. Belenguer, L. Pelloquin, J. Grosgeorge, C. Turc-Carel, E. Perret, C. Astarie-Dequeker, L. Lasquellec, B. Arnaud, B. Ducommun, J. Kaplan and C. P. Hamel (2000). "Nuclear gene OPA1, encoding a mitochondrial dynamin-related protein, is mutated in dominant optic atrophy." Nat Genet **26**(2): 207-210.

DeVay, R. M., L. Dominguez-Ramirez, L. L. Lackner, S. Hoppins, H. Stahlberg and J. Nunnari (2009). "Coassembly of Mgm1 isoforms requires cardiolipin and mediates mitochondrial inner membrane fusion." J Cell Biol **186**(6): 793-803.

Diao, J., P. Grob, D. J. Cipriano, M. Kyoung, Y. Zhang, S. Shah, A. Nguyen, M. Padolina, A. Srivastava, M. Vrljic, A. Shah, E. Nogales, S. Chu and A. T. Brunger (2012). "Synaptic proteins promote calcium-triggered fast transition from point contact to full fusion." Elife **1**: e00109.

Dimmer, K. S., S. Fritz, F. Fuchs, M. Messerschmitt, N. Weinbach, W. Neupert and B. Westermann (2002). "Genetic basis of mitochondrial function and morphology in Saccharomyces cerevisiae." Mol Biol Cell **13**(3): 847-853.

Dohm, J. A., S. J. Lee, J. M. Hardwick, R. B. Hill and A. G. Gittis (2004). "Cytosolic domain of the human mitochondrial fission protein fis1 adopts a TPR fold." Proteins **54**(1): 153-156.

Ehses, S., I. Raschke, G. Mancuso, A. Bernacchia, S. Geimer, D. Tondera, J. C. Martinou, B. Westermann, E. I. Rugarli and T. Langer (2009). "Regulation of OPA1 processing and mitochondrial fusion by m-AAA protease isoenzymes and OMA1." J Cell Biol **187**(7): 1023-1036.

Eiberg, H., B. Kjer, P. Kjer and T. Rosenberg (1994). "Dominant optic atrophy (OPA1) mapped to chromosome 3q region. I. Linkage analysis." Hum Mol Genet **3**(6): 977-980.

Escobar-Henriques, M. and F. Anton (2013). "Mechanistic perspective of mitochondrial fusion: tubulation vs. fragmentation." Biochim Biophys Acta **1833**(1): 162-175.

Escobar-Henriques, M., B. Westermann and T. Langer (2006). "Regulation of mitochondrial fusion by the F-box protein Mdm30 involves proteasome-independent turnover of Fzo1." J Cell Biol **173**(5): 645-650.

Esser, K., B. Tursun, M. Ingenhoven, G. Michaelis and E. Pratje (2002). "A novel two-step mechanism for removal of a mitochondrial signal sequence involves the mAAA complex and the putative rhomboid protease Pcp1." J Mol Biol **323**(5): 835-843.

Exner, N., A. K. Lutz, C. Haass and K. F. Winklhofer (2012). "Mitochondrial dysfunction in Parkinson's disease: molecular mechanisms and pathophysiological consequences." EMBO J **31**(14): 3038-3062.

Faelber, K., Y. Posor, S. Gao, M. Held, Y. Roske, D. Schulze, V. Haucke, F. Noe and O. Daumke (2011). "Crystal structure of nucleotide-free dynamin." Nature **477**(7366): 556-560.

Ferguson, L. R. and R. C. von Borstel (1992). "Induction of the cytoplasmic 'petite' mutation by chemical and physical agents in Saccharomyces cerevisiae." Mutat Res **265**(1): 103-148.

Ferguson, S. M. and P. De Camilli (2012). "Dynamin, a membrane-remodelling GTPase." Nat Rev Mol Cell Biol **13**(2): 75-88.

Fitzgerald, S. T. (1992). "National Asthma Education Program Expert Panel report: guidelines for the diagnosis and management of asthma." AAOHN J **40**(8): 376-382.

Ford, M. G., S. Jenni and J. Nunnari (2011). "The crystal structure of dynamin." Nature **477**(7366): 561-566.

Furt, F. and P. Moreau (2009). "Importance of lipid metabolism for intracellular and mitochondrial membrane fusion/fission processes." Int J Biochem Cell Biol **41**(10): 1828-1836.

Gammie, A. E., L. J. Kurihara, R. B. Vallee and M. D. Rose (1995). "DNM1, a dynamin-related gene, participates in endosomal trafficking in yeast." J Cell Biol **130**(3): 553-566.

Gao, S., A. von der Malsburg, A. Dick, K. Faelber, G. F. Schroder, O. Haller, G. Kochs and O. Daumke (2011). "Structure of myxovirus resistance protein a reveals intra- and intermolecular domain interactions required for the antiviral function." Immunity **35**(4): 514-525.

Gao, S., A. von der Malsburg, S. Paeschke, J. Behlke, O. Haller, G. Kochs and O. Daumke (2010). "Structural basis of oligomerization in the stalk region of dynamin-like MxA." Nature **465**(7297): 502-506.

Gebert, N., A. S. Joshi, S. Kutik, T. Becker, M. McKenzie, X. L. Guan, V. P. Mooga, D. A. Stroud, G. Kulkarni, M. R. Wenk, P. Rehling, C. Meisinger, M. T. Ryan, N. Wiedemann, M. L. Greenberg and N. Pfanner (2009). "Mitochondrial cardiolipin involved in outer-membrane protein biogenesis: implications for Barth syndrome." Curr Biol **19**(24): 2133-2139.

Gipson, B., X. Zeng, Z. Y. Zhang and H. Stahlberg (2007). "2dx--user-friendly image processing for 2D crystals." J Struct Biol **157**(1): 64-72.

Glauser, L., S. Sonnay, K. Stafa and D. J. Moore (2011). "Parkin promotes the ubiquitination and degradation of the mitochondrial fusion factor mitofusin 1." J Neurochem **118**(4): 636-645.

Gray, M. W., G. Burger and B. F. Lang (1999). "Mitochondrial evolution." Science **283**(5407): 1476-1481.

Guan, K., L. Farh, T. K. Marshall and R. J. Deschenes (1993). "Normal mitochondrial structure and genome maintenance in yeast requires the dynamin-like product of the MGM1 gene." Curr Genet **24**(1-2): 141-148.

Hailey, D. W., A. S. Rambold, P. Satpute-Krishnan, K. Mitra, R. Sougrat, P. K. Kim and J. Lippincott-Schwartz (2010). "Mitochondria supply membranes for autophagosome biogenesis during starvation." Cell **141**(4): 656-667.

Hales, K. G. and M. T. Fuller (1997). "Developmentally regulated mitochondrial fusion mediated by a conserved, novel, predicted GTPase." Cell **90**(1): 121-129.

Haller, O., S. Gao, A. von der Malsburg, O. Daumke and G. Kochs (2010). "Dynamin-like MxA GTPase: structural insights into oligomerization and implications for antiviral activity." J Biol Chem **285**(37): 28419-28424.

Hammermeister, M., K. Schodel and B. Westermann (2010). "Mdm36 is a mitochondrial fission-promoting protein in Saccharomyces cerevisiae." Mol Biol Cell **21**(14): 2443-2452.

He, B., X. Yu, M. Margolis, X. Liu, X. Leng, Y. Etzion, F. Zheng, N. Lu, F. A. Quiocho, D. Danino and Z. Zhou (2010). "Live-cell imaging in Caenorhabditis elegans reveals the distinct roles of dynamin self-assembly and guanosine triphosphate hydrolysis in the removal of apoptotic cells." Mol Biol Cell **21**(4): 610-629.

Head, B., L. Griparic, M. Amiri, S. Gandre-Babbe and A. M. van der Bliek (2009). "Inducible proteolytic inactivation of OPA1 mediated by the OMA1 protease in mammalian cells." J Cell Biol **187**(7): 959-966.

Herlan, M., C. Bornhovd, K. Hell, W. Neupert and A. S. Reichert (2004). "Alternative topogenesis of Mgm1 and mitochondrial morphology depend on ATP and a functional import motor." J Cell Biol **165**(2): 167-173.

Herlan, M., F. Vogel, C. Bornhovd, W. Neupert and A. S. Reichert (2003). "Processing of Mgm1 by the rhomboid-type protease Pcp1 is required for maintenance of mitochondrial morphology and of mitochondrial DNA." J Biol Chem **278**(30): 27781-27788.

Hermann, G. J., E. J. King and J. M. Shaw (1997). "The yeast gene, MDM20, is necessary for mitochondrial inheritance and organization of the actin cytoskeleton." J Cell Biol **137**(1): 141-153.

Hermann, G. J., J. W. Thatcher, J. P. Mills, K. G. Hales, M. T. Fuller, J. Nunnari and J. M. Shaw (1998). "Mitochondrial fusion in yeast requires the transmembrane GTPase Fzo1p." J Cell Biol **143**(2): 359-373.

Hinshaw, J. E. and S. L. Schmid (1995). "Dynamin self-assembles into rings suggesting a mechanism for coated vesicle budding." Nature **374**(6518): 190-192.

Hoppins, S., J. Horner, C. Song, J. M. McCaffery and J. Nunnari (2009). "Mitochondrial outer and inner membrane fusion requires a modified carrier protein." J Cell Biol **184**(4): 569-581.

Hoppins, S., L. Lackner and J. Nunnari (2007). "The machines that divide and fuse mitochondria." Annu Rev Biochem **76**: 751-780.

Huang, B., H. Babcock and X. Zhuang (2010). "Breaking the diffraction barrier: super-resolution imaging of cells." Cell **143**(7): 1047-1058.

Hurley, J. H. and J. E. Hinshaw (2012). "Dynamin: membrane scission meets physics." Curr Biol **22**(24): R1047-1048.

Ichishita, R., K. Tanaka, Y. Sugiura, T. Sayano, K. Mihara and T. Oka (2008). "An RNAi screen for mitochondrial proteins required to maintain the morphology of the organelle in Caenorhabditis elegans." J Biochem **143**(4): 449-454.

Ingerman, E. and J. Nunnari (2005). "A continuous, regenerative coupled GTPase assay for dynamin-related proteins." Methods Enzymol **404**: 611-619.

Ingerman, E., E. M. Perkins, M. Marino, J. A. Mears, J. M. McCaffery, J. E. Hinshaw and J. Nunnari (2005). "Dnm1 forms spirals that are structurally tailored to fit mitochondria." J Cell Biol **170**(7): 1021-1027.

Johansson, L. C., A. B. Wohri, G. Katona, S. Engstrom and R. Neutze (2009). "Membrane protein crystallization from lipidic phases." Curr Opin Struct Biol **19**(4): 372-378.

Jones, B. A. and W. L. Fangman (1992). "Mitochondrial DNA maintenance in yeast requires a protein containing a region related to the GTP-binding domain of dynamin." Genes Dev **6**(3): 380-389.

Joshi, A. S., M. N. Thompson, N. Fei, M. Huttemann and M. L. Greenberg (2012). "Cardiolipin and mitochondrial phosphatidylethanolamine have overlapping functions in mitochondrial fusion in Saccharomyces cerevisiae." J Biol Chem **287**(21): 17589-17597.

Kamimoto, T., Y. Nagai, H. Onogi, Y. Muro, T. Wakabayashi and M. Hagiwara (1998). "Dymple, a novel dynamin-like high molecular weight GTPase lacking a proline-rich carboxyl-terminal domain in mammalian cells." J Biol Chem **273**(2): 1044-1051.

Kim, Y. W., D. S. Park, S. C. Park, S. H. Kim, G. W. Cheong and I. Hwang (2001). "Arabidopsis dynamin-like 2 that binds specifically to phosphatidylinositol 4-phosphate assembles into a high-molecular weight complex in vivo and in vitro." Plant Physiol **127**(3): 1243-1255.

Klein, D. E., A. Lee, D. W. Frank, M. S. Marks and M. A. Lemmon (1998). "The pleckstrin homology domains of dynamin isoforms require oligomerization for high affinity phosphoinositide binding." J Biol Chem **273**(42): 27725-27733.

Kreye, S., J. Malsam and T. H. Sollner (2008). "In vitro assays to measure SNARE-mediated vesicle fusion." Methods Mol Biol **440**: 37-50.

Kroemer, G., B. Dallaporta and M. Resche-Rigon (1998). "The mitochondrial death/life regulator in apoptosis and necrosis." Annu Rev Physiol **60**: 619-642.

Kulikov, A. V., E. S. Shilov, I. A. Mufazalov, V. Gogvadze, S. A. Nedospasov and B. Zhivotovsky (2012). "Cytochrome c: the Achilles' heel in apoptosis." Cell Mol Life Sci **69**(11): 1787-1797.

Kuznetsov, A. V., M. Hermann, V. Saks, P. Hengster and R. Margreiter (2009). "The cell-type specificity of mitochondrial dynamics." Int J Biochem Cell Biol **41**(10): 1928-1939.

Lang, B. F., G. Burger, C. J. O'Kelly, R. Cedergren, G. B. Golding, C. Lemieux, D. Sankoff, M. Turmel and M. W. Gray (1997). "An ancestral mitochondrial DNA resembling a eubacterial genome in miniature." Nature **387**(6632): 493-497.

Lee, Y. J., S. Y. Jeong, M. Karbowski, C. L. Smith and R. J. Youle (2004). "Roles of the mammalian mitochondrial fission and fusion mediators Fis1, Drp1, and Opa1 in apoptosis." Mol Biol Cell **15**(11): 5001-5011.

Lenz, M., S. Morlot and A. Roux (2009). "Mechanical requirements for membrane fission: common facts from various examples." FEBS Lett **583**(23): 3839-3846.

Liu, T. Y., X. Bian, S. Sun, X. Hu, R. W. Klemm, W. A. Prinz, T. A. Rapoport and J. Hu (2012). "Lipid interaction of the C terminus and association of the transmembrane segments facilitate atlastin-mediated homotypic endoplasmic reticulum fusion." Proc Natl Acad Sci U S A **109**(32): E2146-2154.

Loson, O. C., Z. Song, H. Chen and D. C. Chan (2013). "Fis1, Mff, MiD49, and MiD51 mediate Drp1 recruitment in mitochondrial fission." Mol Biol Cell **24**(5): 659-667.

Lovas, J. R. and X. Wang (2013). "The meaning of mitochondrial movement to a neuron's life." Biochim Biophys Acta **1833**(1): 184-194.

Low, H. H. and J. Lowe (2006). "A bacterial dynamin-like protein." Nature **444**(7120): 766-769.

Low, H. H., C. Sachse, L. A. Amos and J. Lowe (2009). "Structure of a bacterial dynamin-like protein lipid tube provides a mechanism for assembly and membrane curving." Cell **139**(7): 1342-1352.

Luo, S., Q. Chen, E. Cebollero and D. Xing (2009). "Mitochondria: one of the origins for autophagosomal membranes?" Mitochondrion **9**(4): 227-231.

Mannella, C. A. (2006). "Structure and dynamics of the mitochondrial inner membrane cristae." Biochim Biophys Acta **1763**(5-6): 542-548.

Mannella, C. A. (2008). "Structural diversity of mitochondria: functional implications." Ann N Y Acad Sci **1147**: 171-179.

Mannella, C. A., D. R. Pfeiffer, P. C. Bradshaw, Moraru, II, B. Slepchenko, L. M. Loew, C. E. Hsieh, K. Buttle and M. Marko (2001). "Topology of the mitochondrial inner membrane: dynamics and bioenergetic implications." IUBMB Life **52**(3-5): 93-100.

Marks, B., M. H. Stowell, Y. Vallis, I. G. Mills, A. Gibson, C. R. Hopkins and H. T. McMahon (2001). "GTPase activity of dynamin and resulting conformation change are essential for endocytosis." Nature **410**(6825): 231-235.

Marsden, H. R., I. Tomatsu and A. Kros (2011). "Model systems for membrane fusion." Chem Soc Rev **40**(3): 1572-1585.

Martens, S. and H. T. McMahon (2008). "Mechanisms of membrane fusion: disparate players and common principles." Nat Rev Mol Cell Biol **9**(7): 543-556.

Martinou, J. C. and R. J. Youle (2011). "Mitochondria in apoptosis: Bcl-2 family members and mitochondrial dynamics." Dev Cell **21**(1): 92-101.

McConnell, S. J., L. C. Stewart, A. Talin and M. P. Yaffe (1990). "Temperature-sensitive yeast mutants defective in mitochondrial inheritance." J Cell Biol **111**(3): 967-976.

McQuibban, G. A., S. Saurya and M. Freeman (2003). "Mitochondrial membrane remodelling regulated by a conserved rhomboid protease." Nature **423**(6939): 537-541.

Mears, J. A. and J. E. Hinshaw (2008). "Visualization of dynamins." Methods Cell Biol **88**: 237-256.

Mears, J. A., L. L. Lackner, S. Fang, E. Ingerman, J. Nunnari and J. E. Hinshaw (2011). "Conformational changes in Dnm1 support a contractile mechanism for mitochondrial fission." Nat Struct Mol Biol **18**(1): 20-26.

Mears, J. A., P. Ray and J. E. Hinshaw (2007). "A corkscrew model for dynamin constriction." Structure **15**(10): 1190-1202.

Meeusen, S., R. DeVay, J. Block, A. Cassidy-Stone, S. Wayson, J. M. McCaffery and J. Nunnari (2006). "Mitochondrial inner-membrane fusion and crista maintenance requires the dynamin-related GTPase Mgm1." Cell **127**(2): 383-395.

Meeusen, S., J. M. McCaffery and J. Nunnari (2004). "Mitochondrial fusion intermediates revealed in vitro." Science **305**(5691): 1747-1752.

Meglei, G. and G. A. McQuibban (2009). "The dynamin-related protein Mgm1p assembles into oligomers and hydrolyzes GTP to function in mitochondrial membrane fusion." Biochemistry **48**(8): 1774-1784.

Morlot, S., V. Galli, M. Klein, N. Chiaruttini, J. Manzi, F. Humbert, L. Dinis, M. Lenz, G. Cappello and A. Roux (2012). "Membrane shape at the edge of the dynamin helix sets location and duration of the fission reaction." Cell **151**(3): 619-629.

Morlot, S. and A. Roux (2013). "Mechanics of dynamin-mediated membrane fission." Annu Rev Biophys **42**: 629-649.

Moss, T. J., C. Andreazza, A. Verma, A. Daga and J. A. McNew (2011). "Membrane fusion by the GTPase atlastin requires a conserved C-terminal cytoplasmic tail and dimerization through the middle domain." Proc Natl Acad Sci U S A **108**(27): 11133-11138.

Moss, T. J., A. Daga and J. A. McNew (2011). "Fusing a lasting relationship between ER tubules." Trends Cell Biol **21**(7): 416-423.

Muhlberg, A. B., D. E. Warnock and S. L. Schmid (1997). "Domain structure and intramolecular regulation of dynamin GTPase." EMBO J **16**(22): 6676-6683.

Nass, S. and M. M. Nass (1963). "Intramitochondrial Fibers with DNA Characteristics. Ii. Enzymatic and Other Hydrolytic Treatments." J Cell Biol **19**: 613-629.

Nunnari, J., W. F. Marshall, A. Straight, A. Murray, J. W. Sedat and P. Walter (1997). "Mitochondrial transmission during mating in Saccharomyces cerevisiae is determined by mitochondrial fusion and fission and the intramitochondrial segregation of mitochondrial DNA." Mol Biol Cell **8**(7): 1233-1242.

Okamoto, K. and J. M. Shaw (2005). "Mitochondrial morphology and dynamics in yeast and multicellular eukaryotes." Annu Rev Genet **39**: 503-536.

Orso, G., D. Pendin, S. Liu, J. Tosetto, T. J. Moss, J. E. Faust, M. Micaroni, A. Egorova, A. Martinuzzi, J. A. McNew and A. Daga (2009). "Homotypic fusion of ER membranes requires the dynamin-like GTPase atlastin." Nature **460**(7258): 978-983.

Osman, C., M. Haag, C. Potting, J. Rodenfels, P. V. Dip, F. T. Wieland, B. Brugger, B. Westermann and T. Langer (2009). "The genetic interactome of prohibitins: coordinated control of cardiolipin and phosphatidylethanolamine by conserved regulators in mitochondria." J Cell Biol **184**(4): 583-596.

Osman, C., D. R. Voelker and T. Langer (2011). "Making heads or tails of phospholipids in mitochondria." J Cell Biol **192**(1): 7-16.

Otera, H., N. Ishihara and K. Mihara (2013). "New insights into the function and regulation of mitochondrial fission." Biochim Biophys Acta **1833**(5): 1256-1268.

Otera, H., C. Wang, M. M. Cleland, K. Setoguchi, S. Yokota, R. J. Youle and K. Mihara (2010). "Mff is an essential factor for mitochondrial recruitment of Drp1 during mitochondrial fission in mammalian cells." J Cell Biol **191**(6): 1141-1158.

Otsuga, D., B. R. Keegan, E. Brisch, J. W. Thatcher, G. J. Hermann, W. Bleazard and J. M. Shaw (1998). "The dynamin-related GTPase, Dnm1p, controls mitochondrial morphology in yeast." J Cell Biol **143**(2): 333-349.

Palmer, C. S., K. D. Elgass, R. G. Parton, L. D. Osellame, D. Stojanovski and M. T. Ryan (2013). "Adaptor proteins MiD49 and MiD51 can act independently of Mff and Fis1 in Drp1 recruitment and are specific for mitochondrial fission." J Biol Chem **288**(38): 27584-27593.

Palmer, C. S., L. D. Osellame, D. Laine, O. S. Koutsopoulos, A. E. Frazier and M. T. Ryan (2011). "MiD49 and MiD51, new components of the mitochondrial fission machinery." EMBO Rep **12**(6): 565-573.

Pandey, A., D. M. Gordon, J. Pain, T. L. Stemmler, A. Dancis and D. Pain (2013). "Frataxin directly stimulates mitochondrial cysteine desulfurase by exposing substrate-binding sites and a mutant Fe-S cluster scaffold protein with frataxin-bypassing ability acts similarly." J Biol Chem.

Park, J., Y. Kim and J. Chung (2009). "Mitochondrial dysfunction and Parkinson's disease genes: insights from Drosophila." Dis Model Mech **2**(7-8): 336-340.

Patterson, G. H. and J. Lippincott-Schwartz (2002). "A photoactivatable GFP for selective photolabeling of proteins and cells." Science **297**(5588): 1873-1877.

Pendin, D., J. Tosetto, T. J. Moss, C. Andreazza, S. Moro, J. A. McNew and A. Daga (2011). "GTP-dependent packing of a three-helix bundle is required for atlastin-mediated fusion." Proc Natl Acad Sci U S A **108**(39): 16283-16288.

Perez-Iratxeta, C. and M. A. Andrade-Navarro (2008). "K2D2: estimation of protein secondary structure from circular dichroism spectra." BMC Struct Biol **8**: 25.

Perkins, G. A., M. G. Sun and T. G. Frey (2009). "Chapter 2 Correlated light and electron microscopy/electron tomography of mitochondria in situ." Methods Enzymol **456**: 29-52.

Pfeiffer, K., V. Gohil, R. A. Stuart, C. Hunte, U. Brandt, M. L. Greenberg and H. Schagger (2003). "Cardiolipin stabilizes respiratory chain supercomplexes." J Biol Chem **278**(52): 52873-52880.

Pizzo, P., I. Drago, R. Filadi and T. Pozzan (2012). "Mitochondrial Ca(2)(+) homeostasis: mechanism, role, and tissue specificities." Pflugers Arch **464**(1): 3-17.

Praefcke, G. J. and H. T. McMahon (2004). "The dynamin superfamily: universal membrane tubulation and fission molecules?" Nat Rev Mol Cell Biol **5**(2): 133-147.

Quiros, P. M., A. J. Ramsay, D. Sala, E. Fernandez-Vizarra, F. Rodriguez, J. R. Peinado, M. S. Fernandez-Garcia, J. A. Vega, J. A. Enriquez, A. Zorzano and C. Lopez-Otin (2012). "Loss of mitochondrial protease OMA1 alters processing of the GTPase OPA1 and causes obesity and defective thermogenesis in mice." EMBO J **31**(9): 2117-2133.

Rambold, A. S. and J. Lippincott-Schwartz (2011). "Mechanisms of mitochondria and autophagy crosstalk." Cell Cycle **10**(23): 4032-4038.

Rizzuto, R., D. De Stefani, A. Raffaello and C. Mammucari (2012). "Mitochondria as sensors and regulators of calcium signalling." Nat Rev Mol Cell Biol **13**(9): 566-578.

Roux, A., K. Uyhazi, A. Frost and P. De Camilli (2006). "GTP-dependent twisting of dynamin implicates constriction and tension in membrane fission." Nature **441**(7092): 528-531.

Rubinstein, J. L. (2007). "Structural analysis of membrane protein complexes by single particle electron microscopy." Methods **41**(4): 409-416.

Rujiviphat, J., G. Meglei, J. L. Rubinstein and G. A. McQuibban (2009). "Phospholipid association is essential for dynamin-related protein Mgm1 to function in mitochondrial membrane fusion." J Biol Chem **284**(42): 28682-28686.

Sanjuan Szklarz, L. K. and L. Scorrano (2012). "The antiapoptotic OPA1/Parl couple participates in mitochondrial adaptation to heat shock." Biochim Biophys Acta **1817**(10): 1886-1893.

Santel, A. and M. T. Fuller (2001). "Control of mitochondrial morphology by a human mitofusin." J Cell Sci **114**(Pt 5): 867-874.

Schatz, G. (1963). "The Isolation of Possible Mitochondrial Precursor Structures from Aerobically Grown Baker's Yeast." Biochem Biophys Res Commun **12**: 448-451.

Scherz-Shouval, R., E. Shvets, E. Fass, H. Shorer, L. Gil and Z. Elazar (2007). "Reactive oxygen species are essential for autophagy and specifically regulate the activity of Atg4." EMBO J **26**(7): 1749-1760.

Schlame, M. and K. Y. Hostetler (1997). "Cardiolipin synthase from mammalian mitochondria." Biochim Biophys Acta **1348**(1-2): 207-213.

Sesaki, H., C. D. Dunn, M. Iijima, K. A. Shepard, M. P. Yaffe, C. E. Machamer and R. E. Jensen (2006). "Ups1p, a conserved intermembrane space protein, regulates mitochondrial shape and alternative topogenesis of Mgm1p." J Cell Biol **173**(5): 651-658.

Sesaki, H. and R. E. Jensen (1999). "Division versus fusion: Dnm1p and Fzo1p antagonistically regulate mitochondrial shape." J Cell Biol **147**(4): 699-706.

Sesaki, H. and R. E. Jensen (2001). "UGO1 encodes an outer membrane protein required for mitochondrial fusion." J Cell Biol **152**(6): 1123-1134.

Sesaki, H. and R. E. Jensen (2004). "Ugo1p links the Fzo1p and Mgm1p GTPases for mitochondrial fusion." J Biol Chem **279**(27): 28298-28303.

Sesaki, H., S. M. Southard, A. E. Hobbs and R. E. Jensen (2003). "Cells lacking Pcp1p/Ugo2p, a rhomboid-like protease required for Mgm1p processing, lose mtDNA and mitochondrial structure in a Dnm1p-dependent manner, but remain competent for mitochondrial fusion." Biochem Biophys Res Commun **308**(2): 276-283.

Sesaki, H., S. M. Southard, M. P. Yaffe and R. E. Jensen (2003). "Mgm1p, a dynamin-related GTPase, is essential for fusion of the mitochondrial outer membrane." Mol Biol Cell **14**(6): 2342-2356.

Seth, R. B., L. Sun, C. K. Ea and Z. J. Chen (2005). "Identification and characterization of MAVS, a mitochondrial antiviral signaling protein that activates NF-kappaB and IRF 3." Cell **122**(5): 669-682.

Sever, S., H. Damke and S. L. Schmid (2000). "Dynamin:GTP controls the formation of constricted coated pits, the rate limiting step in clathrin-mediated endocytosis." J Cell Biol **150**(5): 1137-1148.

Sever, S., H. Damke and S. L. Schmid (2000). "Garrotes, springs, ratchets, and whips: putting dynamin models to the test." Traffic **1**(5): 385-392.

Sever, S., A. B. Muhlberg and S. L. Schmid (1999). "Impairment of dynamin's GAP domain stimulates receptor-mediated endocytosis." Nature **398**(6727): 481-486.

Shaw, J. M. and J. Nunnari (2002). "Mitochondrial dynamics and division in budding yeast." Trends Cell Biol **12**(4): 178-184.

Shepard, K. A. and M. P. Yaffe (1999). "The yeast dynamin-like protein, Mgm1p, functions on the mitochondrial outer membrane to mediate mitochondrial inheritance." J Cell Biol **144**(4): 711-720.

Shi, G., J. R. Lee, D. A. Grimes, L. Racacho, D. Ye, H. Yang, O. A. Ross, M. Farrer, G. A. McQuibban and D. E. Bulman (2011). "Functional alteration of PARL contributes to mitochondrial dysregulation in Parkinson's disease." Hum Mol Genet **20**(10): 1966-1974.

Shih, Y. L., K. F. Huang, H. M. Lai, J. H. Liao, C. S. Lee, C. M. Chang, H. M. Mak, C. W. Hsieh and C. C. Lin (2011). "The N-terminal amphipathic helix of the topological specificity factor MinE is associated with shaping membrane curvature." PLoS One **6**(6): e21425.

Shim, S. H., C. Xia, G. Zhong, H. P. Babcock, J. C. Vaughan, B. Huang, X. Wang, C. Xu, G. Q. Bi and X. Zhuang (2012). "Super-resolution fluorescence imaging of organelles in live cells with photoswitchable membrane probes." Proc Natl Acad Sci U S A **109**(35): 13978-13983.

Simbeni, R., L. Pon, E. Zinser, F. Paltauf and G. Daum (1991). "Mitochondrial membrane contact sites of yeast. Characterization of lipid components and possible involvement in intramitochondrial translocation of phospholipids." J Biol Chem **266**(16): 10047-10049.

Smirnova, E., L. Griparic, D. L. Shurland and A. M. van der Bliek (2001). "Dynamin-related protein Drp1 is required for mitochondrial division in mammalian cells." Mol Biol Cell **12**(8): 2245-2256.

Smirnova, E., D. L. Shurland, S. N. Ryazantsev and A. M. van der Bliek (1998). "A human dynamin-related protein controls the distribution of mitochondria." J Cell Biol **143**(2): 351-358.

Stowell, M. H., B. Marks, P. Wigge and H. T. McMahon (1999). "Nucleotide-dependent conformational changes in dynamin: evidence for a mechanochemical molecular spring." Nat Cell Biol **1**(1): 27-32.

Sweitzer, S. M. and J. E. Hinshaw (1998). "Dynamin undergoes a GTP-dependent conformational change causing vesiculation." Cell **93**(6): 1021-1029.

Tait, S. W. and D. R. Green (2012). "Mitochondria and cell signalling." J Cell Sci **125**(Pt 4): 807-815.

Takei, K., V. Haucke, V. Slepnev, K. Farsad, M. Salazar, H. Chen and P. De Camilli (1998). "Generation of coated intermediates of clathrin-mediated endocytosis on protein-free liposomes." Cell **94**(1): 131-141.

Takei, K., V. I. Slepnev, V. Haucke and P. De Camilli (1999). "Functional partnership between amphiphysin and dynamin in clathrin-mediated endocytosis." Nat Cell Biol **1**(1): 33-39.

Tamura, Y., T. Endo, M. Iijima and H. Sesaki (2009). "Ups1p and Ups2p antagonistically regulate cardiolipin metabolism in mitochondria." J Cell Biol **185**(6): 1029-1045.

Tan, G., M. Chen, C. Foote and C. Tan (2009). "Temperature-sensitive mutations made easy: generating conditional mutations by using temperature-sensitive inteins that function within different temperature ranges." Genetics **183**(1): 13-22.

Taylor, R. C., S. P. Cullen and S. J. Martin (2008). "Apoptosis: controlled demolition at the cellular level." Nat Rev Mol Cell Biol **9**(3): 231-241.

Tooley, J. E., V. Khangulov, J. P. Lees, J. L. Schlessman, M. C. Bewley, A. Heroux, J. Bosch and R. B. Hill (2011). "The 1.75 A resolution structure of fission protein Fis1 from Saccharomyces cerevisiae reveals elusive interactions of the autoinhibitory domain." Acta Crystallogr Sect F Struct Biol Cryst Commun **67**(Pt 11): 1310-1315.

Tucker, C. L. and S. Fields (2003). "Lethal combinations." Nat Genet **35**(3): 204-205.

Ungermann, C. and D. Langosch (2005). "Functions of SNAREs in intracellular membrane fusion and lipid bilayer mixing." J Cell Sci **118**(Pt 17): 3819-3828.

Vogel, F., C. Bornhovd, W. Neupert and A. S. Reichert (2006). "Dynamic subcompartmentalization of the mitochondrial inner membrane." J Cell Biol **175**(2): 237-247.

von der Malsburg, A., I. Abutbul-Ionita, O. Haller, G. Kochs and D. Danino (2011). "Stalk domain of the dynamin-like MxA GTPase protein mediates membrane binding and liposome tubulation via the unstructured L4 loop." J Biol Chem **286**(43): 37858-37865.

Warnock, D. E., J. E. Hinshaw and S. L. Schmid (1996). "Dynamin self-assembly stimulates its GTPase activity." J Biol Chem **271**(37): 22310-22314.

Wei, M. C., W. X. Zong, E. H. Cheng, T. Lindsten, V. Panoutsakopoulou, A. J. Ross, K. A. Roth, G. R. MacGregor, C. B. Thompson and S. J. Korsmeyer (2001). "Proapoptotic BAX and BAK: a requisite gateway to mitochondrial dysfunction and death." Science **292**(5517): 727-730.

Wells, R. C., L. K. Picton, S. C. Williams, F. J. Tan and R. B. Hill (2007). "Direct binding of the dynamin-like GTPase, Dnm1, to mitochondrial dynamics protein Fis1 is negatively regulated by the Fis1 N-terminal arm." J Biol Chem **282**(46): 33769-33775.

Westermann, B. (2010). "Mitochondrial fusion and fission in cell life and death." Nat Rev Mol Cell Biol **11**(12): 872-884.

Whitworth, A. J., J. R. Lee, V. M. Ho, R. Flick, R. Chowdhury and G. A. McQuibban (2008). "Rhomboid-7 and HtrA2/Omi act in a common pathway with the Parkinson's disease factors Pink1 and Parkin." Dis Model Mech **1**(2-3): 168-174; discussion 173.

Williamson, D. (2002). "The curious history of yeast mitochondrial DNA." Nat Rev Genet **3**(6): 475-481.

Wong, E. D., J. A. Wagner, S. W. Gorsich, J. M. McCaffery, J. M. Shaw and J. Nunnari (2000). "The dynamin-related GTPase, Mgm1p, is an intermembrane space protein required for maintenance of fusion competent mitochondria." J Cell Biol **151**(2): 341-352.

Wong, E. D., J. A. Wagner, S. V. Scott, V. Okreglak, T. J. Holewinske, A. Cassidy-Stone and J. Nunnari (2003). "The intramitochondrial dynamin-related GTPase, Mgm1p, is a component of a protein complex that mediates mitochondrial fusion." J Cell Biol **160**(3): 303-311.

Yoon, Y., K. R. Pitts and M. A. McNiven (2001). "Mammalian dynamin-like protein DLP1 tubulates membranes." Mol Biol Cell **12**(9): 2894-2905.

Youle, R. J. and A. M. van der Bliek (2012). "Mitochondrial fission, fusion, and stress." Science **337**(6098): 1062-1065.

Zhang, P. and J. E. Hinshaw (2001). "Three-dimensional reconstruction of dynamin in the constricted state." Nat Cell Biol **3**(10): 922-926.

Zhao, X., D. Alvarado, S. Rainier, R. Lemons, P. Hedera, C. H. Weber, T. Tukel, M. Apak, T. Heiman-Patterson, L. Ming, M. Bui and J. K. Fink (2001). "Mutations in a newly identified GTPase gene cause autosomal dominant hereditary spastic paraplegia." Nat Genet **29**(3): 326-331.

Zick, M., S. Duvezin-Caubet, A. Schafer, F. Vogel, W. Neupert and A. S. Reichert (2009). "Distinct roles of the two isoforms of the dynamin-like GTPase Mgm1 in mitochondrial fusion." FEBS Lett **583**(13): 2237-2243.

Zinser, E. and G. Daum (1995). "Isolation and biochemical characterization of organelles from the yeast, Saccharomyces cerevisiae." Yeast **11**(6): 493-536.

Ziviani, E., R. N. Tao and A. J. Whitworth (2010). "Drosophila parkin requires PINK1 for mitochondrial translocation and ubiquitinates mitofusin." Proc Natl Acad Sci U S A **107**(11): 5018-5023.

Zuchner, S., I. V. Mersiyanova, M. Muglia, N. Bissar-Tadmouri, J. Rochelle, E. L. Dadali, M. Zappia, E. Nelis, A. Patitucci, J. Senderek, Y. Parman, O. Evgrafov, P. D. Jonghe, Y. Takahashi, S. Tsuji, M. A. Pericak-Vance, A. Quattrone, E. Battaloglu, A. V. Polyakov, V. Timmerman, J. M. Schroder and J. M. Vance (2004). "Mutations in the mitochondrial GTPase mitofusin 2 cause Charcot-Marie-Tooth neuropathy type 2A." Nat Genet **36**(5): 449-451.